

Studies on water and nutrient balances and their mechanisms in tropical
lowland and montane rainforests in Malaysian Borneo

ボルネオ島低地・山地熱帯雨林における水・物質収支と
そのメカニズムに関する研究

五名 美江

Studies on water and nutrient balances and their mechanisms in tropical lowland and
montane rainforests in Malaysian Borneo

Mie Gomyo

The University of Tokyo

2010

Contents

List of Figures

List of Tables

List of Abbreviations

1. Introduction	1
1.1 Background	1
1.2 Climate and ENSO-rainfall relationship	2
1.3 Water balance and hydrological cycle	6
1.4 Nutrient input/output balances and nutrient cycle	7
1.5 Streamwater chemistry	11
1.6 Objectives of this thesis	13
1.7 Structure of this thesis	13
1.8 References	15
2. Site descriptions	22
2.1 Lambir Hills National Park site	23
2.1.1 Location	23
2.1.2 Climate	23
2.1.3 Geology and lithology	24
2.1.4 Watersheds and soils	24
2.1.5 Vegetation	25
2.2 Mount Kinabalu National Park site	26
2.2.1 Location	26
2.2.2 Climate	26
2.2.3 Geology and lithology	26
2.2.4 Watersheds and soils	27
2.2.5 Vegetation	29
2.3 References	29
3. Spatial and temporal variations in rainfall and the ENSO-rainfall relationship	32
3.1 Introduction	32
3.2 Methods	33
3.2.1 Rainfall data	33

Contents

3.2.2	SST data	34
3.3	Results	35
3.3.1	Spatial variation of rainfall	35
3.3.2	Seasonal variation of rainfall	36
3.3.3	ENSO-rainfall relationship	40
3.3.4	DJF rainfall	42
3.4	Discussion	45
3.4.1	Spatial and seasonal variations of rainfall	45
3.4.2	ENSO-rainfall relationship	50
3.5	Conclusion	52
3.6	References	53
4.	Water balance and nutrient balances	54
4.1	Introduction	54
4.2	Methods	57
4.2.1	Site descriptions	57
4.2.2	Rainfall and discharge observation	58
4.2.3	Rainfall, throughfall and streamwater sampling, intense observation during rainfall-induced stormflow	58
4.2.4	Chemical analysis	59
4.2.5	Convert water level to discharge	59
4.2.6	Imputation of missing data	61
4.2.7	Annual input fluxes by rainfall and throughfall	63
4.2.8	Annual output fluxes	64
4.3	Results	68
4.3.1	Water balance	68
4.3.2	Estimation of output fluxes	68
4.3.3	Nutrient balance	74
4.4	Discussion	76
4.4.1	Water balance	76
4.4.2	Rainfall and flow duration curves	78
4.4.3	Output flux estimation methods	80
4.4.4	Partitioning output flux into baseflow and stormflow	81
4.4.5	Nutrient balances in LT and KM	84
4.5	Conclusion	89
4.6	References	91

5. Factors controlling pH and ion concentrations of streamwater	97
5.1 Introduction	97
5.2 Methods	98
5.2.1 Watersheds descriptions	98
5.2.2 Rainfall and discharge observation	98
5.2.3 Intensive observation of streamwater and rainwater during rainfall-induced stormflow	98
5.2.4 Chemical analysis	98
5.3 Results	99
5.3.1 Streamwater and rainwater chemistry	99
5.4 Discussion	102
5.4.1 Characteristics of streamwater chemistry in LHNP and MKNP	102
5.4.2 Effects of SO_4^{2-} concentration on pH	108
5.5 Conclusion	110
5.6 References	110
6. Sources and possible generation mechanism for controlling ion concentrations of streamwater	112
6.1 Introduction	112
6.2 Methods	113
6.2.1 Study watershed	113
6.2.2 Sampling design and chemical analysis	114
6.3 Results	116
6.3.1 Spatial and vertical distribution	116
6.4 Discussion	126
6.4.1 Spatial and Vertical Distributions of SO_4^{2-} Concentration and pH	126
6.4.2 Balance: The Ratio of Ca and Fe Concentrations	127
6.5 Conclusion	129
6.6 References	130
7. Conclusion	133
8. Acknowledgements	137

List of Figures

1.1	World map showing distribution of the three climatic sub-types (humid, sub-humid, wet-dry) of the humid tropics (Chang and Lau, 1993).	3
1.2	Nutrient cycling pathways in forest (Bruijnzeel, 1991)	8
1.3	The major pathways linking terrestrial and stream ecosystems (Proctor, 2005).	9
1.4	The chemical S cycle and fluxes of S within the environment (Hawakesford and De Kok, 2007).	11
1.5	Biogeochemical cycling in forest (Berner and Berner, 1995).	12
1.6	The structure of this thesis.	14
2.1	Map showing the study sites.	22
2.2	Location and topography of the LT, LC and LM watersheds in LHNP based on the map (Wakahara and Shiraki, per.com.).	25
2.3	Location of two watersheds based on the map in Jacobson (1970). Climate station is located near the park headquarters.	28
2.4	Location and topography of the KM and KB watersheds in MKNP.	28
3.1	Tree diagram of the cluster analysis of the 18 observation stations over Sarawak.	35
3.2	Tree diagram of the cluster analysis of the 25 observation stations over Sabah.	35
3.3	Anomalies of the mean monthly rainfall for (a) C1, C2, C3 and C4, and (b) LHNP. The anomaly was calculated by taking the average of the normalized anomaly in each month at each station, which was obtained by dividing the anomaly by the mean monthly rainfall.	36
3.4	Anomalies of the mean monthly rainfall for (a) C1, (b) C2, (c) C3 and (d) C4. The anomaly was calculated by taking the average of the normalized anomaly in each month at each station, which was obtained by dividing the anomaly by the mean monthly rainfall.	37
3.5	Anomalies of the mean monthly rainfall for (a) S1, S2, S3 and S4, and (b) MKNP. The anomaly was calculated by taking the average of the normalized anomaly in each month at each station, which was obtained by dividing the anomaly by the mean monthly	

List of Figures

rainfall.	38
3.6 Anomalies of the mean monthly rainfall for (a) S1, (b) S2, (c) S3 and (d) S4. The anomaly was calculated by taking the average of the normalized anomaly in each month at each station, which was obtained by dividing the anomaly by the mean monthly rainfall.	39
3.7 Mean annual rainfall of the cluster in Sarawak and Sabah, respectively. The mean rainfall for LHNP (2000-2008) and MKNP (1996-2000, 2006-2008) are shown. The bars are standard deviation.	40
3.8 Coefficients for the simultaneous and lag correlations between the three-month sliding sum of rainfall and SST (a) Sarawak, (b) Sabah.	41
3.9 El Niño minus all-years composite of the three-month sliding sum of rainfall anomaly for the four clusters.	41
3.10 Mean DJF rainfall of the cluster, LHNP and MKNP, respectively. The bars are standard deviation.	43
3.11 (a) Mean DJF rainfall, and (b) El Niño years mean DJF rainfall of all stations over Sarawak(left) and Sabah(right), respectively.	44
3.12 DJF rainfall reductions in the El Niño years of all stations over Sarawak (left) and Sabah (right), respectively.	45
3.13 The NCEP/NCAR reanalysis wind velocity of pentad 2(6 Jan – 10 Jan). Mean of 1979-2000 at 850 hPa (Oki, 2002).	46
3.14 The NCEP/NCAR reanalysis wind velocity of pentad 9(10 Feb – 14 Feb). Mean of 1979-2000 at 850 hPa (Oki, 2002).	47
3.15 The NCEP/NCAR reanalysis wind velocity of pentad 26(6 May – 10 May). Mean of 1979-2000 at 850 hPa (Oki, 2002).	48
3.16 The NCEP/NCAR reanalysis wind velocity of pentad 38(5 Jul. – 10 Jul.). Mean of 1979-2000 at 850 hPa (Oki, 2002).	49
3.17 The NCEP/NCAR reanalysis wind velocity of pentad 64(12 Nov. – 16 Nov.). Mean of 1979-2000 at 850 hPa (Oki, 2002).	50
4.1 Relationship between water level (water depth in this figure) and discharge at LT (TL in this figure) watershed (Wakahara et al., in reviewing).	60
4.2 Relationship between water level and discharge at KM watershed.	61
4.3 Schematic diagram of the proposed hydrological cycle model.	62
4.4 Model output and observed hourly discharge of the KM watershed from September 2006 to April 2007.	63
4.5 Relationship between discharge and ion concentration of (a) NO_3^- , (b) NH_4^+ , (c) K^+ , (d)	

List of Figures

	Mg ²⁺ , (e) Ca ²⁺ , (f) Na ⁺ , (g) Cl ⁻ , and (h) SO ₄ ²⁻ at LT and KM watersheds.	66
4.6	Flow duration curves for hourly discharge data from 2006 to 2007 in the (a) LT and (b) KM watersheds. MD2Y = mean discharge over 2 years.	67
4.7	Comparison of NO ₃ -N AOF estimated by six different methods, in (a) LT and (b) KM.	71
4.8	Comparison of NH ₄ -N AOF estimated by six different methods, in (a) LT and (b) KM.	72
4.9	Comparison of K AOF estimated by six different methods, in (a) LT and (b) KM.	72
4.10	Comparison of Mg AOF estimated by six different methods, in (a) LT and (b) KM.	72
4.11	Comparison of Ca AOF estimated by six different methods, in (a) LT and (b) KM.	73
4.12	Comparison of Na AOF estimated by six different methods, in (a) LT and (b) KM.	73
4.13	Comparison of Cl AOF estimated by six different methods, in (a) LT and (b) KM.	73
4.14	Comparison of SO ₄ -S AOF estimated by six different methods, in (a) LT and (b) KM.	74
4.15	Comparison of relationship between (a) rainfall and discharge, (b) loss and rainfall, (c) loss and elevation, and (d) loss and watershed area in the tropical forested catchments in Malaysia. Water balance in the tropical forested catchments in Malaysia (<100 ha).	77
4.16	Daily rainfall and daily discharge at LT (a) and KM (b) watersheds from January 2006 to December 2007).	78
4.17	(a) Daily rainfall and (b) daily flow duration curves for two years daily rainfall and discharge data (LT and KM = 2006 and 2007, SP and UK = 1991 and 1992).	79
4.18	Relationship between discharge and NO ₃ ⁻ concentration, NO ₃ ⁻ concentration values estimated by used six methods, and frequency of each flow in LT watershed.	80
4.19	Percentage frequencies, discharge, and AOF by discharge in different flow classes (2006-2007) in the LT and KM watersheds.	83
4.20	AIF _R , AIF _T , and AOF of (a and b) NO ₃ -N, (c and d) NH ₄ -N, and (e and f) Inorg-N from 2006 to 2008 in the LT and KM watersheds. The bars are standard deviation.	84
4.21	AIF _R , AIF _T , and AOF of K from 2006 to 2008 in the (a) LT and (b) KM watersheds. The bars are standard deviation.	85
4.22	AIF _R , AIF _T , and AOF of Mg from 2006 to 2008 in the (a) LT and (b) KM watersheds. The bars are standard deviation.	86

List of Figures

4.23	AIF _R , AIF _T , and AOF of Ca from 2006 to 2008 in the (a) LT and (b) KM watersheds. The bars are standard deviation.	87
4.24	AIF _R , AIF _T , and AOF of Na (a and c) and Cl (b and d) from 2006 to 2008 in the LT and KM watersheds. The bars are standard deviation.	88
4.25	AIF _R , AIF _T , and AOF of SO ₄ -S from 2006 to 2008 in the (a) LT and (b) KM watersheds. The bars are standard deviation.	89
5.1	Relationship between anions and cations based on Table 5.1.	100
5.2	Relationship between anions and cations of rainwater based on Table 5.1. The legends in this figure are the same as in Figure 5.1.	101
5.3	(a) Scatter graph of the ion balance of streamwater chemistry in watersheds in tropical rainforest. (b) Scatter graph of the relationship between anion and SO ₄ ²⁻ concentration. KM = Kinabalu Mempening, KB = Kinabalu Bukit Ular, LC = Lambir Crane Large, LT = Lambir Tower Large, M1 = Mendolong W3, M2 = Mendolong W6, B1 = Bukit Tarek C1, B2 = Bukit Tarek C2.	104
5.4	Schematic diagram of the input, pool, and runoff of SO ₄ ²⁻ for (a) LT and (b) KM.	106
5.5	Ternary diagram of (a) anions Cl ⁻ – SO ₄ ²⁻ – (TC-TA) and (b) cations (Na ⁺ + K ⁺) – Mg ²⁺ – Ca ²⁺ . The labels LT, LC, KM, KB, M1, M2, B1, and B2 are the same as in Figure 5.3.	108
5.6	(a) Scatter graph of the relationship between the SO ₄ ²⁻ concentration and pH. The solid line depicts when the ion composition is 100% H ₂ SO ₄ . (b) Scatter graph of the relationship between SO ₄ ²⁻ concentration and cations ([Na ⁺] + [K ⁺] + 2[Mg ²⁺] + 2[Ca ²⁺]). The labels LT, LC, KM, KB, M1, M2, B1, and B2 are the same as in Figure 5.3.	109
6.1	Location and topography of the LM watershed showing locations of soil water, groundwater, and streamwater sampling sites.	115
6.2	Arithmetic mean concentrations of SO ₄ ²⁻ for soil water, groundwater, and streamwater in the LM watershed. The numbers in parentheses indicate the number of samples, and the bars are standard deviation. Significant differences between LM1 streamwater and all soil water, groundwater, and LM4 streamwater, and between LM4 streamwater and soil water at LM4 and LM5 and groundwater are indicated by *'s on the right side of the figure (t-test, **: p < 0.001; *: p < 0.01).	117
6.3	Arithmetic mean concentrations of [TA]for soil water, groundwater, and streamwater in the LM watershed. The numbers in parentheses indicate the number of samples, and the bars are standard deviation. Significant differences are the same as in Figure 6.2.	118

List of Figures

6.4 Arithmetic mean concentrations of NO_3^- for soil water, groundwater, and streamwater in the LM watershed. The numbers in parentheses indicate the number of samples, and the bars are standard deviation. Significant differences are the same as in Figure 6.2. ...119

6.5 Arithmetic mean concentrations of Cl^- for soil water, groundwater, and streamwater in the LM watershed. The numbers in parentheses indicate the number of samples, and the bars are standard deviation. Significant differences are the same as in Figure 6.2. ...120

6.6 Arithmetic mean concentrations of Ca^{2+} for soil water, groundwater, and streamwater in the LM watershed. The numbers in parentheses indicate the number of samples, and the bars are standard deviation. Significant differences are the same as in Figure 6.2. ...121

6.7 Arithmetic mean concentrations of Mg^{2+} for soil water, groundwater, and streamwater in the LM watershed. The numbers in parentheses indicate the number of samples, and the bars are standard deviation. Significant differences are the same as in Figure 6.2. ...122

6.8 Arithmetic mean concentrations of [TC] for soil water, groundwater, and streamwater in the LM watershed. The numbers in parentheses indicate the number of samples, and the bars are standard deviation. Significant differences are the same as in Figure 6.2. ...123

6.9 The pH for soil water, groundwater, and streamwater in the LM watershed. The numbers in parentheses indicate the number of samples, and the bars are standard deviation. Significant differences are the same as in Figure 6.2.124

6.10 Arithmetic mean concentrations of [TC]-[TA] for soil water, groundwater, and streamwater in the LM watershed. The numbers in parentheses indicate the number of samples, and the bars are standard deviation. Significant differences are the same as in Figure 6.2.125

6.11 Arithmetic mean concentrations of Fe for soil water, groundwater, and streamwater in the LM watershed. The numbers in parentheses indicate the number of samples, and the bars are standard deviation. Significant differences are the same as in Figure 6.2. ..126

6.12 Scatter graph showing the relationship between $[\text{SO}_4^{2-}]$ and (a) (TC – TA) (b) $[\text{SO}_4^{2-}]$ and the ratio of $[\text{Ca}^{2+}]$ and $/([\text{Ca}^{2+}] + [\text{Mg}^{2+}])$, and (c) $[\text{SO}_4^{2-}]$ and [Fe] for soil water, groundwater, and streamwater.128

List of Tables

2.1	Weather stations and watersheds description in LHNP	23
2.2	Weather stations and watersheds description in MKNP	26
3.1	List of rainfall stations used in Sarawak. Cluster name, station number, name, location (latitude values are degrees north and longitude values are degrees east), elevation, mean annual rainfall and mean DJF rainfall.	33
3.2	List of rainfall stations used in Sabah. Cluster name, station number, name, location (latitude values are degrees north and longitude values are degrees east), elevation, mean annual rainfall and mean DJF rainfall.	34
4.1	Features of the LT and KM watersheds.	58
4.2	List of the parameters.	63
4.3	Definition of AOF estimated by six different methods.	64
4.4	Annual rainfall, discharge, loss, mean air temperature, and mean water temperature from 2006 to 2008 in the LT and KM watersheds.	68
4.5	Parameters of the exponential equation, $\text{Log}(\text{Concentration}) = a + b \text{Log}(\text{Discharge})$, of the relationship between concentration (C , $\mu\text{mol}_c\text{L}^{-1}$) and discharge (Q , mm/10 min) in LT and KM. (a) Linear regression. (b) Piecewise continuous linear function with two parts.	69
4.6	Occurrence distributions of sampled, hour and discharge over the four classes of LT and KM watersheds. (a) Jan 2006 – Dec 2006, (b) Jan 2007 – Dec 2007, and (c) Intensive observation during rainfall-induced stormflow.	70
4.7	Comparison of nutrient AOF estimated by five different methods, in LT and KM.	71
4.8	AIF_R , AIF_T , and AOF from 2006 to 2008 in the LT and KM watersheds.	75
4.9	Water balance in the tropical forested catchments in Malaysia (<100 ha).	77
4.10	(a) Mean hour (b) Mean discharge and (c) mean AOF by discharge in different flow classes (2006 – 2007). Percentage values indicate the fraction of total AOF for the corresponding flow class.	82
5.1	Volume-weighted mean (VWM) concentrations of ions from January 2006 to December 2007 for (a) streamwater in 4 watersheds and (b) rainwater in 2 sites.	99

List of Tables

5.2	Significance level of difference between sites tested by t-test. Data used were volume-weighted mean concentrations of ions except ‘storm’.....	102
5.3	Volume-weighted mean concentrations of Fe, Si, and Al from January 2006 to December 2007 for streamwater in four watersheds.....	102
5.4	Ion concentrations of streamwater in tropical rainforests worldwide, as reported in the literature. The metal concentrations are shown for reference.....	103
6.1	Arithmetic mean concentration of soil water, groundwater, and streamwater sampled at five sites and various depths.....	116
6.2	The pH of soil samples.	129

List of Abbreviations

1. AIF_R : annual input flux through rainfall
2. AIF_T : annual input flux through throughfall
3. AOF : annual output flux
4. CPC : Climate Prediction Center
5. CMAP : Climate Analysis of Precipitation
6. DID : Department of Irrigation and Drainage
7. DJF : December to February
8. ENSO : El-Niño/Southern Oscillation
9. FM : February to March
10. ITCZ : Intertropical convergence zone
11. JFM : January to March
12. JJA : June to August
13. KB : Kinabalu Bukit Ular
14. KM : Kinabalu Mempening
15. LC : Lambir Crane Large
16. LHNP : Lambir Hills National Park
17. LM : Lambir Crane Micro
18. LT : Lambir Tower Large
19. MEM : northeast monsoon
20. MJ : May to June
21. MKNP : Mount Kinabalu National Park
22. MMS : Malaysian Meteorological Service
23. NES : northeastern Sarawak
24. NOAA : Notional Oceanic and Atmospheric Administration
25. ON : October to November
26. ONDJ : October to January
27. SON : September to November
28. SST : Sea surface temperature
29. SWS : southwestern Sarawak

Chapter 1

Introduction

1.1 Background

Tropical forests are undergoing rapid and extensive change as a result of population growth and economic expansion. Such change has induced deforestation, defined as the conversion of tropical forest to other land uses such as subsistence cultivation and large-scale mono-crop plantations. Deforestation is accompanied by the irreversible loss of forest biodiversity. Logging and conversion of forests to agricultural land continues at an unprecedented space worldwide. The rate of deforestation in Southeast Asia is among the highest of any tropical region (Turner and Foster, 2009). The expansion of timber harvesting and oil palm plantations continues in Malaysia. The oil palm area throughout the world has increased 3.7-fold from 1,756,000 ha in 1980 to 6,563,000 ha in 2000; in contrast, the oil palm area in Malaysia has remained at a constant level (45-46%) (Wahid et al. 2005). The influence of oil palm expansion on forest ecosystems is unknown.

Tropical peat swamp forests, which are mainly found in Southeast Asia are common in Borneo (Phua et al. 2007; Hooijer, 2005), where they occur on low-lying, poorly drained sites along the coasts of Sarawak, Brunei; Darussalam, Sabah; and Kalimantan. They are located further inland than the neighbouring beach and mangrove forest formations (Phillips, 1998). Peat swamp forests have been rapidly disappearing because of agricultural development and wildfires associated with the ENSO (El-Niño/Southern Oscillation) (Phua et al. 2007). During the El Niño years, droughts in Southeast Asia can have severe environmental effects such as large-scale forest fires (Salafsky, 1994;1998; Idris et al. 2005). Drought can affect the ecology of tropical forests and peat swamp forests via fire, plant mortality, and plant phenology, which in turn affect the timing and amount of resources available to herbivores, pollinators, and seed dispersers (Harrison 2005). The island of Borneo has one of the wettest and most aseasonal climates of any tropical region; therefore, dry periods are rare (Brunig 1969; Walsh and Newbery, 1999). The timing and intensity of El Niño-

1. Introduction

induced droughts over Borneo vary from region to region. The frequency of dry spells may be affected by the ENSO (Gomyo and Kuraji, 2009), leading to an irreversible loss of biodiversity.

Acid sulfur soils are distributed widely around the world, particularly in the coastal lowlands of Southeast Asia, western Africa, eastern Australia, and Latin America, with a total extent of 17 million ha (Andriessse and van Mensvoort, 2006). In Southeast Asia, most acid sulfur soils occur in tidal swampland covered by mangrove swamps, where pyrite (FeS_2) is formed (Arkesteyn, 1980; Attanandana and Vacharotayan, 1986). When these soils are exposed to air during reclamation projects such as irrigation and drainage canal construction, the pyrite oxidizes to produce ferric ions and sulfuric acid in the drainage water. Acid sulfate soils develop where the production of acid exceeds the neutralizing capacity of the parent material, and the pH value falls to 4 (MacKinnon et al. 1996). Pyrite oxidation after peatland development has been found to cause not only acidification of soil but also acidification of the canals ($\text{pH} = 2.0\text{--}3.0$) and connecting rivers (Haraguchi, 2007).

In the tropics, peat swamps as well as hills and valleys include areas of underlying marine sediments uplifted by plate tectonic activities in the Tertiary Age. These marine sedimentary rocks on land are generally covered by terrestrial sedimentary rocks and are rarely exposed on the land surface. However, when exposed by agricultural, industrial, or residential development, these marine sedimentary rocks may chemically react with atmospheric oxygen and rainwater to produce acid sulfate soils.

Next section show the knowledges of (1.2) Climate and ENSO-rainfall relationship as climatology and meteorology, (1.3) Water balance and hydrological cycle as hydrology, (1.4) Nutrient input/output balance and nutrient cycle as biology, ecology, hydrochemistry, (1.5) Streamwater chemistry as hydrochemistry and geochemistry in tropical rainforest.

1.2 Climate and ENSO-rainfall relationship

The most common climate classification of the tropics is based on whether or not the area has a distinct dry season. The natural vegetation of the tropics is predominantly forest. However, forests in areas with a dry season are not as lush as those without, making them deciduous or scrubland depending on their particular conditions, thus it is easier to classify on the basis of vegetation. Köppen defined tropical climates as having a monthly minimum temperature of 18°C ,

1. Introduction

with three subdivisions: tropical rainforest climate (having more than 60mm of monthly rainfall throughout a year), tropical monsoon climate (having a short dry season) and tropical savanna climate (having pronounced wet and dry seasons) (Köppen, 1936). The US President's Council of Advisors on Science and Technology has defined a wet month as having a monthly rainfall of 200mm, dividing the climates into four: humid tropical, humid subtropical, dry-humid and dry, based on the number of wet months (Chang and Lau 1993, *Figure 1.1*).

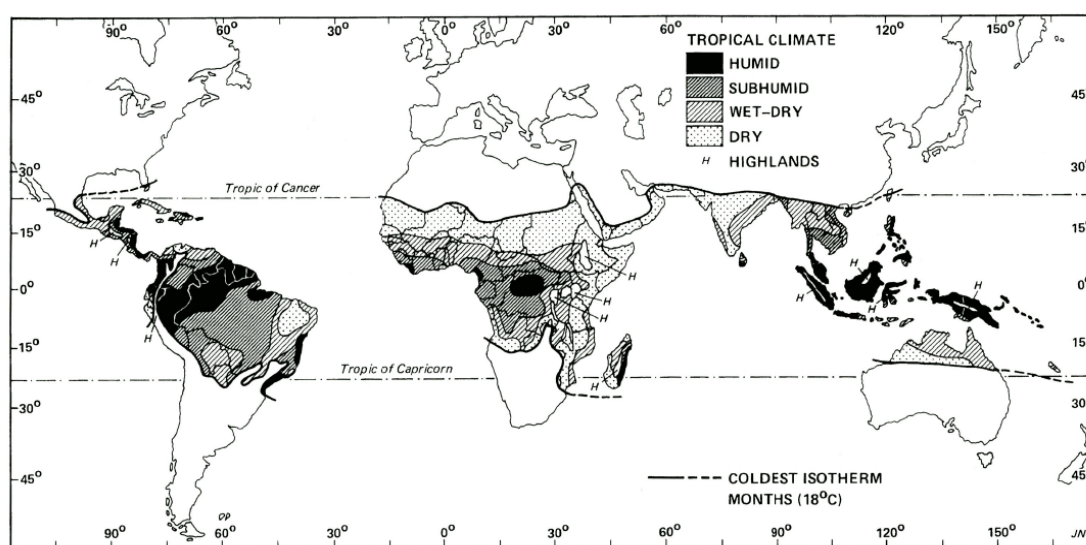


Figure 1.1 World map showing distribution of the three climatic sub-types (humid, sub-humid, wet-dry) of the humid tropics (Chang and Lau 1993).

Ever since the establishment of the Köppen climate classification, it has been commonly recognized that the whole region covering the Malay Peninsula, Sumatra and Borneo islands (the Southeast Asia tropical rainforest region hereafter) belongs to the humid tropics, differentiating it from the Indochina peninsula and northern Philippines, which are regions with dry seasons. Previous studies of the climate of the Southeast Asia tropical rainforest region stated that ‘there is no distinct seasonal variation in rainfall in Borneo’, for example in Sakai et al. (1999), Kato et al. (1999) and Kumagai et al (2005).

However, thanks to the efforts of the meteorological and hydrological offices in relevant countries in collecting and analyzing rainfall data, it is now becoming clearer that there are locations with distinctive seasonal variations in rainfall in the Southeast Asia tropical rainforest region (Kuraji, 2005, Hooijer, 2005), which is traditionally regarded as an year-round wet area with no dry season, and very little seasonal variation in rainfall. It has become clear that variation patterns differ quite

1. Introduction

clearly among locations. For example, Hamada et al. (2002) defined five types of climatological pattern of seasonal rainfall variation using long-term rainfall data collected at 46 locations covering the whole of Indonesia (among which 10 locations are in the Southeast Asia tropical rainforest) with the following findings.

Type A-I (annual cycle, reaching local maximum during September to February): Northern Sumatra (Sigli, Medan), Southeast (Pangkal Pinang), South Borneo (Banjarmasin)

Type A-II (semiannual cycle, reaching local maximum during September to February) : Southeast Sumatra (Jambi), Western Borneo (Pontianak)

Type B-I (annual cycle, reaching local maximum during March to August) : Southeast Borneo (Kotabaru), West (Muara Muntai)

Type C (no seasonal variation) : Western Borneo (Balikpapan, Tarakan)

This study showed that rainfall in the Southeast Asia tropical rainforest region varies, having locations both with and without clear seasonal changes. It was also shown that there are locations, among those without clear seasonal changes, which are spatially unevenly scattered but share the same variation patterns. However, as there are few analyzable locations in this vast region, it has not reached the stage where climatological classification by rainfall, let alone any investigation into the climatological and meteorological causes behind such classification, has actually been conducted.

The biggest landmass in the Southeast Asia tropical rainforest region is the island of Borneo (740, 000 km²), which is divided between three countries, Indonesia, Malaysia and Brunei, with a land area ratio of 73%, 27% and 1% respectively. In order to obtain meteorological data for the whole of Borneo, it is, therefore, effective to use the rainfall observational data from Malaysia as well as that from Indonesia. A geography textbook in Malaysia states that the northern part of Borneo island is affected by monsoons, classifying November to April as the northeast (NE) monsoon season and May to October as the southwest (SW) monsoon season (Penerbit Fajar Bakti Sdn Bhd, 2001; Longman Malaysia, 1989). The section describing the weather in a comprehensive document on national parks in Sarawak (Hans and Abang, 2001) states that there is no prominent dry season in Sarawak, but that there are two relatively humid seasons (the NE monsoon season from

1. Introduction

November to March and the SW monsoon season from June to September with two interval seasons (April/May and October), thus four seasons are recognized there. It also attributes the cause of this seasonal variation to the movement of the intertropical convergence zone (ITCZ). The document does not show the source of this description, but it is assumed that the description is based on the monthly rainfall data collected by a climate mapping project (ACAP) in ASEAN countries.

In Malaysia, rainfall observation is mainly conducted by the Malaysian Meteorological Service (MMS) and the Department of Irrigation and Drainage (DID). While the MMS mainly conducts observation at major airports, DID operates nationwide as part of water resource management and flood control. There are previous studies using these data such as studies by ecologists on the frequency of drought occurrence (Brunig, 1969 ; 1970 ; Walsh and Newbery, 1999). However, seasonal rainfall variation in the whole Sarawak and Sabah have never been analyzed using long-term land surface observation data and mapped out according to the climatological classification.

The temporal and spatial variations between ENSO and rainfall on the maritime continent were studied by Haylock and McBride (2001), Hendon (2003) and Chang et al. (2004). They pointed out that a strong negative simultaneous correlation between Indonesian rainfall and the tropical eastern Pacific sea surface temperature (SST) only occurs in the dry season (June to August; JJA) and transition season (September to November; SON) and not in the wet season (December to February; DJF). However, all station data were from Indonesia and none were from Malaysia, which covers the Malay Peninsula and the northern part of Borneo (Sarawak and Sabah).

The correlation between rainfall and the ENSO in Malaysia was studied by Juneng and Tangang (2005). They found the ENSO–Malaysian rainfall relationship during the northeast monsoon (NEM) period is only apparent in Borneo. Tangang et al. (2006) investigated the difference in the ENSO–rainfall relationship between the Peninsular Malaysia and Borneo and found that only Kuching in southwestern Sarawak (SWS) reported a low simultaneous correlation between the NEM rainfall and SST. The difference in the rainfall–ENSO relationship between SWS and northeastern Sarawak (NES) has never been studied; Tangang et al. (2006) used data recorded by the Malaysian Meteorological Department (MMD), which has too few stations (the three stations of Kuching, Bintulu and Miri) to provide data for the discussion of the difference in the rainfall–ENSO relationship between SWS and NES. The seasonal variation in rainfall in Sarawak was studied by

Walsh and Newbery (1999) but their study was also based on measurements from a limited number of MMD stations.

1.3 Water balance and hydrological cycle

Understanding rainfall and the water balance in undisturbed watersheds is important for assessing the consequences of climate change, land use change, and other anthropogenic impacts on tropical rainforests. Fleischbein et al. (2006) used hydrological modeling to determine components of the water cycle that cannot be measured directly, such as evaporation and transpiration. This approach involved calculating an annual water balance from simulations of catchment areas where classical field hydrological measurements and short-term hydrological observation (Bruijnzeel et al. 1993; Fleischbein et al. 2006) were limited (Bruijnzeel, 2004). Using these principals, the water balance in forests (Jamaica - Hafkenschied, 2000; Puerto Rico – Holwerda, 2005; Malaysia - Kumagai et al. 2005 ; Australia- McJannet et al. 2007) has been analyzed by modeling canopy hydrological components and calculating the canopy water balance(Bruijnzeel,1990).

Several forest water balance studies have been conducted in Borneo at sites such as Sapulut and Ulu Kalumpang, Sabah (Kuraji, 2004); the Danum Valley, Sabah (Donglas, et al. 1992; Chappell et al. 1998; Chappel and Sherlock, 2005); Mendolong, Sabah (Malmer, 1992; 1993; 2004); Temburong, Brunei (Dykes, 1997; Dykes and Thornes, 2000); Lambir Hills, Sarawak (Kume et al. 2008, Manfroi et al. 2004; 2006; Kumagai et al. 2005); and Central Kalimantan (Asdak et al. 1998, Vernimmem et al. 2007). These studies describe a wide range of hydrological observations, such as rainfall, throughfall, stemflow, soil water, groundwater, streamflow, and evapotranspiration. The hydrologic flowpaths in lowland, tropical rainforest soilscales have also been reviewed (Elsenbeer, 2001; Chappell et al. 1998). It was concluded that soil types tentatively define a spectrum of possible hillslope hydrologic flowpaths from predominantly vertical to predominantly lateral. A limited number of hydrological studies have focused on the lowland and montane forests in Borneo. However, a number of comprehensive hydrological studies describe tropical lowland (Nortcliff and Thornes,1989; Lesack, 1993; Elsenbeer et al. 1999) and montane (Hafkenschied, 2000; Bruijnzeel 2001; Fleischbein et al. 2005; 2006) forests in Central and South America.

1.4 Nutrient input/output balances and nutrient cycle

Many reviews of nutrient cycles in tropical rainforest ecosystems are available (Golley et al. 1975; Jordan and Herrera, 1981; Jordan, 1985; Vitousek and Sanford, 1986; Proctor, 1989; 2005; Bruijnzeel, 1991). *Figure 1.2* shows a schematic picture of pools and transport in forest nutrient cycles (Bruijnzeel, 1991).

Nutrients enter forest ecosystems through rainfall, deposition of dust and aerosols, fixation by microorganisms above and below the ground (nitrogen [N]), and weathering of the bedrock (apart from N) (Proctor 2005). There is a flow of nutrients from the major aboveground pool (tree boles, large branches, and other components) to the forest floor in small and large litterfall and in throughfall and stemflow of rainwater enriched by nutrients from leaves and bark. The nutrients in dead organic matter are released gradually by decomposition. In extreme cases immobilization may occur, whereby there is a conversion of litter to stable organic matter that holds nutrients indefinitely. Nutrients are taken up from the soil by roots that provide a living belowground pool and that transfer the nutrients back to the canopy. Permanent loss of nutrients occurs in streamwater and by abiotic or microbial denitrification.

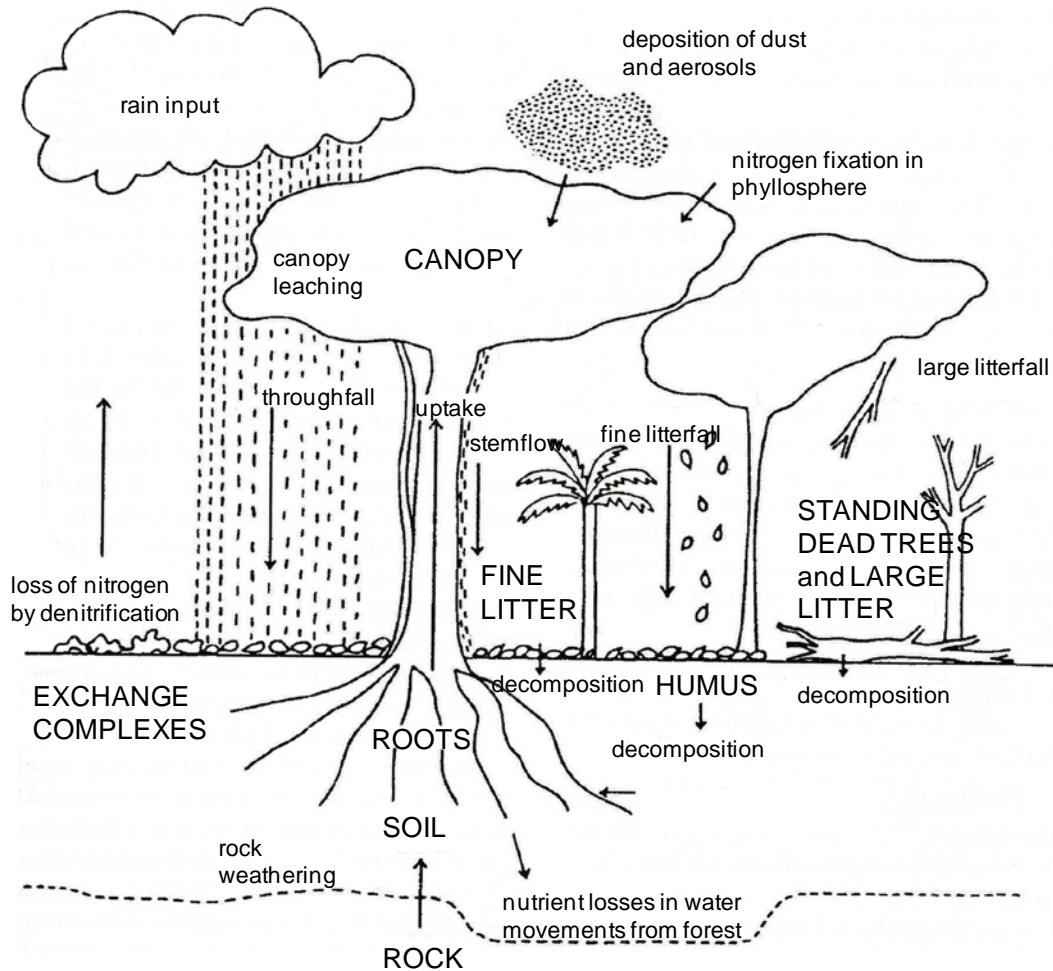


Figure 1.2 Nutrient cycling pathways in forest (Bruijnzeel, 1991).

The links between nutrient cycling and hydrology are numerous (*Figure 1.3*). Nutrient input to the forest floor is provided by rainfall, throughfall, and stemflow, and the chemical composition of the input varies depending on climate, vegetation, and chemical transformation. Nutrient loss from forest ecosystems is reflected in the amount of nutrients in the pools as well as in their flux between these pools and into and out of the system.

Bruijnzeel (1991) examined calcium (Ca), magnesium (Mg), potassium (K), phosphorus (P), and N flux in 25 tropical forest sites and concluded that the annual input flux through rainfall (AIF_R) varies greatly depending on the location relative to the origin of dust and aerosols. He also demonstrated that nutrient losses per unit streamflow increase with increasing site fertility.

1. Introduction

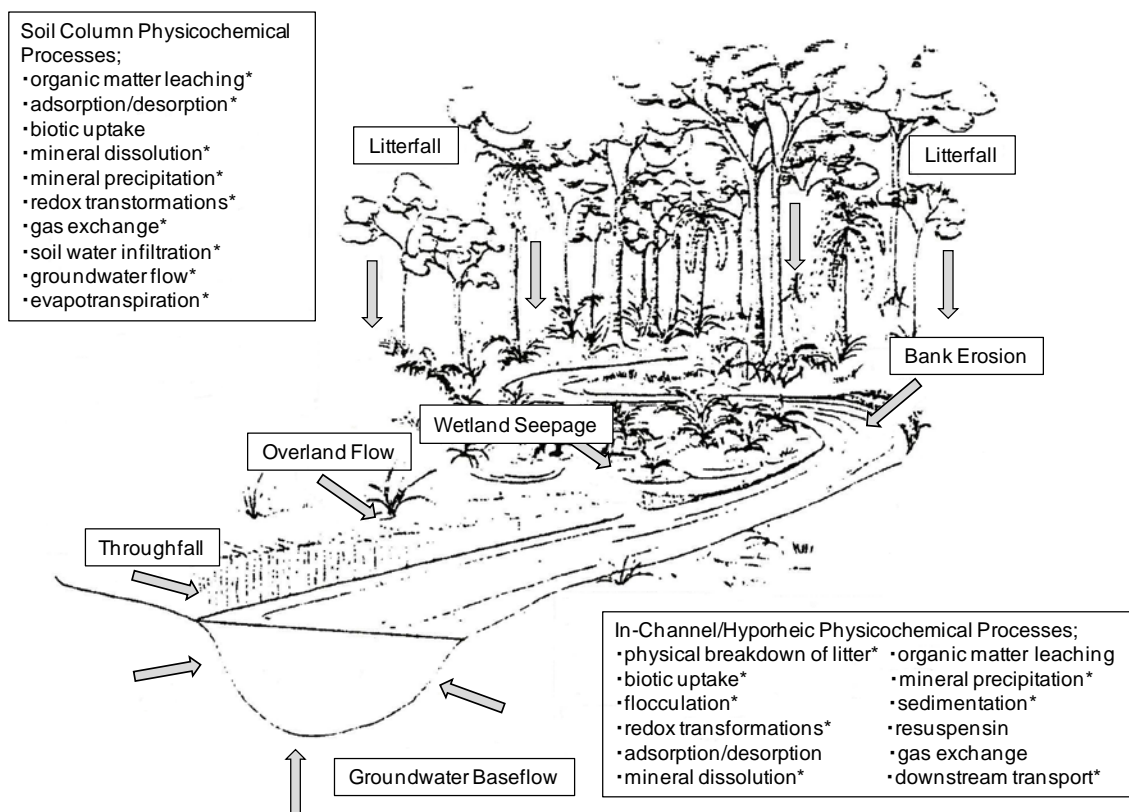


Figure 1.3 The major pathways linking terrestrial and stream ecosystems (Proctor, 2005).

Tropical lowland and montane rainforests differ markedly with respect to their structure and physiognomy (canopy height, leaf mass, dominant leaf size, relative amounts of above- and belowground biomass) as well as their ecological functioning (above- and belowground productivity, transpiration, mineralization of organic matter) (Grubb, 1989; Whitmore, 1998; Bruijnzeel and Veneklaas, 1998; Hafkenscheid, 2000).

With increasing elevation, the stature of the forest decreases and the leaves become smaller, thicker, and harder (more “xeromorphic”) (Grubb, 1989). The reduction in montane forest stature, referred to as “forest stunting” in extreme cases, has received much attention, but the phenomenon is

1. Introduction

not well understood.

In tropical montane forests the N cycle may be restricted by a slower decomposition rate of organic matter that is determined by the relatively low temperatures. Conversely, the N cycle in tropical lowland forests might not be restricted in the same way because of the higher rate of organic matter decomposition that occurs under higher temperatures at the lower elevations (Grubb, 1989). Some studies have estimated that the annual output flux (AOF) of N from tropical montane forests is less than that from tropical lowland forests (Grubb, 1989). However, a review of 25 case studies by Bruijnzeel (1991) found that the AOF of N from tropical montane forests was not necessarily smaller than that from tropical lowland forests. He suggested that the accuracy of previous AOF estimates was limited because the methods used to estimate nutrient AOF varied by site. Schuur (2001) demonstrated that decomposition and N availability is determined by soil water status rather than temperature and that N deficiency leads to tougher leaves that find it harder to decompose.

The literature provides several explanations for the decrease in aboveground net primary productivity and tree stature with increasing elevation in montane forests (Soethe et al. 2008). These include the direct impact of low temperatures on growth (Hoch and Körner, 2003); exposure to strong winds (Lawton, 1982); low rates of photosynthesis due to persistent cloudiness and low radiation input (Bruijnzeel and Veneklass, 1998) or low temperatures; and an increase in rainfall excess due to a change in the relationship between rainfall and streamflow (Kitayama, 1995; Kitayama and Aiba, 2002).

Studies of nutrient cycles in tropical lowland and montane rainforest have focused on sulphur (S), N, P, K, Mg, Ca. *Figure 1.4* shows the S cycle and the flux of S within the environment. Plant requirements for S are closely linked to N availability and growth rate. Adaptive mechanisms exist within plants to optimize supply and demand for S. These range from regulation of uptake and assimilation to modification of growth form (Hawkesford and De Kok, 2007). Data that describe the S cycle and S flux in the tropical rainforest is limited.

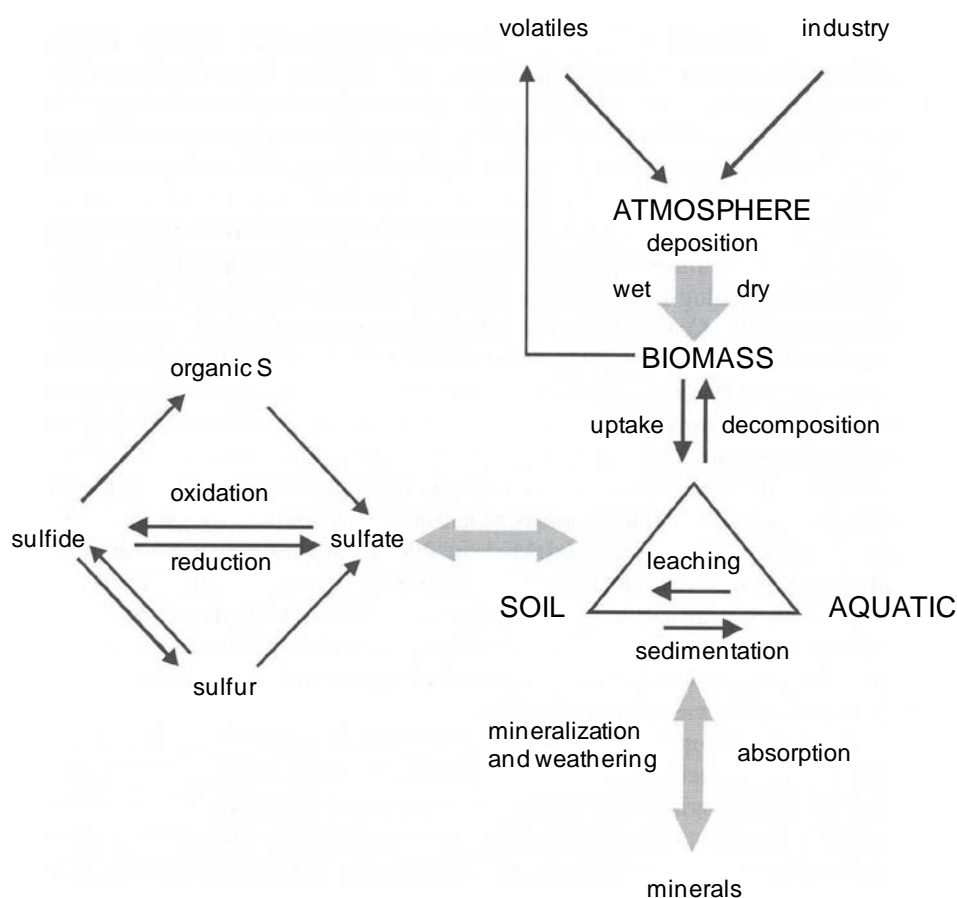


Figure 1.4 The chemical S cycle and fluxes of S within the environment (Hawakesford and De Kok, 2007).

1.5 Streamwater chemistry

The field of tropical forest ecology includes the study of streamwater chemistry. Such studies have typically targeted nutrient cycles and balance (for N, P, K, Mg, and Ca) in tropical forest ecosystems to understand their relationship to tree growth (Bruijnzeel, 1991). Less attention has been paid to other inorganic ions such as chloride (Cl^-), sulfate (SO_4^{2-}), and sodium (Na^+), and only limited consideration has been given to the biogeochemical aspects of ion balance and the relationship between flow volume and solute concentration. Viers et al. (2001) studied the biogeochemical cycle of Cl^- as a tracer of geochemical and hydrological processes in oceanic and continental environments. They reported results for Cl^- , Na^+ , and Ca^{2+} , but not for other ions. Swaine et al. (2006) studied temporal and spatial variations in river conditions and associated river flora in a variety of sites within the forest zone of Ghana. Their results included analyses of inorganic ions, but

1. Introduction

only Cl^- and Ca^{2+} were considered.

In forested areas, natural water chemistry is influenced by the uptake, storage, and release of nutrients by vegetation (Berner and Berner, 1995). *Figure 1.5* shows the biogeochemical cycles that illustrate the interaction of the hydrological cycle with the plant nutrient cycles (Berner and Berner, 1995).

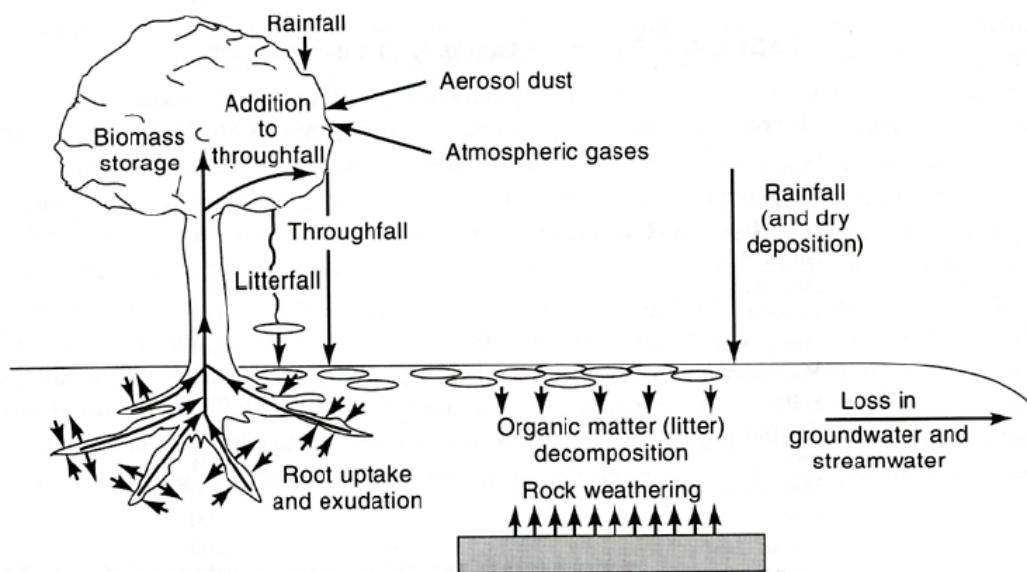


Figure 1.5 Biogeochemical cycling in forests (Berner and Berner, 1995).

For example, Cl^- is an environmental tracer (Leibundgut et al. 2009). Cl^- in rocks are extremely mobile and very soluble. They are not reactive with other ions, do not form complexes, are not greatly absorbed on mineral surfaces, and are not active in the biogeochemical cycle (Berner and Berner, 1995). Natural water chemistry is also affected by the chemical weathering of rocks, which involves several processes that affect the silicate, carbonate, and sulfide minerals.

Recently, a small number of comprehensive watershed studies have been conducted in tropical forests. They examined aspects of ecology, hydrology, and geochemistry. However, few of them were conducted in small sedimentary rock watersheds (the geology of Malaysian Borneo includes tertiary sedimentary rocks, sandstone and mudstone).

A pioneering study by Grip et al. (1994) in Mendolong, Malaysian Borneo, may be the first comprehensive study of two tropical forest watersheds with sedimentary rock. The streamwater chemistry of two soil types was examined, and local differences in the nutrient content of the

bedrock were explained by weathering rates. However, the researchers did not interpret their results by comparing their data with findings from other tropical locations. Zulkifli et al. (2006) conducted a study in Bukit Tarek in Peninsular Malaysia. They examined the pattern of nutrient export in relation to streamflow regimes. The results of these studies together are too diverse to explain the factors that determine the streamwater chemistry of tropical forests on sedimentary rock.

1.6 Objectives of this thesis

The overall goal of my study was to investigate the characteristics of spatial and seasonal variation in rainfall, the ENSO-rainfall relationship, the water and nutrient balances, the difference in water chemistry between tropical montane and lowland forests, and the cause of the streamwater chemistry in Malaysian Borneo.

I collected rainfall data established a series of experimental watersheds and conducted hydrological and hydrochemical observations in Malaysian Borneo.

1.7 Structure of this thesis

Figure 1.6 shows the structure of this thesis.

Chapter 2 describes two study sites located inside the two national parks in Malaysian Borneo.

Chapter 3 discusses the spatial distribution of the seasonal variation in rainfall and the ENSO-rainfall relationship in the two study site (1000×1000 km). The data spanned 20 to 41 years and multiple locations; temporal resolution of daily data was also performed.

Chapter 4 describes the water and nutrient balances at these two sites from 2006 to 2008 and the differences them. The results are compared with data obtained at a number of other locations in tropical rainforests.

Chapter 5 describes the characteristics of inorganic ion concentrations in streamwater in a tropical montane forest and a tropical lowland forest in Malaysian Borneo. By comparing these characteristics with data reported for a number of other tropical forests, this chapter suggests factors that may be responsible for the differences between the two sites.

Chapter 6 describes mechanism that may be responsible for controlling ion concentrations in streamwater. It focuses on spatial and vertical variations in ion concentrations.

Chapter 7 contains the conclusion.

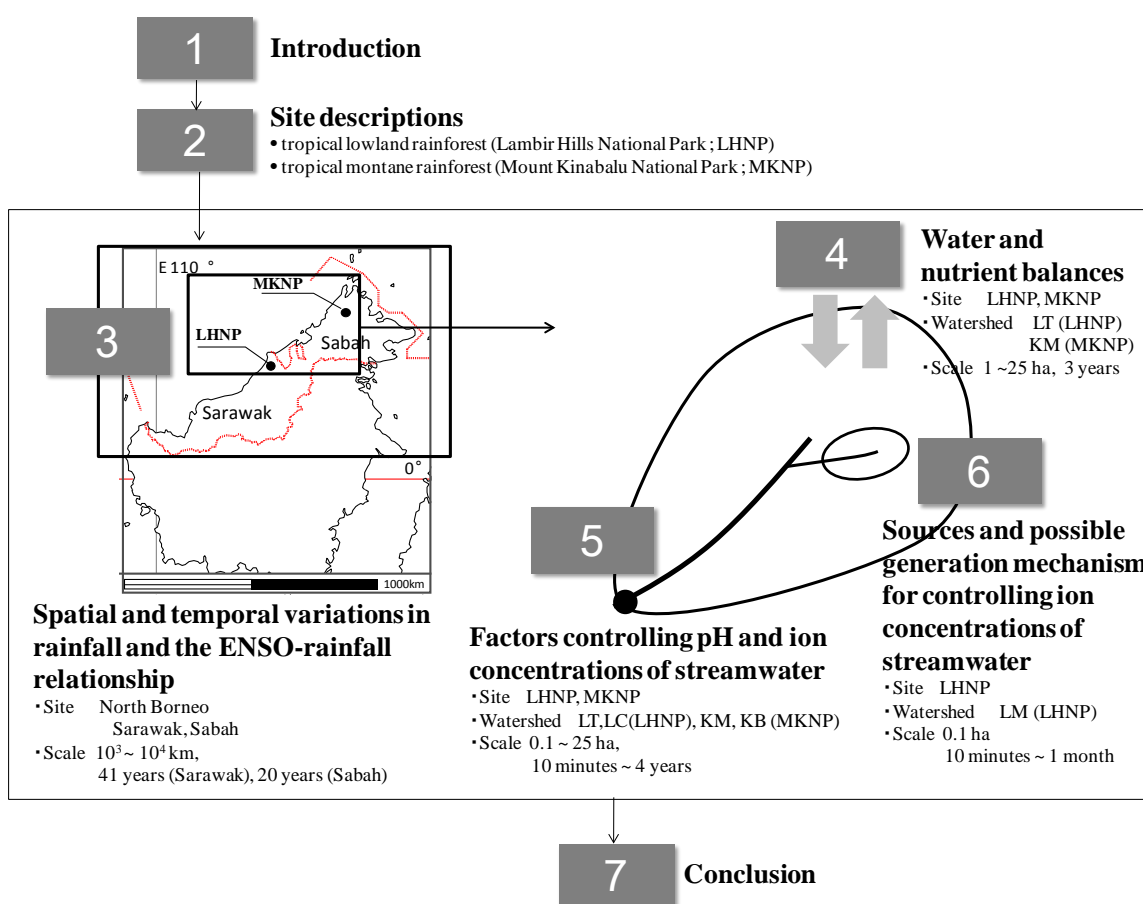


Figure 1.6 The structure of this thesis.

1.8 References

- Andriessse, W., van Mensvoort, M. E. F. 2006. Acid sulfate soils: distribution and extent. In: Lai, R. (Eds.) *Encyclopedia of Soil Science*, 2nd ed. Taylor & Francis, New York, pp. 4-19.
- Arkesteyn, G.J.M.W. 1980. Pyrite oxidation in acid sulphate soils: the role of microorganisms. *Plant and Soil* 54: 119-134.
- Asdak, C., Jarvis, P. G., van Gardingen, P., Fraser, A. 1998. Rainfall interception loss in unlogged and logged forest areas of Central Kalimantan, Indonesia. *Journal of Hydrology* 206: 237–244.
- Attanandana, T., Vacharotayan, S. 1986. Acid sulfate soils: Their characteristics, genesis, amelioration and utilization. *Southeast Asian Studies* 24:154-180.
- Berner, E. K., Berner, R. A. 1995. *Global environment: water, air and geochemical cycles*. Prentice Hall, USA, 376pp.
- Bruijnzeel, L. A. 2004. Hydrological functions of tropical forests : not seeing the soil for the trees? *Agriculture, Ecosystems and Environment* 104:185-228.
- Bruijnzeel, L. A. 2001. Hydrology of tropical montane cloud forests: A Reassessment. *Land Use and Water Resources Research* 1:1-18.
- Bruijnzeel, L. A., Veneklaas, E. J. 1998. Climatological conditions and tropical montane forest productivity : the fog has not lifted yet. *Ecology* 79: 3-9.
- Bruijnzeel, L. A., Waterloo, M. J., Proctor, J., Kuiters, A. T., Kotterink, B. 1993. Hydrological observations in montane rain forests on Gunung Silam, Sabah, Malaysia, with special reference to the ‘Massenerhebung’ effect. *Journal of Ecology* 81:145-167.
- Bruijnzeel, L. A. 1990. *Hydrology of moist tropical forests and effects of conversion: a state of knowledge review*. UNESCO, Paris, and Vrije Universiteit, Amsterdam, The Netherlands, 226pp.
- Brunig, E. F. 1970. On the ecological significance of drought in the equatorial wet evergreen (rain) forest of Sarawak (Borneo). *Aberdeen - Hull Symposia on Malesian Ecology* 1 : 66-96.
- Brunig, E. F. 1969. On the seasonality of droughts in the lowlands of Sarawak (Borneo). *Erdkunde* 23 : 127-133.
- Chang, C. P., Wang, Z., Ju, J., Li, T. 2004. On the relationship between western maritime continent monsoon rainfall and ENSO during northern winter. *Journal of Climate* 17: 665-672.

1. Introduction

- Chang, J. H., Lau, L. S. 1993. Definition of the humid tropics. In : Bonell, M., Hufschmidt, M. M., Gladwell, J. S. (Eds.). *Hydrology and water management in the humid tropics*, UNESCO - Cambridge University Press, Cambridge, pp. 571-574.
- Chappell, N. A., Sherlock, M.D. 2005. Contrasting flow pathways within tropical forest slopes of Ultisol soil. *Earth Surface Processes and Landforms* 30: 735–753.
- Chappell, N. A., Franks, S. W., Larenus, J. 1998. Multi-scale permeability estimation for a tropical catchment. *Hydrological Processes* 12:1507-1523.
- Douglas, I., Spencer, T., Greer, T., Bidin, K., Sinun, W., Wong, W.M. 1992. The impact of selective commercial logging on stream hydrology, chemistry and sediment loads in the Ulu Segama rain forest, Sabah. *Philosophical Transactions of the Royal Society B*335: 397–406.
- Dykes, A. P. Thornes, J. B. 2000. Hillslope hydrology in tropical rainforest steplands in Brunei. *Hydrological Processes* 14; 215–235.
- Dykes, A. P. 1997. Rainfall interception from a lowland tropical rainforest in Brunei. *Journal of Hydrology* 200: 260–279.
- Elsenbeer, H. 2001. Hydrologic flowpaths in tropical rainforest soilscaapes-a review. *Hydrological Processes* 15:1751-1759.
- Elsenbeer, H., Newton, B. E., Dunne, T., de Moraes, J. M. 1999. Soil hydraulic conductivities of latosols under pasture, forest, and teak in Rondonia, Brazil. *Hydrological Processes* 13:1417-1422.
- Fleischbein, K., Wilcke, W., Valarezo, C., Zech, W., Knoblich, K. 2006. Water budgets of three small catchments under montane forest in Equador : experimental and modeling approach. *Hydrological Processes* 20:2491-2507.
- Fleischbein, K., Wilcke, W., Valarezo, C., Zech, W., Knoblich, K. 2006. Water budgets of three small catchments under montane forest in Equador : experimental and modeling approach. *Hydrological Processes* 20:2491-2507.
- Fleischbein, K., Wilcke, W., Goller, R., Boy, J., Valarezo, C., Zech, W. 2005. Rainfall interception in a lower montane forest in Equador : effects of canopy properities. *Hydrological Processes* 19:1355-1371.
- Golley, F. B., McGinnis, J. T., Clements, R. G., Child, G. I., Duever, M. J. 1983. *Mineral Cycling in*

1. Introduction

- a Tropical Moist Forest Ecosystem*. University of Georgia Press, Athens, 248pp.
- Gomyo, M., and Kuraji, K. 2009. Spatial and temporal variations in rainfall and the ENSO-rainfall relationship over Sarawak, Malaysian Borneo. *SOLA* 5:41–44.
- Grip, H., Malmer, A., Wong, F. K. 1994. Converting tropical rain forest to forest plantation in Sabah, Malaysia. Part I. Dynamics and net losses of nutrients in control catchments in control catchment streams. *Hydrological Processes* 8: 179-194.
- Grubb, P. J. 1989. The role of mineral nutrients in the tropics: a plant ecologist's view. In: Proctor, J. (Eds.). *Mineral Nutrients in Tropical Forest and Savanna Ecosystems*, Special publications series of the British ecological society 9, pp.417-437.
- Hafkenscheid, R. L. L. J. 2000. *Hydrology and biogeochemistry of tropical montane rain forests of contrasting stature in the Blue Mountains, Jamaica*. PhD Thesis, VU University Amsterdam, Amsterdam, The Netherlands. 302pp.
- Hamada, J.I., Yamanaka, M.D., Matsumoto, J., Fukao, S., Winarso, P.A., Sribimawati, T. 2002. Spatial and temporal variations of the rainy season over Indonesia and their link to ENSO. *Journal of the Meteorological Society of Japan* 80 : 285-310.
- Hans, P. H., Abang, K. A. M. 2001. Sarawak's physical environment : Climate, Geology and Soils. In : Hazebroek, H. P. Abang Kashim, A. M. (Eds.). *National Parks of Sarawak*, pp.9-16.
- Haraguchi, A. 2007. Effect of sulfuric acid discharge on river water chemistry in peat swamp forests in central Kalimantan, Indonesia. *Limnology* 8:175-182.
- Harrison, R. D. 2005. A severe drought in Lambir Hills National Park. In : Roubik, D. W., Sakai, S. Hamid, A. A. (Eds.). *Pollination Ecology and the Rain Forest*, Ecological Studies 174, pp.51-64.
- Hawkesford, M. J., De Kok, L. J. 2007. *Sulfur in Plants An Ecological Perspective*. Springer, The Netherlands, 264pp.
- Haylock, M., McBride, J. 2001. Spatial coherence and predictability of Indonesian wet season rainfall. *Journal of Climate* 14: 3882-3887.
- Hendon, H. 2003. Indonesia rainfall variability: Impacts of ENSO and local air–sea interaction. *Journal of Climate* 16: 1775-1790.
- Hoch, G., Körner, C. 2003. The carbon changing of pines at the climatic treeline : a global comparison. *Oecologia* 135:10-21.

1. Introduction

- Holwerda, F. 2005. *Water and Energy Budgets of Rain Forests along an Elevational Gradient under Maritime Tropical Conditions*. PhD Thesis, VU University Amsterdam, Amsterdam, The Netherlands. 168pp.
- Hooijer, A. 2005. Hydrology of tropical wetland forests : recent research results from Sarawak peat swamps. In : Bonell, M., Bruijnzeel, L. A. (Eds.), *Forest, Water and People in the Humid Tropics*, UNESCO – Cambridge University Press, Cambridge, pp.447-461.
- Idris, M. H., Kuraji, K., Suzuki, M. 2005. Evaluating vegetation recovery following large-scale forest fires in Borneo and northeastern China using multi-temporal NOAA/AVHRR images. *Journal of Forest Research* 10:101-111.
- Jordan, C. 1985. *Nutrient cycling in tropical forest ecosystems*. John Wiley & Sons, 190pp.
- Jordan, C., Herrera, R. 1981. Tropical rain forests: are nutrients really critical? *American Naturalist* 117:167-180.
- Juneng, L., Tangang, F.T. 2005. Evolution of ENSO-related rainfall anomalies in Southeast Asia region and its relationship with atmosphere–ocean variations in Indo-Pacific sector. *Climate Dynamics* 25: 337-350.
- Kato, M., Inoue, T., Hamid, A.A., Nagamitsu, T., Merdek, M.B., Nona, A.R., Itino, T., Yamane, S., Yumoto, T. 1995. Seasonality and vertical structure of light-attracted insect communities in a dipterocarp forest in Sarawak. *Researches on Population Ecology* 37 : 59-79.
- Kitayama, K., Aiba, S. 2002. Ecosystem structure and productivity of tropical rain forests along altitudinal gradients with contrasting soil phosphorus pools on Mount Kinabalu, Borneo. *Journal of Ecology* 90:37-51.
- Kitayama, K., Mueller-Dombois, D., Vitousek, P. M. 1995. Primary succession of Hawaiian montane rain forest on a chronosequence of eight lava flows. *Journal of Vegetation Science* 6:211-222.
- Köppen, W. 1936. Das geographische System der Klimate. In: Köppen, W. and Geiger, R. (Eds), *Handbuch der Klimatologie*, Gebrüder Borntraeger, Berlin, 46pp.
- Kumagai, T., Saitoh, T. M., Sato, Y., Takahashi, Y., Manfroi, O. J., Morooka, T., Kuraji, K., Suzuki, M., Yasunari, T., Komatsu, H. 2005. Annual water balance and seasonality of evapotranspiration in a Borneo tropical rainforest. *Agricultural and Forest Meteorology* 128 : 81-92.

1. Introduction

- Kume, T., Manfroi, O. J., Kuraji, K., Tanaka, N., Horiuchi, T., Suzuki, M., Kumagai, T. 2008. Estimation of canopy water storage capacity from sap flow measurements in a Bornean tropical rainforest. *Journal of Hydrology* 352: 288–295.
- Kuraji, K. 2005. Comments on “Nighttime CO₂ flux over a Bornean tropical rainforest.” *Journal of Japan Society of Hydrology & Water Resources* 18: 321 (in Japanese with English abstract).
- Kuraji, K. 2004. Hydrological characteristics of small watersheds in Sabah: hill dipterocarp forest in Sapulut and Macaranga forest in Ulu Kalumpang. In: Sidle, R. C., Tani, M., Abdul Rahim, A.N., Twodros (Eds.), *Forests and Water in Warm, Humid Asia, Proceedings, 2004 IUFRO Forest Hydrology Workshop (Kota Kinabalu)*, IUFRO, Malaysia, pp: 57–60.
- Leibundgut, C., Maloszewski, P., Külls, C. 2009. *Tracers in Hydrology*. Wiley-Brackwell, UK, 415pp.
- Lesack, L. F. W. 1993. Export of nutrients and major ionic solutes from a rain forest catchment in the central Amazon basin. *Water Resources Research* 29: 743–758.
- Longman Malaysia. 1989. *Kajian Atlas KBSM Tingkatan 1*, Longman Malaysia Sdn. Bhd, 29pp.
- MacKinnon, K., Hatta, G., Halim, H., Mangalik, A. 1996. *The ecology of Kalimantan*. Periplus Editions, Singapore, 802pp.
- Malmer, A. 2004. Streamwater quality as affected by wild fires in natural and manmade vegetation in Malaysian Borneo. *Hydrological Processes* 18: 853–864.
- Malmer, A. 1993. *Dynamics of hydrology and nutrient losses as response to establishment of forest plantation, A case study on tropical rainforest land in Sabah, Malaysia*. Thesis, Department of Forest Ecology, Umeå, Sweden, 182pp.
- Malmer, A. 1992. Water-yield changes after clear-felling tropical rainforest and establishment of forest plantation in Sabah, Malaysia. *Journal of Hydrology* 134:77-94.
- Manfroi, O. J., Kuraji, K., Suzuki, M., Tanaka, N., Kume, T., Nakagawa, M., Kumagai, T., Nakashizuka, T. 2006. Comparison of conventionally observed interception evaporation in a 100-m² subplot with that estimated in a 4-ha area of the same Bornean lowland tropical forest. *Journal of Hydrology* 329: 329-349.
- Manfroi, O.J., Kuraji, K., Tanaka, N., Suzuki, M., Nakagawa, M., Nakashizuka, T., Chong, L. 2004. The stemflow of trees in a Bornean lowland tropical forest. *Hydrological Processes* 18:2455-2474.

1. Introduction

- McJannet, D., Wallace, J., Fitch, P., Disher, M., Reddell, P. 2007. Water balance of tropical rainforest canopies in north Queensland, Australia. *Hydrological Processes* 21: 3473-3484.
- Nortcliff, S., Thornes, J. B. 1989. Variations in soil nutrients in relation to soil moisture status in a tropical forested ecosystem. In: Proctor, J. (ed.) *Mineral Nutrients in Tropical Forest and Savanna Ecosystems*. Blackwell, Oxford. pp.43-54.
- Penerbit Fajar Bakti Sdn. Bhd. 2001. *Atlas Informatid KBSR*. Kum-Vivar Printing Sdn, Bhd, pp.96.
- Phillips, V. D. 1998. Peatswamp ecology and sustainable development in Borneo. *Biodiversity and Conservation* 7:651-671.
- Phua, M. H., Tsuyuki, S., Lee, J. S., Sawakawa, H. 2007. Detection of burned peat swamp forest in a heterogeneous tropical landscape: A case study of the Klias Peninsula, Sabah, Malaysia. *Landscape and Urban Planning* 82:103-116.
- Proctor, J. 2005. Rainforest mineral nutrition: the 'black box' and a glimpse inside it. In: Bonell, M., Bruijnzeel, L. A. (Eds). *Forest, Water and People in the Humid Tropics*, Cambridge University Press, pp.422-446.
- Proctor, J. 1989. *Mineral Nutrients in Tropical Forest and Savanna Ecosystems, Special publications series of the British ecological society* 9. Blackwell Scientific Publications, Oxford, London, 473pp.
- Sakai, S., Momose, K., Yumoto, T., Nagamitsu, T., Nagamasu, H., Abang, A. H., Nakashizuka, T. 1999. Plant reproductive phenology over four years including an episode of general flowering in a lowland dipterocarp forest, Sarawak, Malaysia. *American Journal of Botany* 86(10) : 1414-1436.
- Salafsky, N. 1998. Drought in the rain forest, Part II, An update based on the 1994 ENSO event. *Climatic Change* 39: 601-603.
- Salafsky, N. 1994. Drought in the rain forest: Effects of the 1991 El Nino-Southern Oscillation event on a rural economy in west Kalimantan, Indonesia. *Climatic Change* 27 : 373-396.
- Schuur, E. A. G. 2001. The effect of water on decomposition dynamics in mesic to wet Hawaiian montane forests. *Ecosystems* 4:259-273.
- Soethe, N., Lehmann, J., Engels, C. 2008. Nutrient availability at different altitudes in a tropical montane forest in Ecuador. *Journal of Tropical Ecology* 24:397-406.
- Swaine, M. D., Adomako, J., Ameka, G., de Graft-Johnston, K.A.A., Cheek, M. 2006. Forest river

1. Introduction

- plants and water quality in Ghana. *Aquatic Botany* 85: 299–308.
- Tangang, F. T., Juneng, L., Bahari, A. 2006. The covariability between anomalous northeast monsoon rainfall in Malaysia and sea surface temperature in Indian-Pacific sector: a singular value decomposition analysis approach. Symposium on Asia Monsoon Winter MONEX Abstracts, 33-37.
- Turner, E. C., Foster, W. A. 2009. The impact of forest conversion to oil palm on arthropod abundance and biomass in Sabah, Malaysia. *Journal of Tropical Ecology* 25:23-30.
- Vernimmen, R. R. E., Bruijnzeel, L.A., Romdoni, A., Proctor, J. 2007. Rainfall interception. I. Three contrasting lowland rain forest types in Central Kalimantan, Indonesia. *Journal of Hydrology* 340: 217–232.
- Viers, J., Dupre, B., Braun, J. J., Freydier, R., Greenberg, S., Ngoupayou, J. N., Nkamdjou, L. S. 2001. Evidence for non-conservative behavior of chlorine in humid tropical environments. *Aquatic Geochemistry* 7: 127–154.
- Vitousek, P. M., Sanford, R. L. 1986. Nutrient cycling in moist tropical forest. *Annual Review of Ecology and Systematics* 17: 137-167.
- Wahid, M. B., Abdullah, S. B. A., Henson, I. E. 2005. Oil palm-achievements and potential. *Plant Production Science* 8:288-297.
- Walsh, R. P. D., Newberry, D. M. 1999. The ecoclimatology of Danum, Sabah, in the context of the world's rainforest regions with particular reference to dry periods and their impact. In : Newbery, D. M., Clutton-Brock, T. H., Prance, G. T. (Eds.). *Changes and Disturbance in Tropical Rainforest in South-East Asia*, Philosophical Transactions of the Royal Society London B354 : 1869-1883.
- Whitmore, T. C. 1998. *An introduction to tropical rain forest*. 2nd ed., Clarendon Press, Oxford. 282pp.
- Yamakura, T., Kanzaki, M., Itoh, A., Ohkubo, T., Ogino, K., Ernest, C., Lee, H. S., Ashton, P. S. 1995. Topography of a large-scale research plot established within a tropical rain forest at Lambir, Sarawak. *Tropics* 5:41–56.
- Zulkifli, Y., Douglas, I., Nik, A. R. 2006. Export of dissolved and undissolved nutrients from forested catchments in Peninsular Malaysia. *Forest Ecology and Management* 224: 26–44.

Chapter 2

Site descriptions

The two study sites were located inside the two national parks in Malaysian Borneo (*Figure 2.1*), the Lambir Hills National Park (LHNP) in Sarawak and the Mount Kinabalu National Park (MKNP) in Sabah.

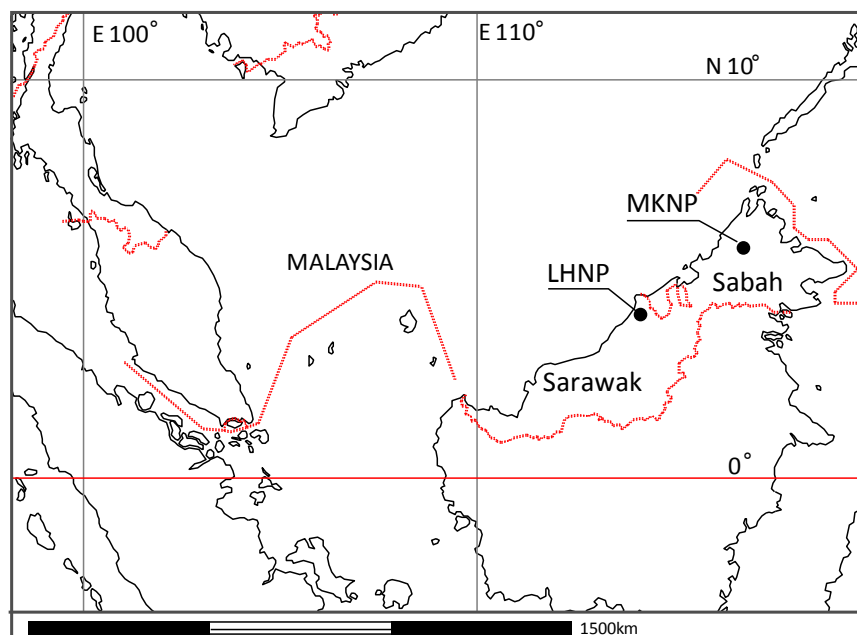


Figure 2.1 Map showing the study sites.

Chapter 3 analyzes the rainfall characteristics and the ENSO-rainfall relationship for Sarawak and Sabah. Chapter 4 describes how water and nutrient balances were examined in the Tower Large (LT) watershed in LHNP and the Mempening (KM) watershed in MKNP. Chapter 5 describes how streamwater chemistry was examined in the LT and Crane Large (LC) watersheds in LHNP and the KM and Bukit Ular (KB) watersheds in MKNP. Chapter 6 describes how the mechanisms responsible for generating streamwater chemistry were identified in Crane Micro (LM)

2. Site descriptions

a micro watershed located in LC.

2.1 Lambir Hills National Park site

2.1.1 Location

Situated about 25 km southwest of Miri, an eastern city of Sarawak, LHNP encompasses an area of 6,949 ha (Ishizuka et al. 1998). The distance from the nearest coast is 13.7 km, and the highest peak of LHNP is Lambir Hill (465 m above sea level). Hereafter, I refer to this site as site LHNP.

2.1.2 Climate

Rainfall at Miri has obvious seasonal fluctuation (Gomyo and Kuraji, 2006). In LHNP, annual mean temperature for the 8 years from 2000 to 2007 and rainfall for the 9 years from 2000 to 2008 were 25.9°C and 2650 mm, respectively (*Table 2.1*). Micrometeorological and hydrological research has been conducted in LHNP, including studies of rainfall interception (Manfroi et al. 2006), transpiration (Kumagai et al. 2004), and water balance (Kumagai et al. 2005). Stream flow sometimes ceases during dry spells (a period of 30 days with less than 100 mm rainfall). This region has been identified as the most vulnerable to El Niño-induced droughts in Sarawak (Gomyo and Kuraji, 2009). Dry spells have been observed frequently in February and March, but rarely from October to December (Kuraji, 2005).

Table 2.1 Weather stations and watershed descriptions in LHNP.

Site name	Weather station					Experimental watershed				
	Location	Distance from the nearest coast (km)	Elevation (m.a.s.l.)	Annual mean rainfall (mm)	Annual mean air temperature (°C)	Name	Area (ha)	Geology	Soil (USDA)	Vegetation
Lambir Hills (LHNP)	4°20'N, 113°50'E	13.7	200	2,650 (2000-2008)	25.9 (2000-2007)	Tower Large (LT)	23.25	Tertiary sedimentary rocks, Sandstone and mudstone	Ultisol	Dipterocarpaceae
						Crane Large (LC)	21.97			
						Crane Micro (LM)	0.59			

2.1.3 Geology and lithology

The bedrock of LHNP is predominantly sandstone and is considered transitional between

2. Site descriptions

the predominantly sandstone Lambir Formation and the predominantly shale Setap Formation (Ashton, 1998; Hutchison, 2005). According to Hazebroek and Abang Kashim (2001), thin beds of limestone near the base of the hills contain tiny fossils (foraminifera and nanoplankton) that suggest an age between 6 and 13 million years old (Middle and Late Miocene). The sea probably reached its greatest depth near Lambir about 12.8 million years ago, as shown by the concentration of fossils in massive blue claystones, which is thought to represent a peak in the abundance and diversity of the animals living in, on, and above the sea bed. Sandstone and mudstone accumulated and consolidated to form a considerable thickness of about 2,100 m of rocks, together forming the Lambir Formation. In the northern part of LHNP, the sands and clays are poorly consolidated. The sandstone is soft and medium grained (Yamakura et al. 1995), which often also forms thin layers of lignite (a brownish-black, poor-quality coal that originates from peat). These rocks are part of the Tukau Formation (Hazebroek and Abang Kashim, 2001). Lambir's rocks were uplifted and gently folded about 1.6 million years ago at the onset of the Pleistocene (Wilford, 1961).

2.1.4 Watersheds and soils

Two experimental watersheds, named Tower Large (LT), Crane Large (LC) and Crane Micro (LM) in LC were used in this study (*Figure 2.2*). The elevations of the lowest points of LT, LC and LM are 90.4, 176.4 and 190 m above sea level, respectively. Whereas LC has gentle topography, LT is more rugged and includes several waterfalls and exposed mutual strata.

Mudstone appears in these places and may include pyrite (Potter et al. 2005). No reports have indicated the presence of gypsum at LHNP or of any hydrothermal activity in the system. Soils at LHNP have been identified as mainly clay udult ultisols over shale, with the rest on sandy humults ultisols (Hazebroek and Abang Kashim, 2001). Other soils include immature alluvial soils around river banks, red-yellow podsols (ultisols) on slopes and ridges, podsols around the hill summit of Bukit Lambir, and immature regosols on very steep slopes (Yamakura et al. 1995; Baille et al. 2006).

2. Site descriptions

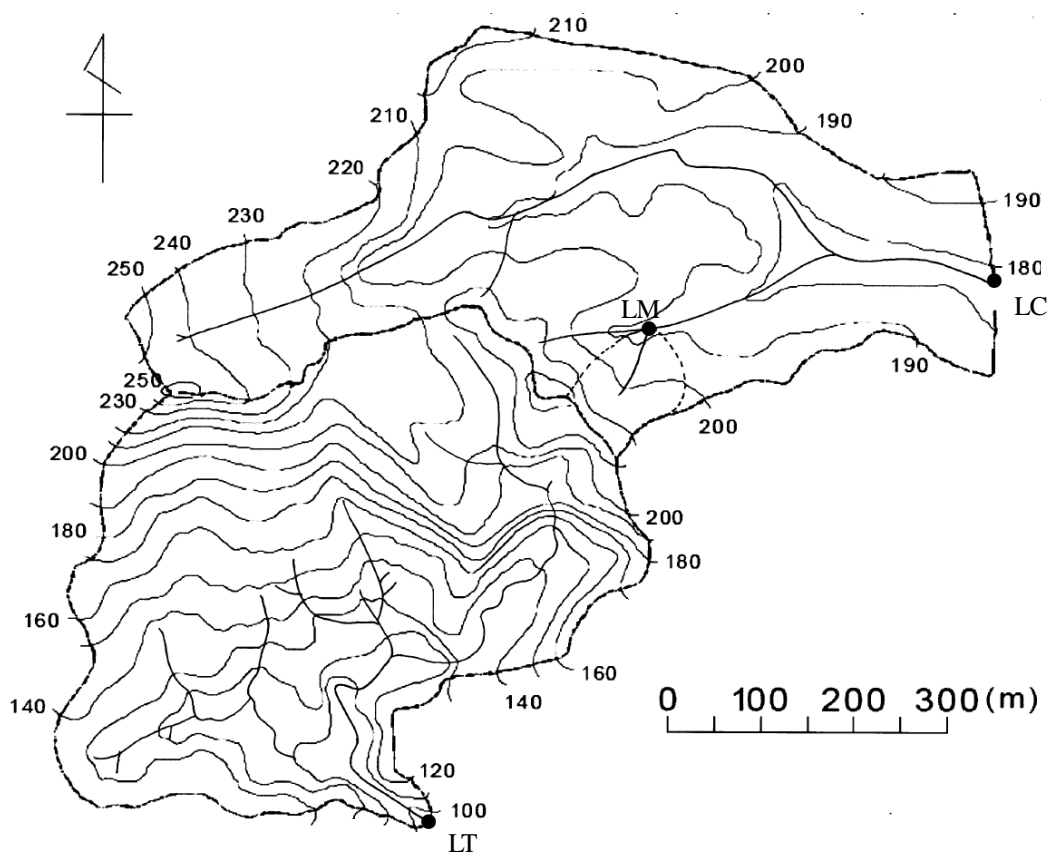


Figure 2.2 Location and topography of the LT, LC and LM watersheds in LHNP based on the map (Wakahara and Siraki, *per.com.*).

2.1.5 Vegetation

The forest in LHNP consists of two types of indigenous vegetation common throughout Borneo: mixed dipterocarp forest and tropical heath forest (Yamakura et al. 1995; Ashton, 1998; Potts et al. 2002). The study site was established within the mixed dipterocarp forest, where red-yellow podzols (ultisols) are the predominant soils. In the LT plot there were 53 families, 134 genera, and 404 species; in the LC plot there were 60 families, 195 genera, and 590 species (Nakagawa, *per.com.*).

2.2 Mount Kinabalu National Park site

2.2.1 Location

Encompassing 75,400 ha, MKNP is situated approximately 50 km east of Kota Kinabalu (KK), the capital city of the state of Sabah, which contains Mount Kinabalu (4,095.2 m above sea level), the highest peak in Southeast Asia. The distance from the nearest coast is 44.5 km. The study site consisted of two experimental watersheds, one of the four weather stations in MKNP (Kitayama et al. 1999), and a rainwater sampling point, located near the park headquarters (6°01'N, 116°32'E, 1,560 m a.s.l.). Hereafter, I refer to this site as site MKNP.

2.2.2 Climate

The annual rainfall observed at site MKNP is normally around 3,000 mm, but it was extraordinarily low in 1997 and 1998 (*Table 2.2*), which were years associated with El Niño events (Malmer, 2004; Walsh and Newberry, 1999). The mean annual air temperature at site MKNP is normally around 18°C, but slightly higher values were recorded in 1997 and 1998 (*Table 2.2*).

Table 2.2 Weather stations and watersheds description in MKNP

Site name	Weather station				Experimental watershed					
	Location	Distance from the nearest coast (km)	Elevation (m.a.s.l.)	Annual mean rainfall (mm)	Annual mean air temperature (°C)	Name	Area (ha)	Geology	Soil (USDA)	Vegetation
Mount Kinabalu (MKNP)	6°01'N, 116°32'E	44.5	1560	1709 (1997-1998)	18.6 (1997-1998)	1.78	1697.7	Tristaniaopsis, Dacrycarpus, Podocarpus	Spodosol	Tertiary sedimentary rocks
				3168 (1996, 1999-2008)	17.2 (1996, 1999-2008)	4.06	1866.8	Lithocarpus, Syzygium, Madhuca	Inceptisol	Tertiary sedimentary rocks accumulated by the collapse occurred in Quaternary

2.1.3 Geology and lithology

The oldest rocks are upfaulted slices of crystalline basement of Mesozoic or earlier age. These sedimentary rocks (Trusmadi and Crocker Formations) were intensely folded in an orogeny that culminated in the middle Miocene. Ultrabasic intrusive rocks were upfaulted at this time. The Mount Kinabalu intrusion is a pluton composed mainly of hornblende adamellite that was emplaced diapirically into the complex of older rocks. It is part of a large batholith underlying the area and was

2. Site descriptions

emplaced 9 million years ago. The central part of the batholith was probably uplifted by faulting in the lower Pleistocene to form the present mountain (Jacobson, 1970; Hutchison, 2005).

In MKNP, dark colored argillaceous rocks predominate and are either thick-bedded or interbedded with thin sandstone and siltstone beds. Cataclasites are commonly developed, and some crush conglomerate is present. A few thick sandstone beds occur, as do isolated exposures of volcanic rocks. Limestone has not been found. Quartz veining is widespread in the Trusmadi Formation rocks (Jacobson, 1970).

2.2.4 Watersheds and soils

Two experimental watersheds, named Mempening (KM) and Bukit Ular (KB), were used in this study (*Figure 2.3 and 2.4*). The KM watershed is located on soils derived from old sedimentary rocks folded in the Tertiary period (Kitayama et al. 2004). The KB watershed is located on soils derived from colluvial deposits passed down from upper elevations in the early Quaternary period (approximately 30,000 to 40,000 years ago) (Kitayama et al. 2004). The elevations of the lowest points of KM and KB are 1,697.7 and 1,866.8 m above sea level, respectively. Both sites are located within the same vegetation zone and have comparable climate and parent rocks, but they are of different ages (Kitayama et al. 2004). As a consequence, the soil of KB did not show horizonation, whereas KM soils appeared to be at a more advanced stage of soil development and were classified as spodosols (Kitayama et al. 2004).

2. Site descriptions

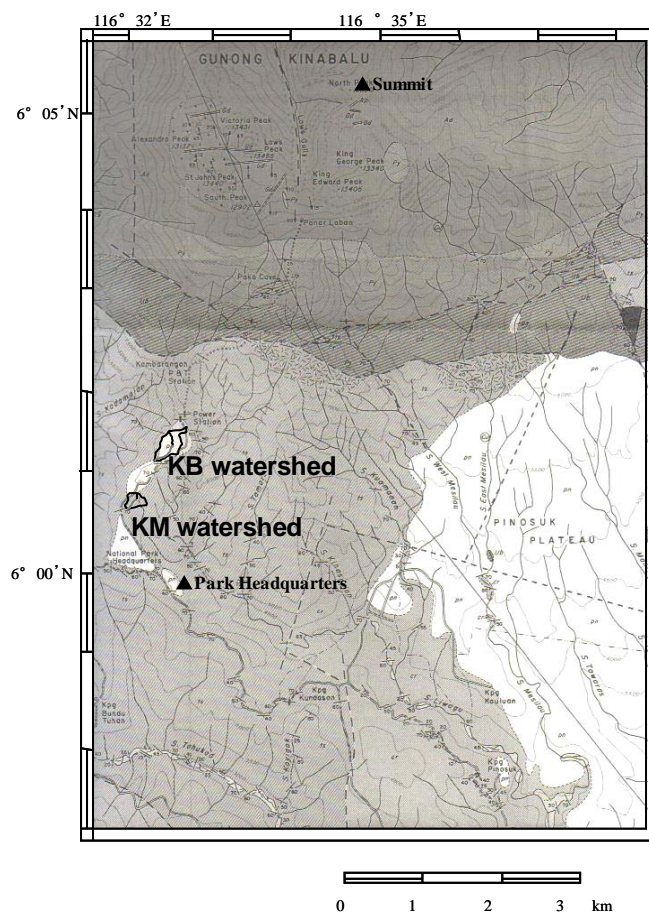


Figure 2.3 Location of two watersheds based on the map in Jacobson (1970). Climate station is located near the park headquarters.

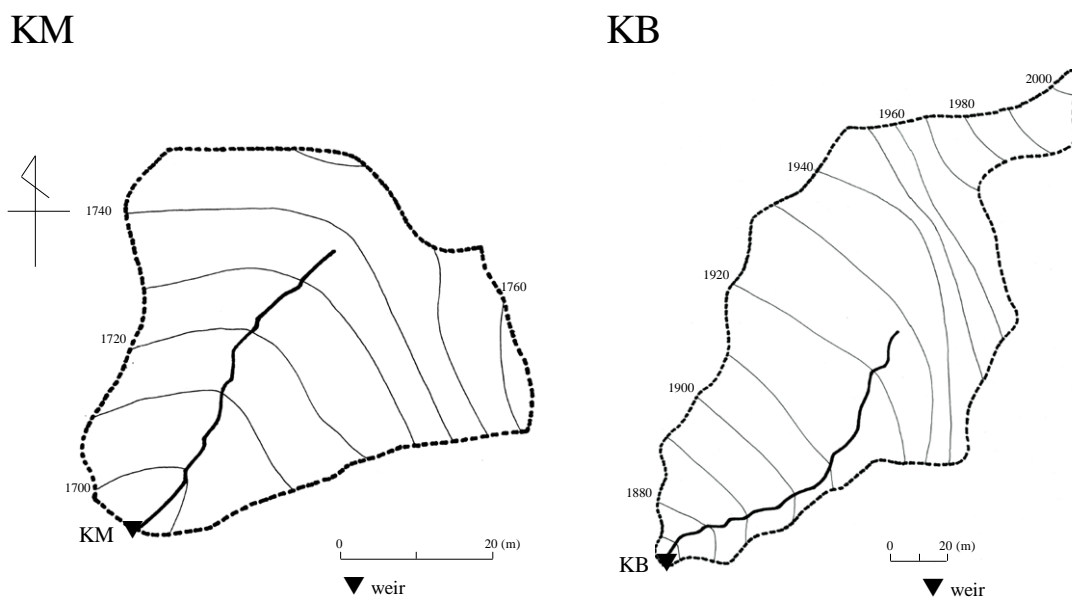


Figure 2.4 Location and topography of KM and KB watersheds in MKNP.

2. Site descriptions

Vegetation

The floristic composition and abundance of canopy tree species were considerably different at KM and KB (Takyu et al. 2002). Notably, *Tristaniopsis* (Myrtaceae) and coniferous *Dacrycarpus* and *Dacrydium* (Podocarpaceae) were abundant at KM, but these species did not occur (or were only minor) at KB (Kitayama et al. 2004). Species of *Lithocarpus* (Fagaceae), *Syzygium* (Myrtaceae), and *Madhuca* (Sapotaceae) dominated at KB, whereas the same species occurred at KM with lesser abundance. Therefore, more site-specific species dominated the older KM (Kitayama et al. 2004).

2.3 References

- Ashton, P.S., 1998. Lambir's forest: The world's most diverse known tree assemblage? In: Roubik, D.W., Sakai, S., Abang Hamid, A.K. (Eds.), *Pollination Ecology and the Rain Forest Sarawak Studies*, Ecological Studies 174: 191–216.
- Baillie, I. C., Ashton, P. S., Chin, S. P., Davies, S. J., Palmiotto, P. A., Russo, S. E., Tan, S., 2006. Spatial associations of humus, nutrients and soils in mixed dipterocarp forest at Lambir, Sarawak, Malaysian Borneo. *Journal of Tropical Ecology* 22: 543–553.
- Gomyo, M., Kuraji, K. 2006. Spatial distribution of seasonal variation in rainfall in the state of Sarawak, Malaysia. *Journal of Japan Society of Hydrology & Water Resources* 19: 128-138. (in Japanese with English abstract).
- Hazebroek, H.P., Abang Kashim, A.M. 2001. National Parks of Sarawak. Natural History Publications (Borneo), Kota Kinabalu, 502pp.
- Hutchison, C. S. 2005. *Geology of North-West Borneo Sarawak, Brunei and Sabah*. Elsevier, London. 421pp.
- Ishizuka, S., Tanaka, S., Sakurai, K., Hirai, H., Hirotani, H., Ogino, K., Lee, H. S., Kendawang, J. J., 1998. Characterization and distribution of soils at Lambir Hills National Park in Sarawak, Malaysia, with special reference to soil hardness and soil texture. *Tropics* 8: 31–44.
- Jacobson, G., 1970. *Gunung Kinabalu Area, Sabah, Malaysia*. Geological Survey Malaysia, Report 8 (with a colored geological map on a scale of 1:500,000). Kuching (Malaysia): Geological Survey Malaysia, 111pp.
- Kitayama, K., Aiba, S., Takyu, M., Majalap, N., Wagai, R. 2004. Soil phosphorus fractionation and

2. Site descriptions

- phosphorus-use efficiency of a Bornean tropical montane rain forest during soil aging with podzolization. *Ecosystems* 7: 259–274.
- Kitayama, K., Maklarin, L., Mohd, Z. W. 1999. Climate profile of Mount Kinabalu during late 1995–early 1998 with special reference to the 1998 drought. *Sabah Parks Nature Journal* 2: 85–100.
- Kumagai, T., Saitoh, T. M., Sato, Y., Takahashi, Y., Manfroi, O. J., Morooka, T., Kuraji, K., Suzuki, M., Yasunari, T., Komatsu, H. 2005. Annual water balance and seasonality of evapotranspiration in a Borneo tropical rainforest. *Agricultural and Forest Meteorology* 128 : 81-92.
- Kumagai, T., Saitoh, T., Sato, Y., Morooka, T., Manfroi, O.J., Kuraji, K. and Suzuki, M. 2004. Transpiration, canopy conductance and the decoupling coefficient of a lowland mixed Dipterocarp forest in Sarawak, Borneo: dry spell effects. *Journal of Hydrology* 287: 237-251.
- Kuraji, K. 2005. Comments on “Nighttime CO₂ flux over a Bornean tropical rainforest.” *Journal of Japan Society of Hydrology & Water Resources* 18: 321 (in Japanese with English abstract).
- Malmer, A. 2004. Streamwater quality as affected by wild fires in natural and manmade vegetation in Malaysian Borneo. *Hydrological Processes* 18: 853–864.
- Manfroi, O. J., Kuraji, K., Suzuki, M., Tanaka, N., Kume, T., Nakagawa, M., Kumagai, T., Nakashizuka, T. 2006. Comparison of conventionally observed interception evaporation in a 100-m² subplot with that estimated in a 4-ha area of the same Bornean lowland tropical forest. *Journal of Hydrology* 329: 329-349.
- Potter, P.E., Maynard, J.B., Deoetris, P.J. 2005. *Mud and mudstones: introduction and overview*. Springer, 297pp.
- Potts, M. D., Ashton, P. S., Kaufman, L. S., Plotkin, J. B. 2002. Habitat patterns in tropical rain forests: A comparison of 105 plots in northwest Borneo. *Ecology* 83: 2782-2797.
- Takyu, M., Aiba, S., Kitayama, K. 2002. Effects of topography on tropical lower montane forests under different geological conditions on Mount Kinabalu, Borneo. *Plant Ecology* 159: 35–49.
- Walsh, R. P. D., Newberry, D. M. 1999. The ecoclimatology of Danum, Sabah, in the context of the world’s rainforest regions with particular reference to dry periods and their impact. In : Newberry, D. M., Clutton-Brock, T. H., Prance, G. T. (Eds.). *Changes and Disturbance in Tropical Rainforest in South-East Asia*, Philosophical Transactions of the Royal Society London

2. Site descriptions

B354 : 1869-1883.

Wilford, G.E. 1961. *The Geology and Mineral Resources of Brunei and Adjacent Parts of Sarawak.*

Memoir 10. Geology Survey Department, British Territories in Borneo, 319pp.

Yamakura, T., Kanzaki, M., Itoh, A., Ohkubo, T., Ogino, K., Ernest, C., Lee, H. S., Ashton, P. S.

1995. Topography of a large-scale research plot established within a tropical rain forest at

Lambir, Sarawak. *Tropics* 5:41–56.

Chapter 3

Spatial and temporal variations in rainfall and the ENSO-rainfall relationship

3.1 Introduction

It is widely recognized that during El Niño years, droughts tend to occur over the maritime continent, which consists of Malaysia, Indonesia, Papua New Guinea and the surrounding land and oceanic areas.

I examined the seasonal variation in rainfall over Sarawak using rainfall data observed by the Department of Irrigation and Drainage (DID) at 17 stations (Gomyo and Kuraji, 2006). However, I did not analyze the frequency, timing, intensity or spatial heterogeneity of drought and the rainfall–ENSO relationship. To my knowledge, there are no studies involving the combined analysis of the spatial and temporal variations in the ENSO–rainfall relationship and seasonal variation in rainfall in Borneo. Grid rainfall data such as data of the Climate Prediction Center (CPC) Merged Analysis of Precipitation (CMAP) are of limited use in detecting seasonal variations in rainfall on a small scale.

The 1st objective of this chapter is to analyze, in more detail than Gomyo and Kuraji (2006), the characteristics of the spatial distribution of the seasonal variation in rainfall at Sarawak and Sabah, using long-term multi-location rainfall data collected by DID and MMD, and to classify climatologically the areas of Sarawak and Sabah states. The 2nd objective of this chapter is to examine differences in the rainfall–ENSO relationship and seasonal variation in rainfall by analyzing rainfall data from 18 stations throughout Sarawak for 1963–2003, 25 stations throughout Sabah for 1987–2006. A precise understanding of the ENSO relationship with local rainfall is achieved by collecting rainfall data. The combined analysis is necessary for determining the most vulnerable regions in an El Niño-induced drought.

3.2 Methods

3.2.1 Rainfall data

I used rainfall data obtained at 18 stations (*Table 3.1*) throughout Sarawak from 1963 to 2003 by DID (stations 1, 3-9, 13-18) and MMD (stations 2, 10-12), and 25 stations (*Table 3.2*) throughout Sabah from 1987 to 2006 by DID. The DID rainfall data throughout Sarawak were taken daily and published in the form of yearbooks. I digitalized all daily data from the yearbooks and conducted quality control by comparing the monthly rainfall at a station with those of adjacent stations. If there is a month which includes at least one day data missing, the month is defined as data missing month.

Table 3.1 List of rainfall stations used in Sarawak. Cluster name, station number, name, location (latitude values are degrees north and longitude values are degrees east), elevation, mean annual rainfall and mean DJF rainfall.

Cluster	No.	Station Name	Location		Elevation (m.a.s.l.)	Mean annual rainfall (mm)	Mean DJF rainfall (mm)
			Latitude N	Longitude E			
C1	1	Telok Assam	1° 43'	110° 26'	5	4047 [34]	1856 [33]
	2	Kuching	1° 28'	110° 20'	25	4123 [41]	1641 [41]
	3	Semongok	1° 23'	110° 19'	32	4104 [33]	1528 [37]
	4	Sebuyau	1° 31'	110° 55'	3	3835 [33]	1518 [37]
	5	Mukah	2° 54'	112° 05'	1	3644 [40]	1562 [40]
	6	Balingian	2° 55'	112° 32'	16	3649 [33]	1403 [35]
C2	7	Kabong	1° 48'	110° 06'	1	3594 [36]	1190 [37]
	8	Pantu	1° 08'	111° 06'	104	3653 [34]	1156 [39]
	9	Saratok	1° 44'	111° 20'	39	3284 [37]	1026 [42]
	10	Sibu	2° 20'	111° 50'	8	3245 [39]	1016 [40]
	11	Bintulu	3° 10'	113° 02'	13	3732 [40]	1091 [41]
C3	12	Miri	4° 19'	113° 59'	47	2785 [40]	795 [41]
	13	Lutong	4° 28'	114° 00'	1	3038 [32]	897 [31]
C4	14	Marudi	4° 10'	114° 19'	70	2675 [36]	796 [39]
	15	Ukong	4° 33'	114° 51'	15	3826 [35]	1079 [36]
	16	Lawas	4° 50'	115° 24'	10	4078 [31]	951 [33]
	17	Lio Matu	3° 10'	115° 13'	285	3759 [34]	894 [38]
	18	Bario	3° 44'	115° 27'	1005	2250 [30]	533 [37]
			LHNP	4°11' 23"	114°01' 09"	90.4	2650 [9]

Note: [] years with 12 months rainfall data available are used for calculation.

[] years with DJF rainfall data available are used for calculation.

3. Spatial and temporal variations in rainfall and the ENSO-rainfall relationship

Table 3.2 List of rainfall stations used in Sabah. Cluster name, station number, name, location (latitude values are degrees north and longitude values are degrees east), elevation, mean annual rainfall and mean DJF rainfall.

Cluster	No.	Station Name	Location		Elevation (masl)	Mean annual rainfall (mm)	Mean DJF rainfall (mm)
			Latitude N	Longitude E			
S1	1	Kiansam	5° 59' 05"	116° 10' 40"	70	3131 [20]	596 [19]
	2	Tamu Darat	6° 15' 50"	116° 27' 10"	52	2899 [17]	550 [19]
	3	Rosok	6° 23' 30"	116° 31' 30"	76	2271 [17]	492 [18]
	4	Beaufort	5° 21' 15"	115° 43' 25"	10	3428 [18]	661 [19]
	5	Ulu Moyog	5° 51' 50"	116° 15' 50"	960	5408 [17]	985 [18]
	6	Mempakul	5° 17' 50"	115° 10' 55"	15	2774 [16]	420 [18]
	7	Inanam	5° 59' 45"	116° 06' 55"	5	2525 [16]	403 [19]
S2	8	Sapulut	4° 42' 10"	116° 28' 55"	280	2651 [17]	496 [18]
	9	Bonor	-	-	-	2092 [17]	455 [18]
	10	Kalampun	-	-	-	1733 [18]	370 [18]
	11	Sook	5° 09' 00"	116° 18' 20"	350	1880 [18]	387 [18]
	12	Kemabong	4° 54' 50"	115° 34' 15"	183	1615 [18]	397 [19]
	13	Keningau	5° 20' 45"	116° 09' 40"	290	1291 [18]	304 [17]
	14	Kalabakan	4° 25' 00"	117° 29' 10"	47	2067 [17]	455 [17]
	15	Tampias	5° 42' 40"	116° 51' 35"	220	2609 [16]	658 [17]
S3	16	Trusan Sugut	6° 25' 20"	117° 41' 40"	30	2547 [16]	952 [18]
	17	Kudat	6° 53' 20"	116° 50' 35"	20	1999 [18]	893 [19]
	18	Pitas	6° 03' 40"	117° 03' 15"	15	2257 [16]	1060 [18]
S4	19	Tandek	-	-	-	2538 [17]	1018 [19]
	20	Trusan Sapi	5° 54' 10"	117° 22' 25"	15	3270 [18]	1137 [18]
	21	Basai	6° 03' 03"	117° 18' 52"	30	2961 [18]	1060 [19]
	22	Kuamut	5° 13' 20"	117° 29' 10"	20	3100 [18]	1086 [19]
	23	Sukau	5° 32' 15"	118° 17' 15"	30	2488 [18]	924 [19]
	24	Bilit	5° 29' 00"	118° 12' 00"	-	2413 [16]	928 [17]
	25	Tangkulap	5° 18' 15"	117° 16' 40"	80	2791 [17]	886 [19]
		MKNP	6° 00' 42"	116° 32' 27"	1698	2803 [8]	655 [10]

Note: [] years with 12 months rainfall data available are used for calculation.

[] years with DJF rainfall data available are used for calculation.

3.2.2 SST data

The SST data over the Niño-3.4 area (5°S–5°N, 170°–120°W) were obtained from the National Weather Service Climate Prediction Center of the National Oceanic and Atmospheric Administration (NOAA) (<http://www.cpc.ncep.noaa.gov/>). I selected the DJF mean Niño-3.4 SST as the ENSO index because the Niño-3.4 SST anomaly reached a maximum during the DJF(0/1) warm phase of the ENSO (Rasmusson and Carpenter, 1982). DJF (0/1) denotes three consecutive months starting from December (year 0) to the following February (year 1). Hereafter all SSTs are DJF mean

SSTs over the Niño-3.4 area and simply noted as SSTs.

3.3 Results

3.3.1 Spatial variation of rainfall

To analyze the spatial variation in the seasonal fluctuation of rainfall over Sarawak and Sabah, cluster analysis was applied on the basis of the anomaly of the mean monthly rainfall. If there is a year which includes only one data missing month, the rainfall anomaly was calculated by the other 11 months data. *Figure 3.1 and 3.2* are tree diagrams showing the results of the cluster analysis over Sarawak and Sabah, respectively. I used a minimum distance hierarchical method, which calculates the sum of squared Euclidean distances from each case in a cluster to the mean of all variables (Ward's method).

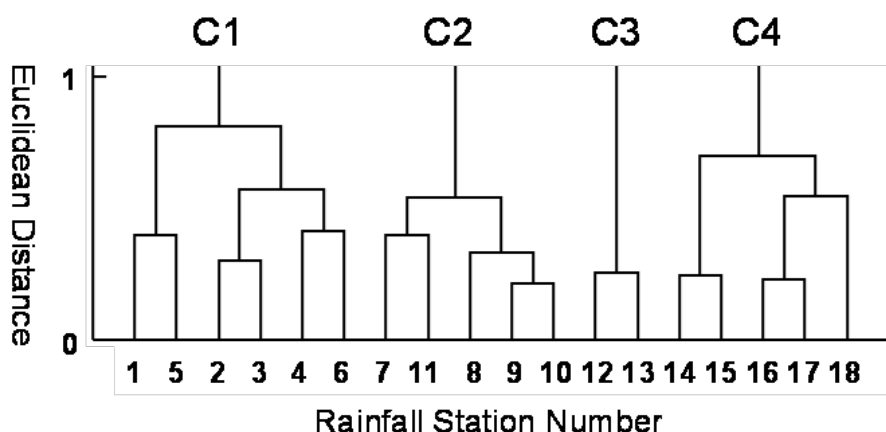


Figure 3.1 Tree diagram of the cluster analysis of the 18 observation stations over Sarawak.

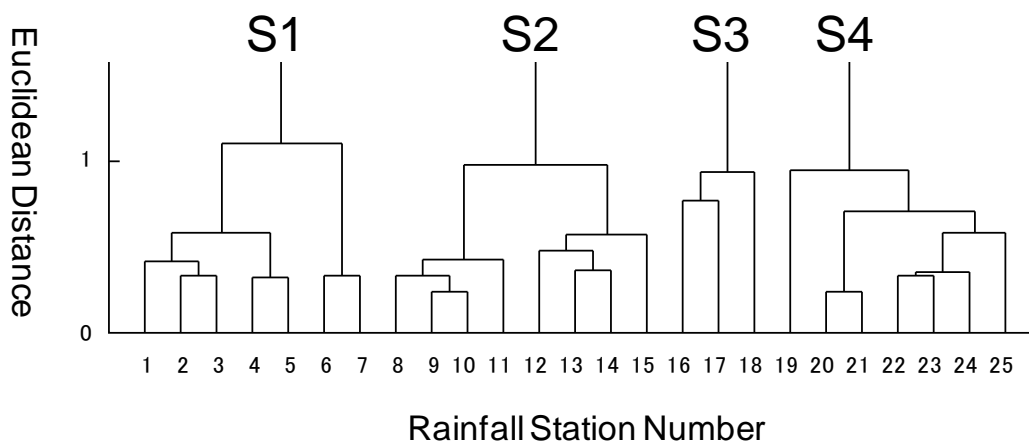


Figure 3.2 Tree diagram of the cluster analysis of the 25 observation stations over Sabah.

3.3.2 Seasonal variation of rainfall

Figure 3.3 (a and b) show the anomalies of the mean seasonal variation in rainfall for the four clusters over Sarawak and LHNP, respectively. In Figure 3.3 (b), the anomaly of the mean seasonal variation in rainfall for LHNP (2000-2008) is shown. Figure 3.4 (a b c and d) show the anomalies of the mean seasonal variation in rainfall for the all stations over Sarawak, respectively. The mean annual rainfalls for C1, C2, C3 and C4 were 3900, 3502, 2912 and 3318 mm, which means the C3 region received about 25% less rainfall than the C1 region did (Figure 3.4 a). For C1, there was a distinct rainy season (DJF) and dry season (JJA) whereas there were no such distinct seasons for C4. For C3, there were relatively wet (from October to January; ONDJ) and relatively dry (February to March; FM) seasons. C2 had a transitional pattern between the patterns of C1 and C3. C2 had a transitional pattern between the patterns of C1 and C3.

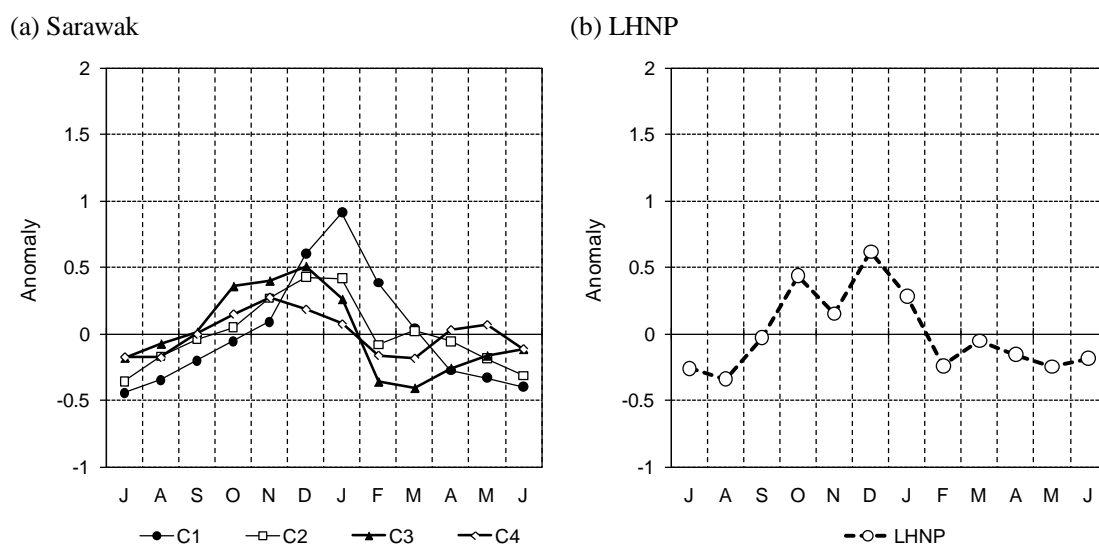


Figure 3.3 Anomalies of the mean monthly rainfall for (a) C1, C2, C3 and C4, and (b) LHNP. The anomaly was calculated by taking the average of the normalized anomaly in each month at each station, which was obtained by dividing the anomaly by the mean monthly rainfall.

3. Spatial and temporal variations in rainfall and the ENSO-rainfall relationship

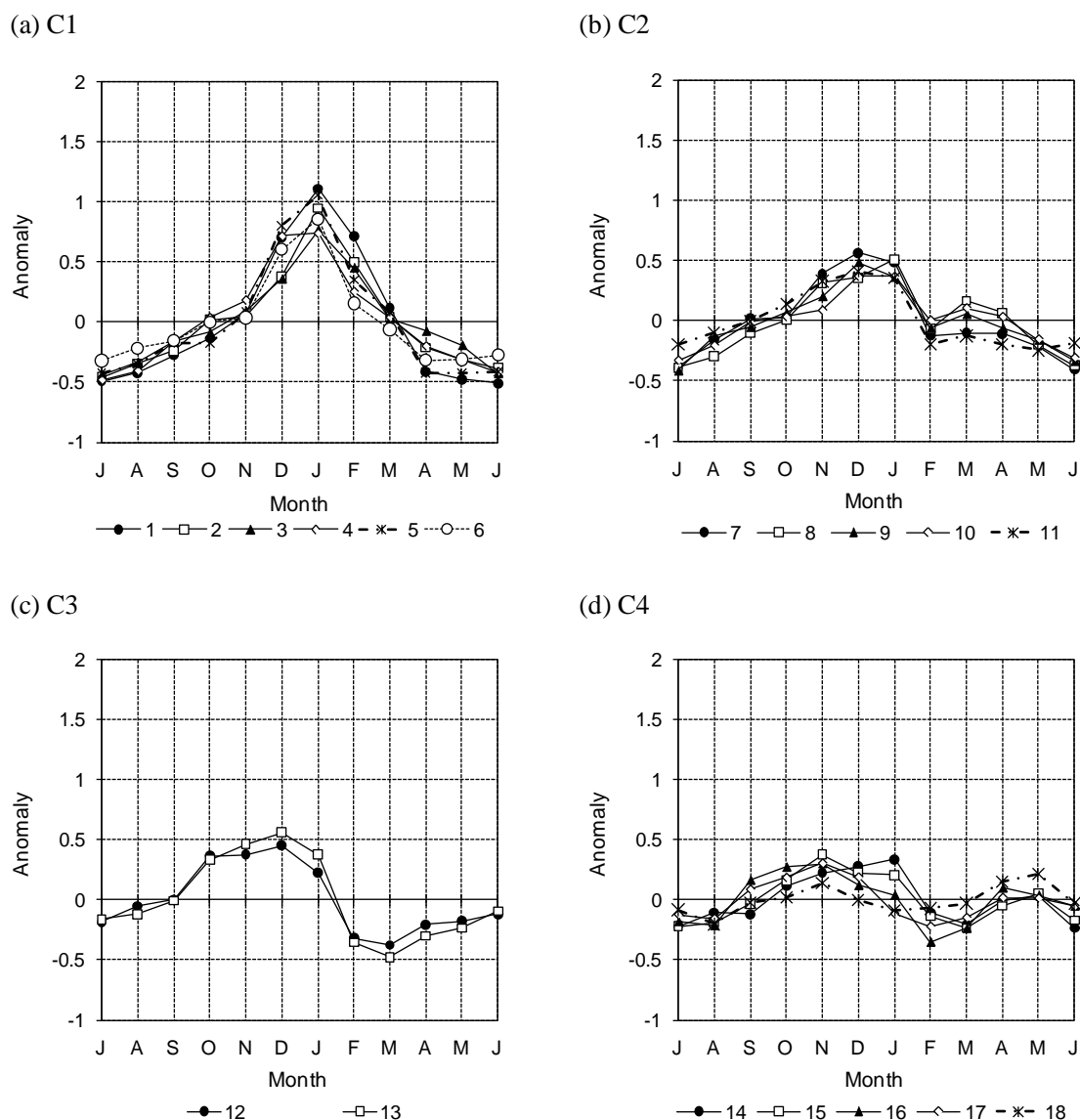


Figure 3.4 Anomalies of the mean monthly rainfall for (a) C1, (b) C2, (c) C3 and (d) C4. The anomaly was calculated by taking the average of the normalized anomaly in each month at each station, which was obtained by dividing the anomaly by the mean monthly rainfall.

Figure 3.5 (a and b) show the anomalies of the mean seasonal variation in rainfall for the four clusters over Sabah and MKNP, respectively. In Figure 3.5 (b), the anomaly of the mean seasonal variation in rainfall for MKNP (1996-2000, 2006-2008) is shown. Figure 3.6 (a b c and d) show the anomalies of the mean seasonal variation in rainfall for the all stations over Sabah, respectively.

3. Spatial and temporal variations in rainfall and the ENSO-rainfall relationship

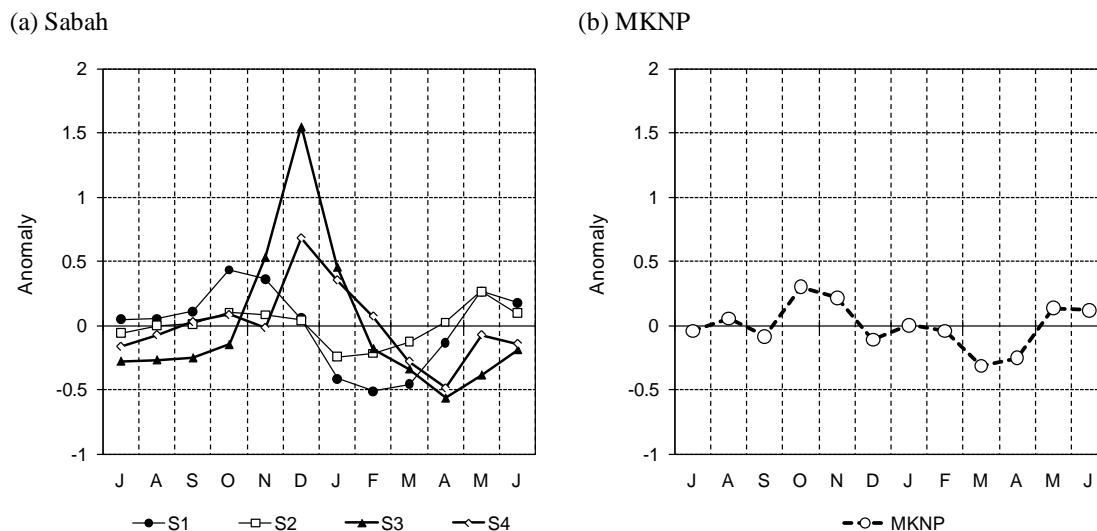


Figure 3.5 Anomalies of the mean monthly rainfall for (a) S1, S2, S3 and S4, and (b) MKNP. The anomaly was calculated by taking the average of the normalized anomaly in each month at each station, which was obtained by dividing the anomaly by the mean monthly rainfall.

The mean annual rainfalls for S1, S2, S3 and S4 were 3205, 1992, 2268 and 2795 mm, which means the S2 region received about 38% less rainfall than the S1 region did (Figure 3.7 b). For S1, there was distinct rainy season (ON, MJ) and dry season (JFM). For S2, there was no such distinct season variation. For S3, the anomaly of DJF was greater than other region.

3. Spatial and temporal variations in rainfall and the ENSO-rainfall relationship

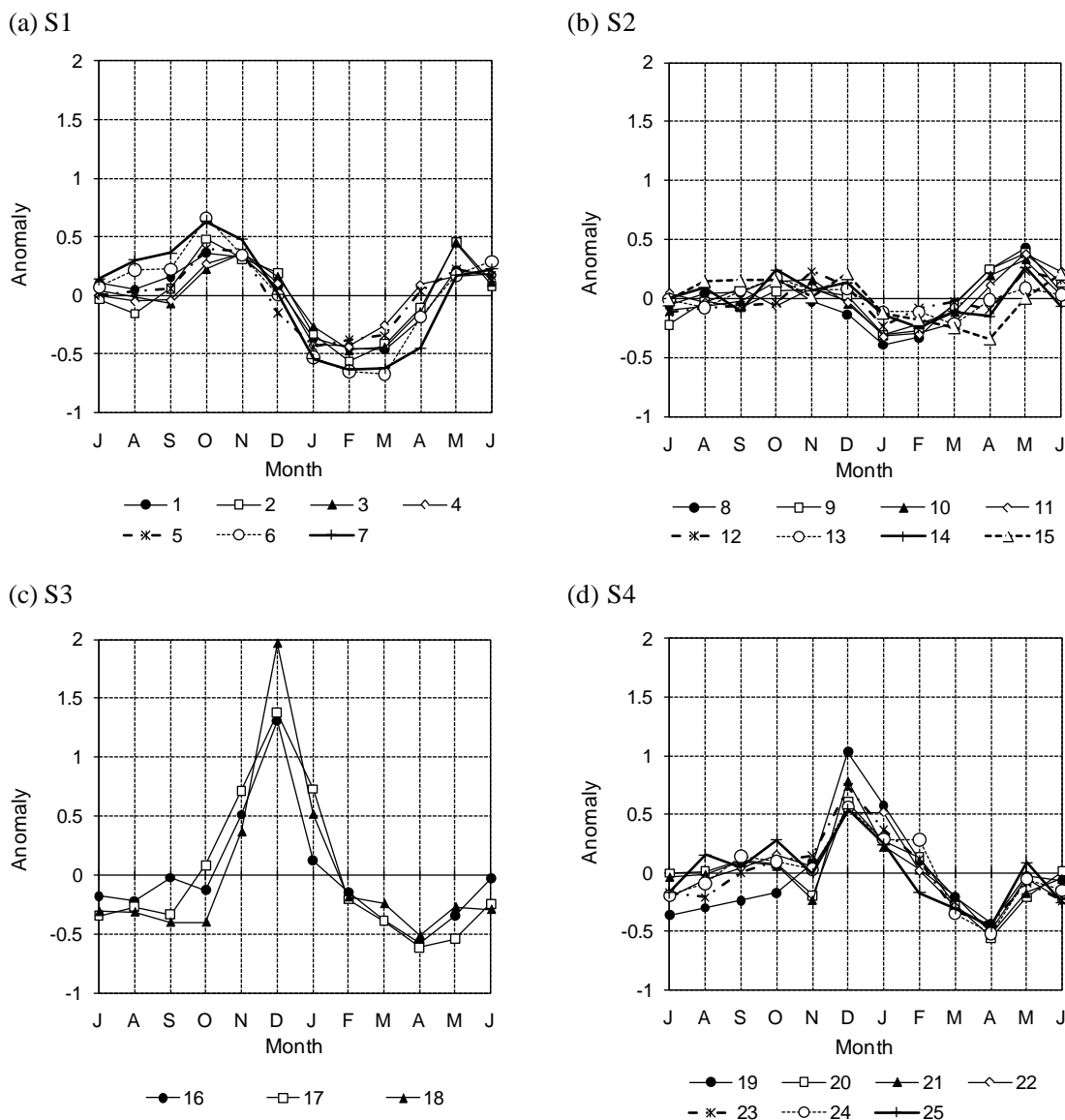


Figure 3.6 Anomalies of the mean monthly rainfall for (a) S1, (b) S2, (c) S3 and (d) S4. The anomaly was calculated by taking the average of the normalized anomaly in each month at each station, which was obtained by dividing the anomaly by the mean monthly rainfall.

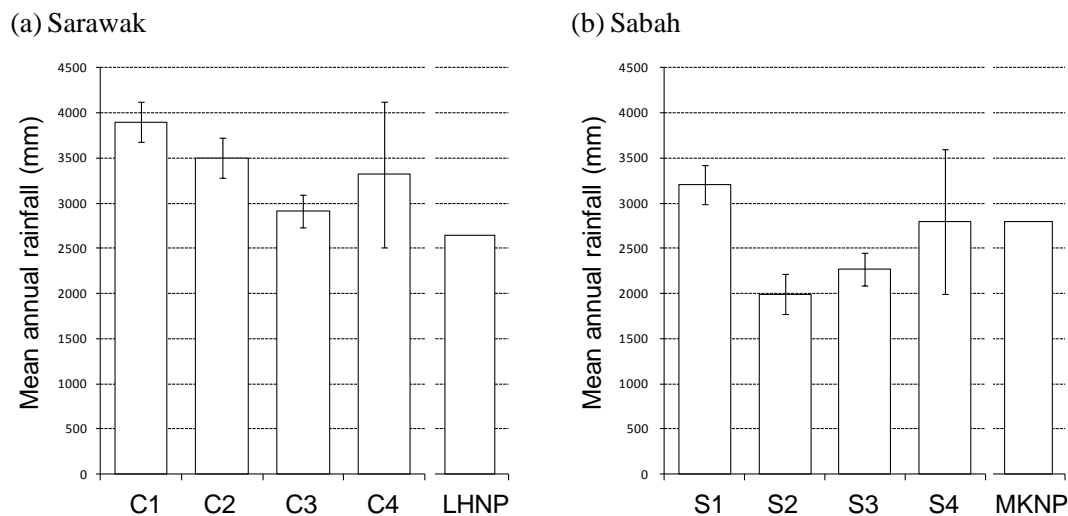


Figure 3.7 Mean annual rainfall of the cluster in Sarawak and Sabah, respectively. The mean rainfall for LHNP (2000-2008) and MKNP (1996-2000, 2006-2008) are shown. The bars are standard deviation.

3.3.3 ENSO-rainfall relationship

Figure 3.8 (a and b) show coefficients for the lag correlation between SST and the three-month sliding sum of rainfall for all clusters. In Sarawak, the significance levels of the negative lag correlation between July- September (JAS) (0) rainfall and SST were higher for C1 and C2 than for C3 and C4. The significance level of negative simultaneous correlations between January-March (JFM)(1) rainfall and SST were higher for C4 and C3 than for C2 and C1. A positive lag correlation between JJA(1) rainfall and SST appears for all clusters and the significant levels are higher for C2 and C4 than for C1.

3. Spatial and temporal variations in rainfall and the ENSO-rainfall relationship

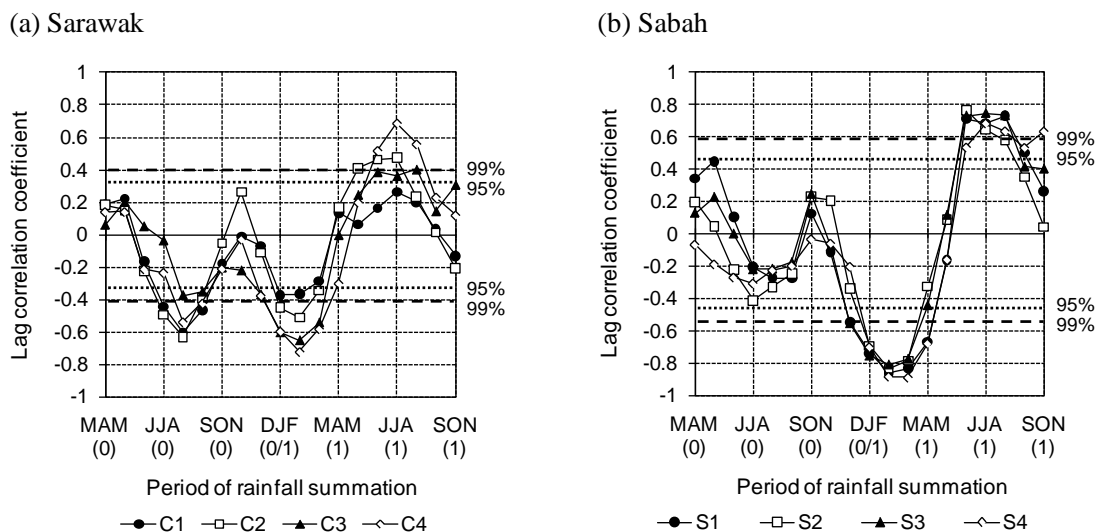


Figure 3.8 Coefficients for the simultaneous and lag correlations between the three-month sliding sum of rainfall and SST (a)Sarawak, (b) Sabah.

To determine the spatial and temporal variations in the effect of El Niño on drought over Sarawak and Sabah, the El Niño minus all-years composites of rainfall anomaly for all clusters were examined (Figure 3.6). The El Niño years used for the composite analysis are 1963-64, 65-66, 68-69, 72-73, 76-77, 77-78, 82-83, 86-87, 87-88, 91-92, 94-95 and 97-98 (Juneng and Tangang, 2005).

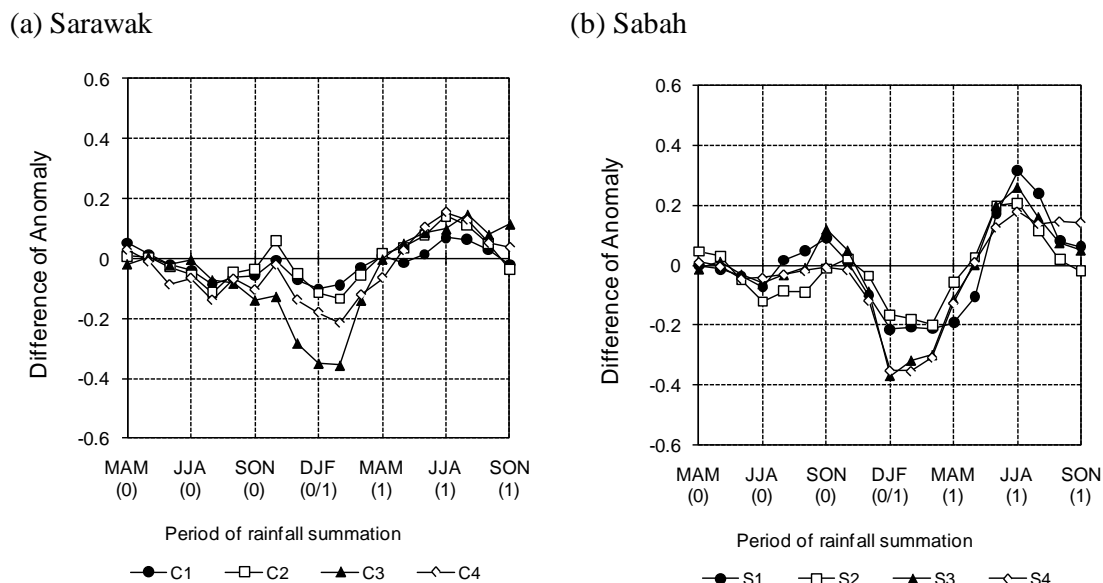


Figure 3.9 El Niño minus all-years composite of the three-month sliding sum of rainfall anomaly for the four clusters.

3. Spatial and temporal variations in rainfall and the ENSO-rainfall relationship

In JAS(0), a small reduction of rainfall anomaly in the El Niño years was observed for all four clusters, which corresponds to a significant negative lag correlation between JAS(0) rainfall and SST in Sarawak (*Figure 3.8 a*). In DJF(0/1) and JFM(1), the largest reduction of rainfall anomaly was observed for C3 and the second largest for C4, which correspond to a significant negative simultaneous correlation between rainfall and SST for C3 and C4 (*Figure 3.8 a*). For C3, the wet season is from October to the following January and the dry season is the following February and March. In *Figure 3.9(a)*, a reduction in rainfall can be observed from October(0) to the following March(1), encompassing both the wet season and the following dry season. For C1, there is no such obvious reduction in rainfall in these months and this corresponds to a weak simultaneous correlation between rainfall and SST (*Figure 3.8 a*). This result indicates the wet season (DJF(0/1)) rainfall for C1 and C2 has relatively weaker significant relation with the ENSO than for C3 and C4. In DJF(0/1), the largest reduction of rainfall anomaly was observed for all regions. In JJA(1), an increase of rainfall anomaly in the El Niño years was observed for all four clusters, which corresponds to a positive lag correlation between JJA(1) rainfall and SST (*Figure 3.8 b*) but the range of increase was less than 0.2, which is smaller than the range of reduction during DJF(0/1) and JFM(1) for C3 and C4. In S3 and S4 regions, the ratio of rainfall reduction (DJFMA) was greater than S1 and S2 regions (*Figure 3.9 b*).

3.3.4 DJF rainfall

Figure 3.10 (a and b) show the mean DJF rainfall of the cluster, LHNP and MKNP, and *Figure 3.11 (a and b)* show the mean DJF rainfall and El Niño years mean DJF rainfall of all stations over Sarawak and Sabah, respectively, and *Figure 3.12* shows the DJF rainfall reductions in the El Niño years of all stations over Sarawak and Sabah.

In DJF(0/1), the smallest DJF rainfall over Sarawak and Sabah in El Niño years (except LHNP and MKNP) was 207 mm at Mempakul (Station No.6) in S1, and the second smallest was 217 mm at Keningau (Station No. 13) in S2. For the rainfall reductions in the El Niño years of all stations over Sarawak and Sabah, the greatest rainfall reduction is 515 mm at Bilit (Station No. 24) in S4. The S4 and S3 regions are greater rainfall reduction in the El Niño years than the other regions. In Sarawak, the DJF rainfall for C1 and C2 has relatively weaker significant relation with the ENSO than for C3 and C4 (except No.14, 17 and 18).

3. Spatial and temporal variations in rainfall and the ENSO-rainfall relationship

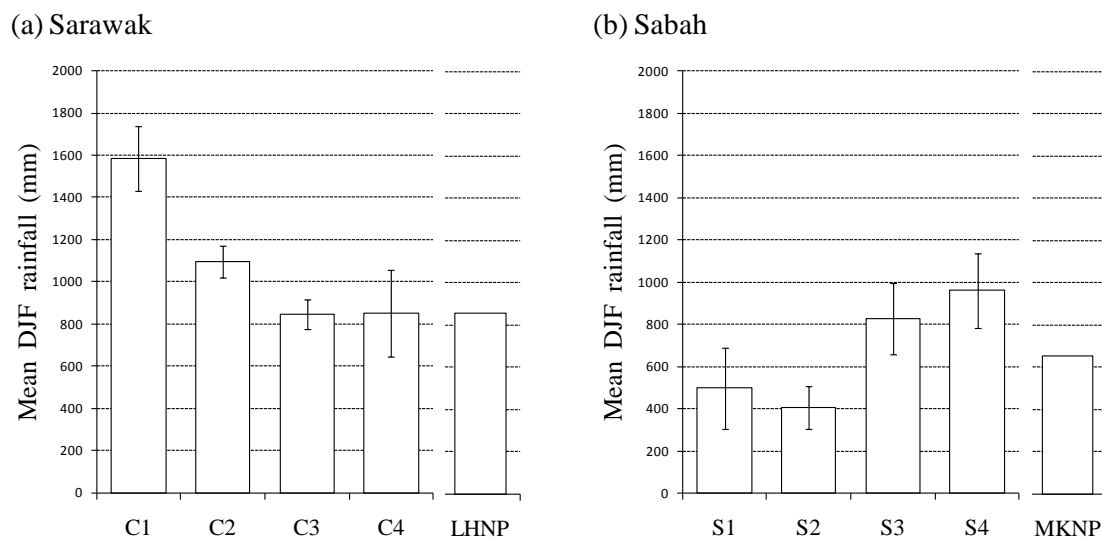
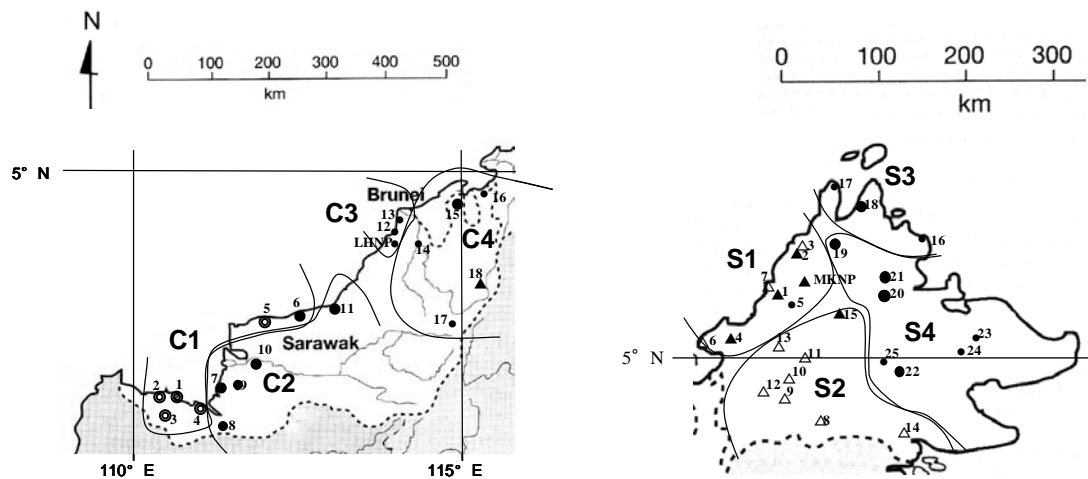


Figure 3.10 Mean DJF rainfall of the cluster, LHNP and MKNP, respectively. The bars are standard deviation.

(a) Mean DJF Rainfall



(b) El Niño Years Mean DJF Rainfall

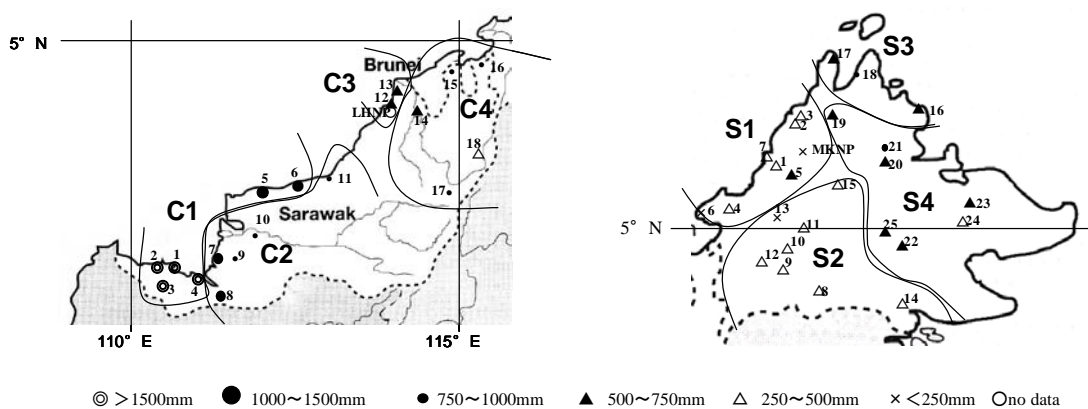


Figure 3.11 (a) Mean DJF rainfall, and (b) El Niño years mean DJF rainfall of all stations over Sarawak (left) and Sabah (right), respectively.

3. Spatial and temporal variations in rainfall and the ENSO-rainfall relationship

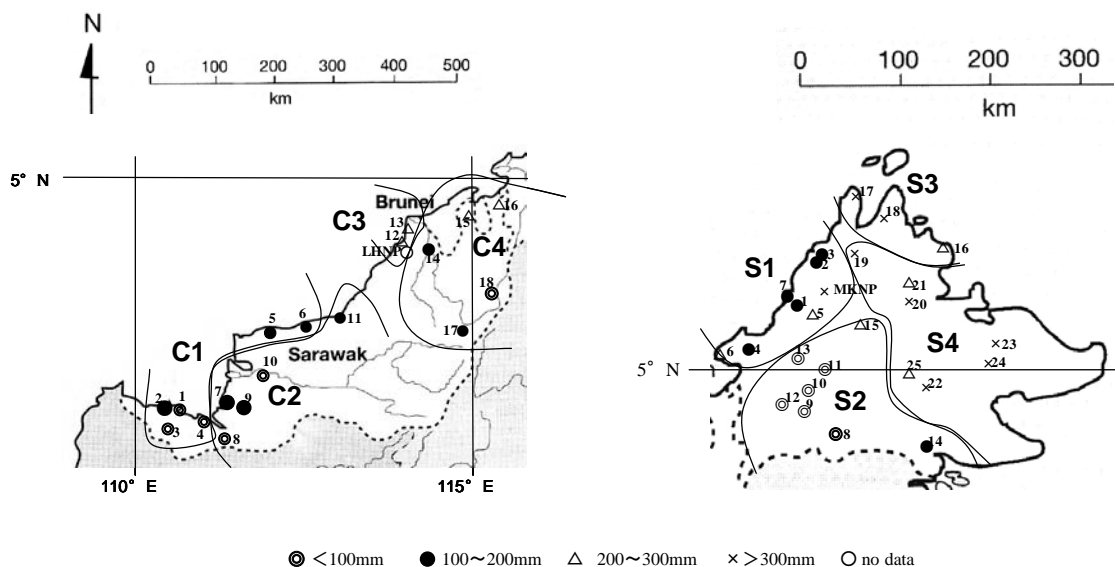


Figure 3.12 DJF rainfall reductions in the El Niño years of all stations over Sarawak (left) and Sabah (right), respectively.

3.4 Discussion

3.4.1 Spatial and seasonal variations of rainfall

In order to discuss the seasonal rainfall fluctuations in Sarawak and Sabah, as shown in the previous section, it is necessary to set out firstly the validity of seasonal divisions in this region.

In a study of the seasonal rainfall variations of the areas spanning the Bay of Bengal, Indochina, Philippines and Maritime Continent, Chang et al. (2005 a;b) divided the year into four seasons; NE monsoon season = winter in Asia (summer in Australia); monsoon season = DJF; Interval season (spring in northern hemisphere) = MAM; SW monsoon season = Asia (India) summer monsoon season = JJA; Interval season (autumn in northern hemisphere) = SON. It describes the seasonal rainfall variations in northern Borneo as follows:

- In the NE monsoon season, the ITCZ is situated on the Maritime Continent in the southern hemisphere with its northern limit further south than Sarawak and Sabah. Because of this Sarawak and Sabah are affected by the wet NE wind from the South China Sea with plenty of rain.
- In the SW monsoon season, the ITCZ migrates north to Indochina and the Philippines with its southern limit situated near Sarawak and Sabah. The dry SE wind from Australia changes direction

3. Spatial and temporal variations in rainfall and the ENSO-rainfall relationship

to SW around the equator to reach Sarawak and Sabah. Because of this Sarawak and Sabah have little overall rainfall.

In DJF, the rainfalls are generally high everywhere. *Figure 3.13* shows a diagram of the wind system in the 850 hPa field. In Sarawak and Sabah, the area along the coast is affected by strong NE or N wind that is thought to bring rain. During the first half of DJF, the ITCZ is situated on the Maritime Continent in the southern hemisphere with its northern limit south of Sarawak and Sabah with its northern limit near the equator, thus Sarawak and Sabah are outside the ITCZ. The C4 and S2 groups located inland have less rainfall. It is presumed that this is because these groups are not affected by the NE monsoon and are situated outside ITCZ.

In the latter half of DJF, the rainfalls start to decrease between groups; however, the timing is not the same. The northward migration of the northern limit of the ITCZ and subtle changes of wind direction may be considered as possible causes for the difference in onsets but a clear-cut conclusion could not be reached from this investigation using the wind system diagrams for every 5-day unit.

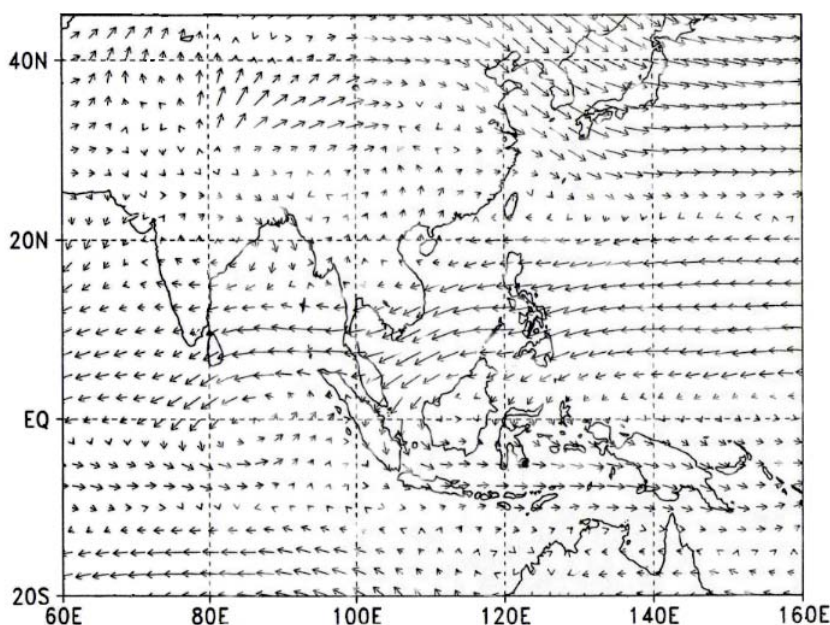


Figure 3.13 The NCEP/NCAR reanalysis wind velocity of pentad 2(6 Jan – 10 Jan).
Mean of 1979-2000 at 850 hPa (Oki, 2002).

Figure 3.14 shows a diagram of the wind system in the 850hPa field in the 9th 5-day unit. Compared to *Figure 3.13*, the wind speed decreased around Sarawak and Sabah and its direction changed from northeasterly to easterly. It can be assumed that the decreasing wind speed is the cause

3. Spatial and temporal variations in rainfall and the ENSO-rainfall relationship

of decreasing rainfall in group C1. The cause of low rainfall during this season for groups C3 might be connected to their locations, with their coastline facing NE. While the monsoon wind is northerly during the first half of DJF and the wind from the sea reached the locations directly, the wind changed to easterly during the latter half of DJF, which brings rain to the eastern coast of groups S3 and S4. The decrease in rain may be caused by the arrival of this easterly wind, now dry, in these locations. The coastlines of all the locations in group two face west. In contrast with these groups, group C1 does not show a local minimum during the latter half of DJF, because its coastline faces NNW, and receives sea winds onto the land even though the wind direction has changed to easterly.

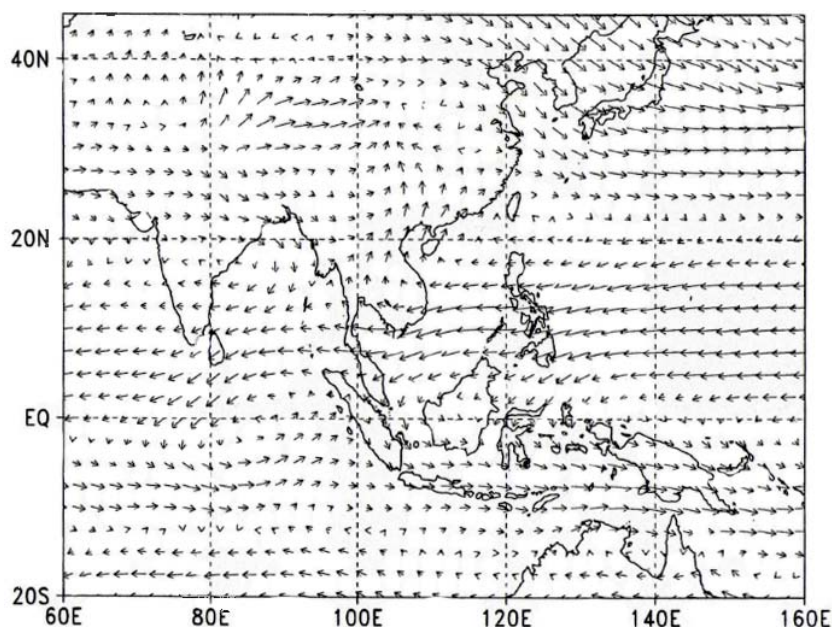


Figure 3.14 The NCEP/NCAR reanalysis wind velocity of pentad 9(10 Feb – 14 Feb).
Mean of 1979-2000 at 850 hPa (Oki, 2002).

MAM is coincident with the latter part of the interval season from the NE monsoon season to the SW monsoon season. *Figure 3.12* shows a diagram of wind directions in the 850hPa field at the 26th 5-day unit. The wind over Sarawak and Sabah are weak and the prevailing direction not clear.

3. Spatial and temporal variations in rainfall and the ENSO-rainfall relationship

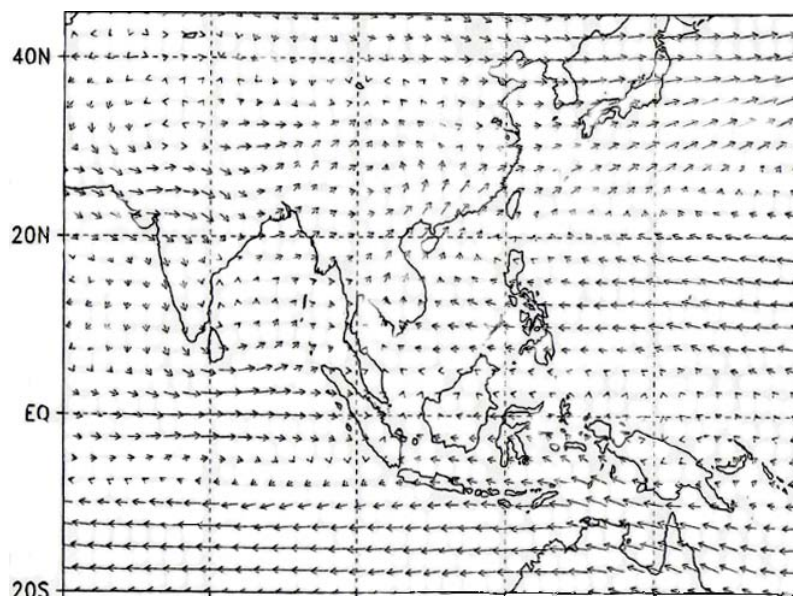


Figure 3.15 The NCEP/NCAR reanalysis wind velocity of pentad 26(6 May – 10 May). Mean of 1979-2000 at 850 hPa (Oki, 2002).

Increased rainfall in groups is thought to be caused by a weakening of the influence of the easterly dry wind as well as by entering the ITCZ-affected area. Under the influence of the SW monsoon, the rainfalls in all groups are low and there is very little difference in the amount of rainfall between the groups.

Figure 3.16 shows a diagram of the wind system in the 850hPa field at the 38th 5-day unit. The dry SE wind from Australia changes direction around the equator to become the dry SW wind reaching Sarawak. The wind speed is not as high as the wind in the NE monsoon. In JJA, the northern limit of the ITCZ reaches the Indochina Peninsula and the whole of the Philippines while its southern limit is situated around the equator (Hans and Abang, 2001), hence the rainfall in the whole of Sarawak and Sabah are thought to be under the influence of the ITCZ.

3. Spatial and temporal variations in rainfall and the ENSO-rainfall relationship

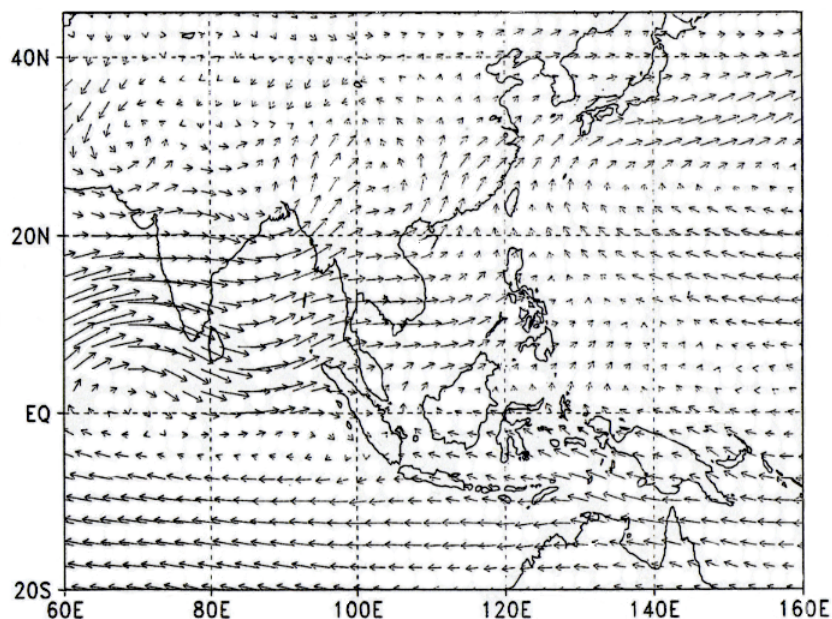


Figure 3.16 The NCEP/NCAR reanalysis wind velocity of pentad 38(5 Jul. – 10 Jul.).
Mean of 1979-2000 at 850 hPa (Oki, 2002).

SON is coincident with the interval season from the SW monsoon to the NE monsoon with the rainfall increasing in all groups. There is no difference seen among the groups as is seen in the interval season from the NE monsoon to the SW monsoon. *Figure 3.17* shows a diagram of the wind system in the 850hPa field at the 64th 5-day unit. As in the JJA, the wind is weak and the prevailing direction not clear. The whole of Sarawak is still under the influence of the ITCZ, but as the ITCZ migrates to southward with strengthening NE and N winds, the amount of rainfall in groups C1, C2, C3, S1 and S3 increases.

3. Spatial and temporal variations in rainfall and the ENSO-rainfall relationship

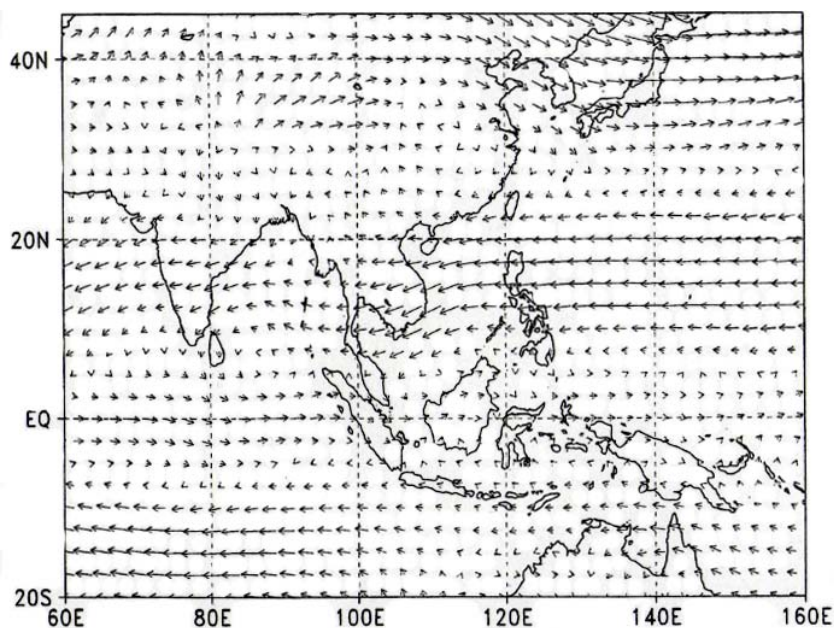


Figure 3.17 The NCEP/NCAR reanalysis wind velocity of pentad 64(12 Nov. – 16 Nov.). Mean of 1979-2000 at 850 hPa (Oki, 2002).

3.4.2 ENSO-rainfall relationship

This study indicates the correlations between rainfall anomalies over Sarawak and Sabah and SST for three different seasons. They were negative lag correlation in JAS(0), negative simultaneous correlation in DJF(0/1) and positive lag correlation in JJA(1). However, as shown in *Figure 3.9*, only small rainfall reduction or increase was observed in JAS(0) and JJA(1). The significant lag correlations in JAS(0) and JJA(1) did not correspond to the distinct rainfall reductions during the El Niño years and less important in terms of the temporal and spatial variation of droughts in this region. Moreover, we have insufficient evidence to explain the possible mechanism why these significant positive / negative lag correlations appeared. According to these reasons, the following discussion is concentrated on the negative simultaneous correlation between rainfall anomaly and SST and rainfall reduction in the El Niño years during DJF(0/1).

The possible mechanism of such correlation and rainfall reduction was well described by Juneng and Tangang (2005) on the basis of $0.5^\circ \times 0.5^\circ$ rainfall data produced by the Global Historical Climatology Network. They suggested that the strong rainfall-ENSO relationship in the East Malaysia during DJF(0/1) is associated with the anomalous cyclonic/anti-cyclonic circulation

3. Spatial and temporal variations in rainfall and the ENSO-rainfall relationship

that stipulated to be a downstream response to the boomerang-shaped SST anomalies. However, this study shows that such mechanism is weakened or masked by other phenomenon in C1 and C2, which rainfall has only weak correlation with SST.

Chang et al. (2004), which examined the localized relationship between the ENSO and DJF rainfall using the CMAP rainfall data. The wet season rainfall for C1 and C2 may be controlled by other mechanisms such as a cold surge, the Borneo vortex and the Madden–Julian Oscillation (MJO). Chang et al. (2005) shows the frequency of Borneo vortex center locations were the highest near the C1 area, suggesting that C1 and C2 is located in the region most affected by the vortex. The vortex may mask the influences of anomalous circulation confined in NES without significantly affecting SWS.

C3, which occupies a small area in northeastern Sarawak around Miri and Lutong, is the most vulnerable to drought during the warm phase of the ENSO because of the following facts. First, the annual rainfall for C3 was the smallest of all clusters. Second, the rainfall–ENSO relationship was continuously significant from July(0) to March(1) including the wet season (ONDJ) and dry season (FM). Third, the anomaly of rainfall reduction in the El Niño year was the largest in January(1) and February(1), about half of the average. February was the second driest month for C3 and the average monthly rainfall was 158.5 mm. The rainfall in El Niño years was insufficient in supplying water for evapotranspiration in this season because the average monthly evapotranspiration in this region is around 100–120 mm.

The C4 region has a similar pattern with that for C3 during DJF(0/1) in terms of the simultaneous correlation with SST (*Figure 3.8*) and the reduction of rainfall anomaly (*Figure 3.9*) but the seriousness of the rainfall reduction is less than that for C3. I have insufficient evidence to explain this fact but I postulate a small-scale mechanism such as land–sea interaction may affect the difference, especially the rainfall decline in February and March.

In S1, the low rainfall period overlaps with the period in which the influence of El Niño is strong. This means that El Niño causes more severe dryness at a point that normally has little rainfall during this period while it causes small impact at a point that normally has much rainfall during the period. There are both low and high rainfall points in S2. The dryness caused by El Niño appears obviously at a low rainfall point and modestly at a high rainfall point. In S3, the monthly average rainfall during the entire year is below 100mm for some months from April to May. This is because

there is relatively low rainfall as well as significant degree of seasonal variation. As for the year that is affected by El Niño, it causes rather severe dryness; the dry season extends to the transition period (from February to March), in which it moves from the high rainfall period to the low rainfall period, in addition to the period from April to May. In S4, the impact of low rainfall caused by El Niño is small because there is higher annual rainfall as well as smaller degree of seasonal variation in S4 than in S3, when based on the average for all years. In Sabah, after it returns from the dryness caused by El Niño, all areas experience higher rainfall than average in the period from July to September. The amount of rainfall and degree of seasonal variation widely vary by locations in this region; however, it was found that the effect of the dryness caused by El Niño occurs at almost the same timing throughout all areas, and it brings dryness in certain points that normally have low rainfall in such timing.

3.5 Conclusion

The rainfall–ENSO relationship and seasonal variation in rainfall over Sarawak and Sabah, Malaysian Borneo, was examined using rainfall data. Rainfall–ENSO relationships were first seen in SWS during JJA and move northeastward to NES in the following DJF. The seasonal variation in rainfall over Sarawak was categorized into four clusters: C1, C2, C3 and C4. For C1, JJA and DJF were dry and wet seasons respectively, whereas for C3, ONDJ and FM were relatively wet and dry seasons respectively. The seasonal variation in rainfall over Sabah was categorized into four clusters: S1, S2, S3 and S4. The seasonal variations were compared with the ENSO–rainfall relationship. It was found that for C1, there was an ENSO-related rainfall decline in the dry season (JJA) but not in the wet season (DJF), whereas for C3, there were rainfall declines in both the wet season (ONDJ) and dry (FM) season.

In Sabah, after it returns from the dryness caused by El Niño, all areas experience higher rainfall than average in the period from July to September. The amount of rainfall and degree of seasonal variation widely vary by locations in this region; however, it was found that the effect of the dryness caused by El Niño occurs at almost the same timing throughout all areas, and it brings dryness in certain points that normally have low rainfall in such timing.

3.6 References

- Chang, C. P., Wang, Z., McBride, J., Liu, C. H. 2005a. Annual cycle of southeast Asia-maritime continent rainfall and the asymmetric monsoon transition. *Journal of climate* 18 : 287-301.
- Chang, C. P., Harr, P. A., Chen, J. H. 2005b. Synoptic disturbances over the equatorial South China Sea and western maritime continent during boreal winter. *Monthly Weather Review* 133:489-503.
- Chang, C. P., Wang, Z., Ju, J., Li, T. 2004. On the relationship between western maritime continent monsoon rainfall and ENSO during northern winter. *Journal of Climate* 17: 665-672.
- Gomyo, M., Kuraji, K. 2006. Spatial distribution of seasonal variation in rainfall in the state of Sarawak, Malaysia. *Journal of Japan Society of Hydrology & Water Resources* 19: 128-138. (in Japanese with English abstract).
- Hans, P. H., Abang, K. A. M. 2001. Sarawak's physical environment : Climate, Geology and Soils. In : Hazebroek, H. P. Abang Kashim, A. M. (Eds.). *National Parks of Sarawak*, pp.9-16.
- Juneng, L., Tangang, F.T. 2005. Evolution of ENSO-related rainfall anomalies in Southeast Asia region and its relationship with atmosphere-ocean variations in Indo-Pacific sector. *Climate Dynamics* 25: 337-350.
- Oki, T. 2002. Investigation on Climate and Water Cycles over Southeast Asia for Future International Cooperation Project. Summary report. (no.13895008) summary report (in Japanese).
- Rasmusson, E. M., Carpenter, T. H. 1982. Variations in tropical sea surface temperature and surface wind fields associated with the southern oscillation / El Niño. *Monthly Weather Review* 110:354-384.

Chapter 4

Water and nutrient balances

4.1 Introduction

Several forest water balance studies have been conducted in Borneo at sites in Sapulut and Ulu Kalumpang, Sabah (Kuraji, 2004), Danum Valley, Sabah (Donglas et al. 1992; Chappell et al. 1998; Chappel and Sherlock, 2005), Mendolong, Sabah (Malmer, 1992; 2004), Temburong, Brunei (Dykes, 1997; Dykes and Thornes, 2000), Lambir Hills, Sarawak (Kume et al. 2008, Manfroi et al. 2006; Kumagai et al. 2005) and Central Kalimantan (Asdak et al. 1998, Vernimmem et al. 2007) among many others. These studies cover a wide range of hydrological observations of rainfall, throughfall, stemflow, soil water, groundwater, streamflow and evapotranspiration. For lowland forests, Elsenbeer (2001) reviewed the hydrologic flowpaths in tropical rainforest soils, including Chappell et al. (1998), and resulted the soil types tentatively define the width of a spectrum of possible hillslope hydrologic flowpaths, from predominantly vertical to predominantly lateral flowpaths. However, only a limited number of hydrological studies have focused on lowland and montane forests in Borneo; notwithstanding that there are a number of comprehensive hydrological studies for Central and South American tropical lowland forests (Nortcliff and Thornes, 1989; Lesack, 1993; Elsenbeer et al. 1999) and montane forests (Hafkenschied, 2000; Bruijnzeel 2001; Fleischbein et al. 2005; 2006).

Nutrients enter forest ecosystems through rain, deposition of dust and aerosols, fixation by microorganisms above and below the ground (in the case of N), and weathering of the substratum (except for N) (Proctor, 2005). Nutrient input to the forest floor is provided by rainfall, throughfall, and stemflow, and the chemical composition of the input varies depending on climate, vegetation, and sources of chemical transformation (Proctor, 2005). Nutrient loss from forest ecosystems is reflected in the nutrients in different pools, as well as their fluxes into and out of the system and between these pools. Bruijnzeel (1991) examined the balance of Ca, Mg, K, P, and N fluxes in 25

4. Water and nutrient balances

tropical forest sites and concluded that annual input flux through rainfall (AIF_R) varied greatly depending on the location of dust and aerosols. He also demonstrated that nutrient losses per unit streamflow increased with increasing site fertility level.

In tropical montane forests, one factor restricting the N cycle may be the relatively slow decomposition rate of organic matter, which is determined by the relatively low temperatures at high elevations. Conversely, the N cycle in tropical lowland forests might not be restricted in the same way because of the higher rate of organic matter decomposition that occurs under high temperatures at low elevations (Grubb, 1989). These perceptions of the differences in N cycling between tropical montane and lowland forests might have been created by some studies which have estimated that the annual output flux (AOF) of N from tropical montane forests was less than that from tropical lowland forests (Grubb, 1989). However, a review of 25 case studies by Bruijnzeel (1991) found that the N AOF from tropical montane forests was not necessarily smaller than that from tropical lowland forests. He suggested that the accuracy of the AOF estimates was limited because the methods used to estimate nutrient AOF varied among sites.

Since the publication of the aforementioned review, several studies have discussed this matter. For example, in a tropical montane forest in the Luquillo Mountains, Puerto Rico, inorganic N AIF_R was 1.89 kg/ha/year, annual input flux through rainfall (AIF_T) was 3.52 kg/ha/year, and AOF was 1.29 kg/ha/year (McDowell, 1998). This study postulated that internal N cycling at Luquillo was limited by N resource availability and that almost all inorganic N input was absorbed by vegetation. This explanation was based on an ecological hypothesis that the balance of inorganic N in forest ecosystems is explained mainly by internal recycling. Since the work of Schuur (2001), however, it is clear that decomposition and N availability is dominated by soil water status rather than temperature. N deficiency also leads to tougher leaves that are harder to decompose, etc. Temperature effect seems to be limited a reduction in ET (rainfall–streamflow) such as water balance, and hence an increase in precipitation-excess (Kitayama, 1995). Markewitz et al. (2006) reported that in a tropical lowland forest in Corrego Roncador, Brazil, inorganic N AIF_R and AOF were 4.1 and 0.2 kg/ha/year, respectively, and suggested the possibility that the output flux of suspended solids might have increased the inorganic N output flux. They pointed out the necessity of considering not only inorganic N that flows out into the internal N cycle without being absorbed by plants but also flow that moves outside the forest ecosystem with the movement of stream water. In

4. Water and nutrient balances

Amazonia, for example, there is an indication that in many cases neither N nor P but base metals are the growth-limiting factors because base metals are often in poor supply in the strongly weathered soils (Cuevas and Medina, 1988; Martinelli et al. 1999).

Determining the nutrient balance in forested watersheds requires characterizing hydrologically mediated nutrient output. Determining the AOF is complicated by the great variability of ion concentrations in discharge waters (McDowell and Asbury, 1994; Godsey et al. 2004; Boy et al. 2008). In southern Ecuador, for example, increasing concentrations of nitrates ($\text{NO}_3\text{-N}$), dissolved organic carbon, dissolved organic nitrogen, and in some cases ammonium nitrate ($\text{NH}_4\text{-N}$) in streamwater were reported when discharge was high. The concentrations of these chemical constituents were greatest during periods of heavy rain (Wilcke et al. 2001; Goller et al. 2006; Boy et al. 2008). In Peninsular Malaysia, Zulkifli et al. (2006) reported that concentrations of K^+ , $\text{NO}_3\text{-N}$, and Mg^{2+} increased during storms. However, in most previous studies nutrient AOF was calculated by multiplying annual discharge with the volume-weighted mean concentration of nutrients or by using the relationship between ion concentration and discharge (C–Q curve; McDowell, 1998; Markewitz et al. 2006). Some studies that have used C–Q curves have not described the equations used or how the coefficients of the C–Q curves were determined. To estimate the contribution of different flow classes to the AOF, Boy et al. (2008) developed a model in which they classified hourly discharge (obtained with TOPMODEL) into their flow classes. They multiplied the cumulative discharge for a given flow class during the 5-year period monitored with the mean concentration of each of the chemical constituents studied in the same flow class. However, their analyses did not include continuous discharge data or intensive water sampling during stormflow periods (Boy et al. 2008; Wilcke et al. 2009). Studies that have used both hydrological and biogeochemical approaches to elucidate the stormflow-related element of the AOF are limited, particularly for the tropics (Saunders et al. 2006).

This chapter involves a discussion of the following three objectives. The first objective was to examine the water balance and hydrological characteristics in the LT and KM watersheds and to compare these results with data obtained at a number of other locations in the humid tropics of Malaysia. The second objective was to reexamine the perception of differences in nutrient balance between tropical lowland and montane forests. Nutrient input and output estimates were made using comparative watershed-based studies through sequential and event-based sampling of rainwater and

streamwater and by continuous hydrological observations. I am unaware of any other comprehensive studies that have included continuous observations of water quality and volume in both tropical lowland and montane forests for the same period. The third objective was to estimate the nutrient AIF and AOF and the balance between them. To evaluate the accuracy of the AOF values, I tested six estimation methods using continuous discharge data and concentration–discharge relationships for each water sampling event.

4.2 Methods

4.2.1 Site descriptions

In this chapter, LT watershed in LHNP and KM watershed in MKNP were used to examine water and nutrient balances. The details of the watersheds are described in Chapter 2.

LT watershed

In the LHNP, the LT experimental watershed was used in this chapter (*Table 4.1*). LT is characterized by rugged topography, with several waterfalls and exposed mutual strata including mudstone and some pyrites. This area was uplifted and gently folded about 1.6 million years ago at the onset of the Pleistocene (Wilford, 1961). No gypsum or any hydrothermal activity has been reported in the LHNP, which is on clay udult ultisol soils over shale and on sandy humult ultisols (Hazebroek and Aband Kashim, 2001). The forest in LHNP consists of two types of indigenous vegetation common throughout Borneo: mixed dipterocarp forest and tropical heath forest (Yamakura et al. 1995; Ashton, 1998; Potts et al. 2002). Our study site was established within the mixed dipterocarp forest on red-yellow podsols (ultisols). The lowest point of LT is at an elevation of 90.4 m a.s.l. and is located about 13.7 km from the nearest coast. The weather station and rainwater sampling point used in this study are about 2.3 km from the LT (4°11'23"N, 114°01'09"E). The mean annual rainfall and mean annual air temperature are normally 2,650 mm (2000–2008) and 25.9°C (2000–2007), respectively (*Table 4.1*).

KM watershed

The KM watershed in MKNP was used in this chapter (*Table 4.1*). KM is located on soils

4. Water and nutrient balances

derived from sedimentary rocks (Trusmadi and Crocker formations) folded in the Tertiary period (Kitayama et al. 2004). These sedimentary rocks were intensely folded in an orogeny that culminated in the middle of the Miocene (Jacobson, 1970). The soil is at an advanced stage of development and is classified as Spodosol (Kitayama et al. 2004). The most abundant canopy tree species are *Tristaniopsis* sp. (Myrtaceae) and the conifers *Dacrycarpus* and *Dacrydium* spp. (Podocarpaceae) (Kitayama et al. 2004). The lowest point of KM has an elevation of 1,697.7 m a.s.l. and is located about 44.5 km from the nearest coast. The weather station and rainwater sampling points used were about 1.4 km from KM. The mean annual rainfall is around 3,000 mm, but it was extraordinarily low in 1997 and 1998 (Table 4.1), which were years associated with El Niño events (Malmer 2004, Walsh and Newberry, 1999). The mean annual air temperature is around 18°C, but it was slightly higher in 1997 and 1998 (Table 4.1).

Table 4.1 Features of the LT and KM watersheds.

Watershed name	Location	Distance from the nearest coast (km)	Elevation at acral area (m.a.s.l.)	Annual mean rainfall (mm)	Annual mean air temperature (°C)	Area (ha)	Vegetation	Soil (USDA)	Geology
Tower Large (LT)	4°11'23" N, 114°01'09" E	13.7	90.4	2650 (2000-2008)	25.9 (2000-2007)	23.25	Dipterocarpaceae	Ultisol	Tertiary sedimentary rocks
Mempening (KM)	6° 00' 42" N, 116°32' 27" E	42.6	1697.7	1709 (1997-1998) 3168 (1996, 1999-2008)	18.6 (1997-1998) 17.2 (1996, 1999-2008)	1.78	<i>Tristaniopsis</i> , <i>Dacrycarpus</i> , <i>Podocarpus</i>	Spodosol	Tertiary sedimentary rocks

4.2.2 Rainfall and discharge observations

Rainfall was measured with a tipping-bucket rain gauge (20-cm diameter, 0.5-mm tip resolution; Ohta Keiki Co., Tokyo, Japan) and a data logger (1-s time resolution; KADEC-PLS, Kona System Co., Sapporo, Japan). At LT, discharge was measured by recording the water height at a site of exposed bedrock, where stream flow velocity was zero in a natural pool, with rapid flow generated at the outlet of the pool (Shiraki and Wakahara, 2005). Discharge was measured through water level measurements of the stilling pool of a V-notch weir at KM using an automatic water level recorder (SE-TR/WT500, TruTrack Co., New Zealand) at 10-min intervals.

4.2.3 Rainwater, throughfall, and stream water sampling: Intensive observations during rainfall-induced stormflow

4. Water and nutrient balances

Rainwater for chemical analysis was collected at LT and KM using bulk samplers consisting of a PVC funnel (20-cm diameter) connected to an 18-L container, installed 0.5 m above the ground. A filter made of glass wool was placed at the bottom of the funnel to prevent contamination by particulate matter and insects. These bulk samplers were also installed above the ground in the forest to collect throughfall for chemical analysis at LT and KM. Rainwater and throughfall were transferred twice a week from the bulk samplers into 100-mL polyethylene bottles. To identify spatial variations in nutrient deposition from rainfall at KM, rainfall was sampled in August 2008 using 10 bulk samplers located around the rain gauge. For the same purpose, throughfall was sampled in June 2007 using 20 bulk samplers located randomly around the throughfall sampler.

Stream water for chemical analysis was collected twice a week into 100-mL polyethylene bottles at the discharge observation points of the two watersheds. Intensive stream water sampling during rainfall-induced stormflow events was performed four times at the watershed discharge observation points using an automatic liquid sampler (Model 900, Sigma Co., USA) at sampling intervals ranging from 10 to 120 min.

4.2.4 Chemical analysis

Sample bottles were transferred to the field laboratory within 30 min of sampling and immediately refrigerated at 2°C. All samples were filtered through a 0.2- μm filter (Minisart RC15, hydrophilic regenerated cellulose) within 2 months of sampling. The concentrations of cations (Na^+ , NH_4^+ , K^+ , Mg^{2+} , and Ca^{2+}) and anions (Cl^- , NO_3^- , SO_4^{2-}) were analysed using ion chromatography (HIC-6A; Shimadzu Co., Kyoto, Japan). The precision of the ion chromatography results was assessed as $\pm 5\%$, based on standard solutions. However, the accuracy of the volatile NO_3^- and NH_4^+ data may have been lower than that of the other ions.

4.2.5 Convert from water level to discharge

To convert water level to discharge, an empirical exponential function was used.

LT watershed

The estimated relationship between water level (H [m]) and discharge (Q [m^3/s]) was calculated as the same method as free fall from weir. Discharge at water level h_0 is calculated as:

4. Water and nutrient balances

$$Q(h_0) = \int_0^{h_0} C \cdot f(h) \cdot v(h) dh$$

where C : contracted coefficient ($= 0.6$), $f(h)$: width of cross section at $h=h_0$ and v : flow velocity

$v(h) = \sqrt{2g(h_0-h)}$ (Wakahara et al. in reviewing). The observed streamflow was checked by observing

the distribution of flow velocity with propeller type current meter (every 10 or 20cm horizontally and every 2cm vertically) at high water level or collecting whole water at low water level. *Figure 4.1* shows the good relationship between the estimated H-Q curve and observed data.

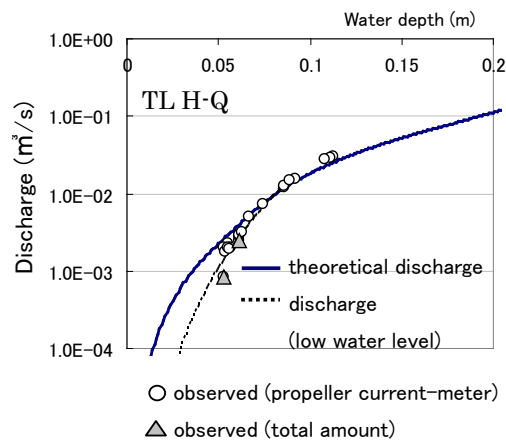


Figure 4.1 Relationship between water level (water depth in this figure) and discharge at LT (TL in this figure) watershed (Wakahara et al. in reviewing).

KM watershed

To determine the parameters of that function, discharge measurements were carried out four times in each watershed between August 2005 and July 2006 using a cylinder, polyethylene bucket, and stopwatch at KM. *Figure 4.2* shows the observed discharge at each water level and the functions between water level and discharge. The respective equations is:

4. Water and nutrient balances

$$Q = 1.548 H^{2.5}$$

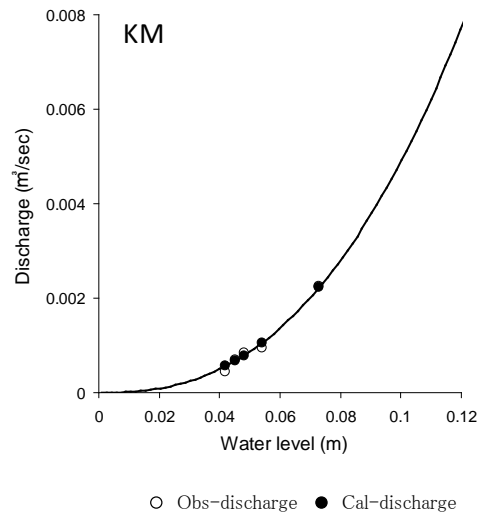


Figure 4.2 Relationship between water level and discharge at KM watershed.

4.2.6 Imputation of missing data

Some discharge measurement data for the 2 year period are missing. In LT, data was no missing (Wakahara et al. in reviewing). In KM, data was missing for 39 days (from 13 October to 20 November) in 2006 and 42 days (from 3 February to 16 March) in 2007. This was because of the greater sediment yield from the watershed which made continuous water level measurement difficult. To fill in for the missing data, a rainfall - runoff simulation model (Kuraji, 1996) was applied. Observation data from 1 September 2005 to 29 February 2006 was used for model calibration. The model was proposed to simulate the rainfall – runoff relationship in the Sapulut (SP) and Ulu Kalumpang (UK) experimental watersheds. The model is a simple lumped model with minimum parameters (*Figure 4.3*). The time resolution of the input rainfall and output discharge data are 1 hour and the calculation time step is also 1 hour. First, rainfall is stored in the canopy storage tank and overflows if the water exceeds the maximum water storage (Sc [mm]). Canopy interception (Ei [mm/hour]) occurs when the canopy storage tank is not empty. The water that overflows is equal to the net rainfall (Rn [mm/hour]), and is separated into effective rainfall (Re [mm/hour]) which enters the discharge tank, and infiltration flow which enters the soil storage tank. The effective rainfall ratio (α) was calculated by a function of the water storage of the soil storage tank (Sb [mm]) as follows:

4. Water and nutrient balances

$$\alpha = S_b - S_0 / S_{100} - S_0$$

where S_{100} [mm] and S_0 [mm] stand for the water storage of the baseflow tank when the effective rainfall ratios are 100% and 0%, respectively. In daytime when the canopy storage tank was empty, transpiration (E_t [mm/hour]) occurs from the soil storage tank. The discharge-storage function of the discharge tank is as follows:

$$S_d = K_d \cdot D_d$$

where D_d [mm/hour], S_d [mm] and K_d [$\text{mm}^{0.7}/\text{hour}^{0.3}$] stand for discharge, water storage in the discharge tank and the coefficient of the discharge tank, respectively.

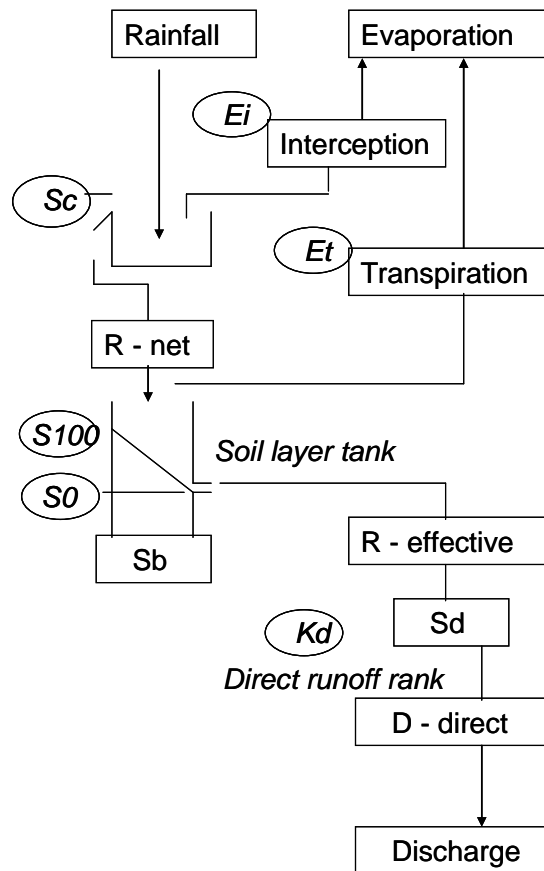


Figure 4.3 Schematic diagram of the proposed hydrological cycle model.

The results of the model calibration and simulation of the periods with data missing and the parameters determined by the calibration period are shown in *Figure 4.4* and *Table 4.2*, respectively.

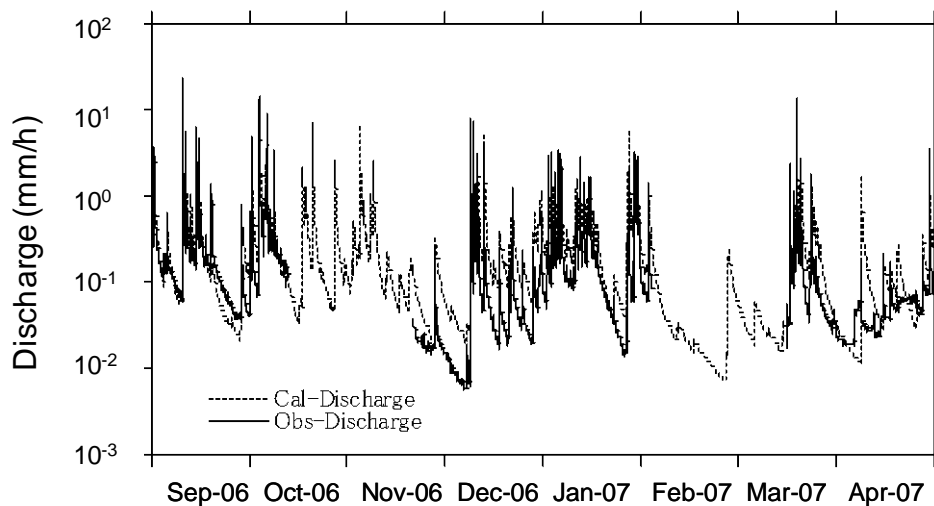


Figure 4.4 Model output and observed hourly discharge of the KM watershed from September 2006 to April 2007.

Table 4.2 List of the parameters.

		KM
Maximum storage of the canopy	Sc [mm]	0.60
Interception rate from the wet canopy	Ei [mm/h]	0.06
Transpiration rate	Et [mm/h]	0.19
Soil storage for the runoff coefficient of 100%	$S100$ [mm]	107.40
Soil storage for the runoff coefficient of 0%	$S0$ [mm]	53.70
Storage function coefficient of the direct runoff	Kd [mm ^{0.7} /hour ^{0.3}]	0.40

4.2.7 Annual input fluxes from rainfall and throughfall

Annual input fluxes from rainfall and throughfall were calculated by summation of the fluxes from each sampling interval, which were calculated by multiplying the volume of water by the concentration of nutrients. Rainfall volume during the sampling period was recorded directly using automatic rain gauges in LT and KM. The volume of throughfall during each sampling period was not observed directly in LT and KM during the study period, but was estimated using the following equations,

4. Water and nutrient balances

$$TF_{(LT)} = -1.825 + 0.899 * P_{(LT)} \quad P_{(LT)} > 2.03 \quad (1)$$

$$= 0 \quad P_{(LT)} \leq 2.03$$

$$TF_{(KM)} = 0.940 * P_{(KM)} \quad (2)$$

where $P_{(LT)}$, $P_{(KM)}$, $TF_{(LT)}$, and $TF_{(KM)}$ are rainfall at KM and LT and throughfall at LT and KM, respectively. Equations (1) and (2) are published data from Manfroi et al. (2004) and based on unpublished data collected from KM in June 2007, respectively.

4.2.8 Annual output fluxes

To increase the accuracy of the nutrient AOF estimations, the following six methods were applied (Table 4.3).

Table 4.3 Definition of AOF estimated by six different methods.

Method	Intensive observation during rainfall-induces stormflow		
	Without	With	With
WWM × Annual Discharge	I	-	
C-Q equation	II	III	IV
Σ (WWM × Discharge) _[flow class]	V	VI	

I : Calculation by multiplying annual discharge by volume weighted mean annual concentration.

II : C-Q equation without stormflow data.

III : C-Q equation with stormflow data.

IV : C-Q equation by piecewise continuous linear function with two pieces.

V : Method of Boy et al (2008).

VI : Method of Boy et al (2008) with stormflow data.

First, the AOF was calculated by multiplying annual discharge with the volume-weighted mean annual concentration of nutrients (Method I). Second, the AOF was calculated from 10-min interval discharge data and the relationship between discharge and concentration (C–Q equation).

4. Water and nutrient balances

The exponential equation $\text{Log}(\text{Concentration}) = a + b \text{Log}(\text{Discharge})$ was adopted, and the coefficients of the C–Q equations were obtained from linear regression on log–log plots both without (Method II) and with (Method III) data from samples taken during rainfall-induced stormflow. *Figure 4.5* shows the relationship between various ion concentrations and discharge in the LT and KM watersheds. These data include periodic samples and samples taken during rainfall-induced stormflow. For example, nitrate ion (NO_3^-) concentration increased when discharge increased from 0 to 0.1318 mm/10 min (LT) or 0.3632 mm/10 min (KM) and decreased at discharge rates above these values (*Figure 4.5a*). When discharge increased, the K^+ concentration tended to increase in LT, but it decreased slightly in KM (*Figure 4.5c*). Chloride ion concentration was almost constant in KM but decreased in LT when discharge increased (*Figure 4.5g*). The concentrations of other nutrients, including Na^+ and SO_4^{2-} , showed trends similar to that of Cl^- . The relationship between ion concentrations and discharge were different in LT and KM.

4. Water and nutrient balances

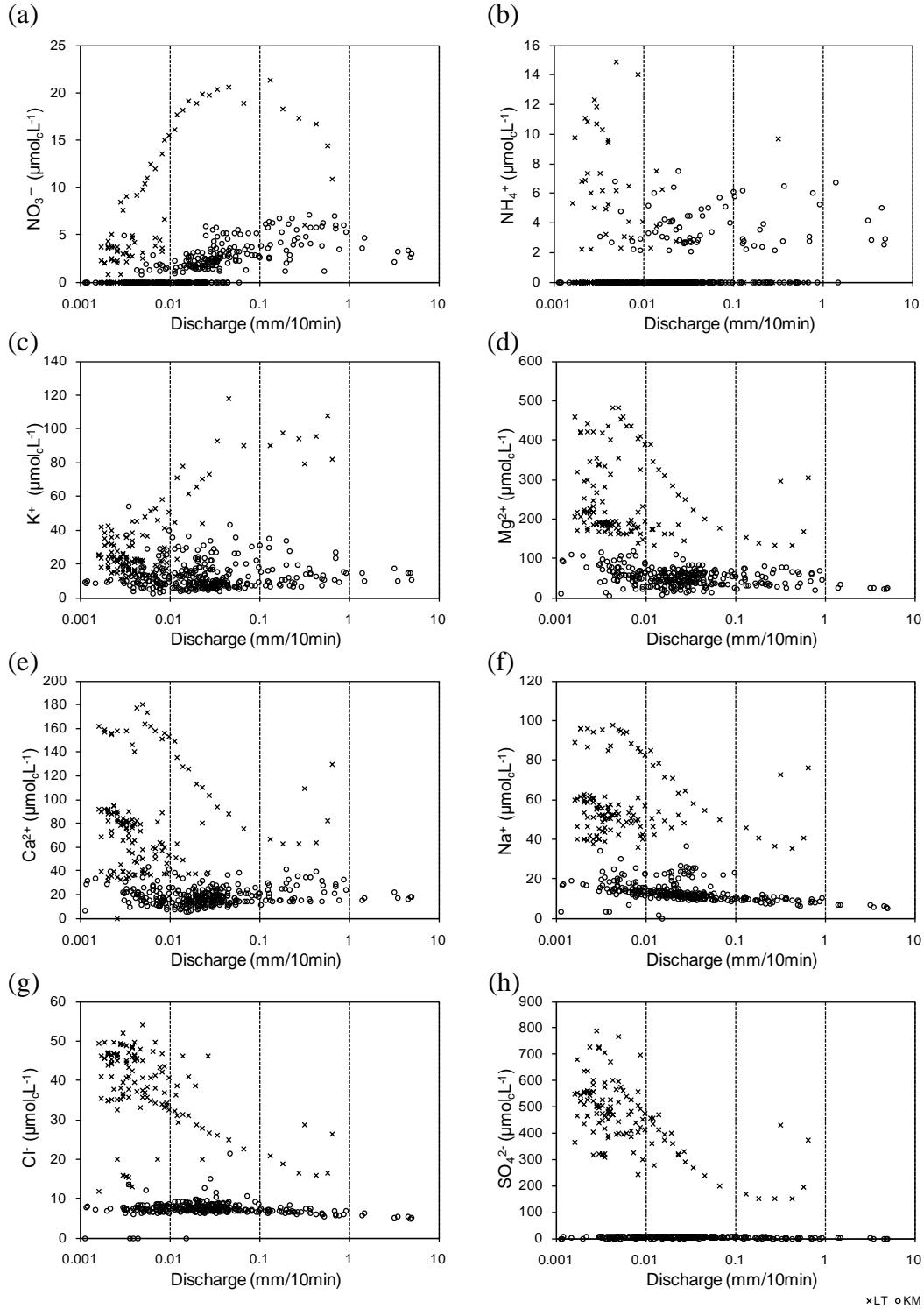


Figure 4.5 Relationship between discharge and ion concentration of (a) NO_3^- , (b) NH_4^+ , (c) K^+ , (d) Mg^{2+} , (e) Ca^{2+} , (f) Na^+ , (g) Cl^- , and (h) SO_4^{2-} at LT and KM watersheds.

4. Water and nutrient balances

Figures 4.6 (a) and (b) show flow duration curves for hourly discharge data from 2006 to 2007 in the LT and KM watersheds, respectively. Flow classes were defined by their relation to the 2-year mean discharge (MD2Y) for each watershed (Boy et al. 2008). The discharge of the flow classes was defined as super dry (less than 25% of the MD2Y of each watershed), baseflow (25%–50% of the MD2Y of each watershed), or intermediate (50%–200% of the MD2Y of each watershed). Stormflow was defined as occurring if the discharge was more than double the 2-year mean. The MD2Y of LT and KM were 0.1452 and 0.2496 mm/h, respectively.

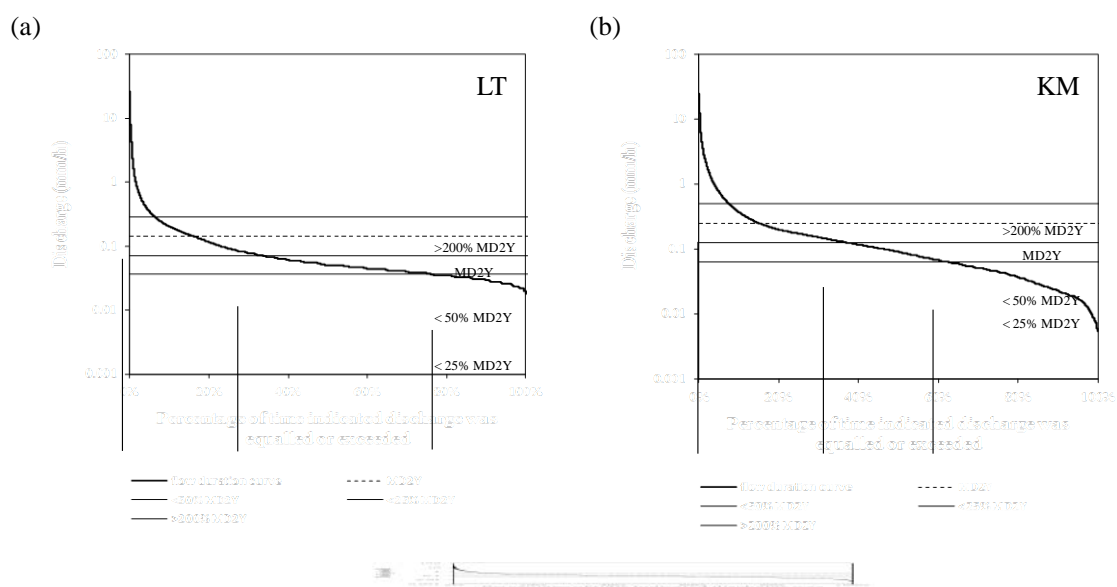


Figure 4.6 Flow duration curves for hourly discharge data from 2006 to 2007 in the (a) LT and (b) KM watersheds. MD2Y = mean discharge over 2 years.

The only data necessary for Method I were the annual discharge (roughly estimated by subtracting rainfall from evapotranspiration), the concentration of periodically sampled water, and the simultaneous discharge at sampling times. For Methods II and V, continuously recorded discharge data were necessary. For Methods III and VI, the concentrations of samples during stormflow were added. Methods III and VI were more accurate but they required the highest quality data.

4.3 Results

4.3.1 Water balance

Table 4.4 shows the values of annual rainfall, discharge, loss, mean air temperature, and mean water temperature for LT in 2006 and 2007 and for KM in 2006, 2007, and 2008. The annual rainfall was $\pm 10\%$ of the long-term average annual rainfall in both LT and KM (Table 4.1). During this observation period, El Niño or La Niña had not occurred. The annual discharge in KM was approximately twice that in LT because the annual rainfall in KM was 120–670 mm greater than that in LT. Furthermore, annual evapotranspiration may be greater in LT than in KM owing to the higher temperatures in LT.

Table 4.4 Annual rainfall, discharge, loss, mean air temperature, and mean water temperature from 2006 to 2008 in the LT and KM watersheds.

		Rainfall (mm)	Discharge (mm)	Loss (mm)	Mean air temperature (°C)	Mean water temperature (°C)
2006	LT	2867.0	1165.7	1701.3	26.8	25.1
	KM	3203.0	2350.5	852.5	16.2	16.4
2007	LT	2986.0	1377.9	1608.1	27.2	-
	KM	3109.0	2022.3	1086.7	16.2	16.4
2008	LT	2661.9	-	-	-	-
	KM	3338.0	2731.7	606.3	16.1	16.3

4.3.2 Estimation of output fluxes

Method II, III and IV

The coefficients of the C–Q equations and the AOF values for nutrients estimated using Methods II, III, and IV are shown in Table 4.5(a). The results of the piecewise continuous linear C–Q curve for the estimation of NO₃-N are shown in parentheses in Table 4.5(b). In KM, the difference between the estimate made by Method III and that from the piecewise continuous linear C–Q curve was relatively small, whereas in LT, Method III gave a 50% underestimate of the AOF of NO₃-N compared to the piecewise continuous linear C–Q curve.

4. Water and nutrient balances

Table 4.5 Parameters of the exponential equation, $\text{Log}(\text{Concentration}) = a + b \text{Log}(\text{Discharge})$, of the relationship between concentration (C , $\mu\text{mol}_c\text{L}^{-1}$) and discharge (Q , $\text{mm}/10 \text{ min}$) in LT and KM.

(a) Linear regression. (b) Piecewise continuous linear function with two parts.

		II				III			
		a	b	n	R ²	a	b	n	R ²
NO ₃ ⁻	LT	-0.1512	-0.1554	89	0.0209	0.6183	0.1058	115	0.0298
	KM	0.5362	0.2213	194	0.2289	0.5910	0.2419	230	0.4326
NH ₄ ⁺	LT	0.2049	-0.0196	89	0.0002	0.0678	-0.0704	115	0.0106
	KM	0.0973	0.0113	194	0.0005	0.3186	0.1224	230	0.1087
K ⁺	LT	1.0248	-0.1186	89	0.0473	2.0827	0.3005	115	0.3940
	KM	0.8513	-0.0801	194	0.0159	0.9821	-0.0111	230	0.0009
Mg ²⁺	LT	1.9434	-0.1533	89	0.1827	2.2632	-0.0359	115	0.0206
	KM	1.5524	-0.0780	194	0.0204	1.4633	-0.1211	230	0.1346
Ca ²⁺	LT	1.4511	-0.1286	89	0.0214	1.9709	0.0658	115	0.0197
	KM	1.0696	-0.0785	194	0.0275	1.1778	-0.0207	230	0.0059
Na ⁺	LT	1.6456	-0.0212	89	0.0089	1.6956	-0.0226	115	0.0000
	KM	0.9407	-0.0939	194	0.0415	0.8726	-0.1284	230	0.2044
Cl ⁻	LT	1.3885	-0.0806	89	0.0209	1.2474	-0.1378	115	0.2345
	KM	1.0984	0.1230	194	0.0944	0.8657	0.0032	230	0.0002
SO ₄ ²⁻	LT	2.2436	-0.1806	89	0.2213	2.2317	-0.1875	115	0.5055
	KM	0.9642	0.1752	194	0.0948	0.5710	-0.0309	230	0.0081

II : C-Q equations were obtained by both linear regression on the log-log plots without samples during stormflow.

III : C-Q equations were obtained by both linear regression on the log-log plots with samples during stormflow.

		Q (mm/h)	a	b	n	R ²
NO ₃ ⁻	LT	≥ 200%MD2Y	1.0138	-0.2567	8	0.2330
		200%MD2Y > 0	1.6038	0.5292	107	0.1456
KM	KM	≥ 200%MD2Y	0.5459	-0.0728	28	0.0408
		200% MD2Y > 0	0.5905	0.2461	202	0.2543

Method V and VI

The occurrence and distribution of discharge levels measured among the four flow classes in the LT and KM watersheds are shown in *Tables 4.6 (a, b, and c)*. As shown in *Tables 4.6 (a) and (b)*, the storm distribution was sampled more frequently in LT than KM, therefore the hourly distribution during the storm was less in LT than KM. It is difficult to periodically sample increased flow classes such as “stormflow” in a watershed such as LT that already has a high hourly distribution in super dry conditions. The discharge distributions during stormflow were 60.4% and 58.9% in LT and KM, respectively, indicating it was necessary to take samples during rainfall-induced stormflow (*Table 4.6c*). Boy et al. (2008) calculated AOF values without continuous discharge data and intensive

4. Water and nutrient balances

water sampling during stormflow periods. I calculated AOF using the continuous discharge data in Method V and using the continuous discharge data and the intensive water sampling during stormflow periods in Method VI.

Table 4.6 Occurrence distributions of sampled, hour and discharge over the four classes of LT and KM watersheds. (a) Jan 2006 – Dec 2006, (b) Jan 2007 – Dec 2007, and (c) Intensive observation during rainfall-induced stormflow.

(a)

2006	Sampled distribution n (%)		Hour distribution n (%)		Discharge distribution mm (%)	
	39	104	8760	8760	1165.7	2350.5
	LT	KM	LT	KM	LT	KM
Superdry	36 (92.3)	30 (28.8)	3763 (43.0)	2547 (29.1)	111.2 (9.5)	96.5 (4.1)
Baseflow	3 (7.7)	37 (35.6)	3152 (36.0)	2529 (28.9)	155.3 (13.3)	232.1 (9.9)
Intermediate	0 (0)	35 (33.7)	1426 (16.2)	2973 (33.9)	195.5 (16.8)	637.4 (27.1)
Storm	0 (0)	2 (1.9)	419 (4.8)	711 (8.1)	703.7 (60.4)	1384.5 (58.9)

(b)

2007	Sampled distribution n (%)		Hour distribution n (%)		Discharge distribution mm (%)	
	50	90	8760	8760	1377.9	2022.3
	LT	KM	LT	KM	LT	KM
Superdry	30 (60.0)	41 (45.6)	367 (4.2)	3965 (45.2)	12.5 (0.9)	131.6 (6.5)
Baseflow	13 (26.0)	17 (18.9)	4532 (51.7)	1955 (22.3)	233.6 (17.0)	176.1 (8.7)
Intermediate	7 (14.0)	31 (34.4)	3171 (36.2)	2233 (25.5)	429.7 (31.2)	485.1 (24.0)
Storm	0 (0)	1 (1.1)	690 (7.9)	607 (6.9)	702.1 (51.0)	1229.5 (60.8)

(c)

Intensive observation	Sampled distribution n (%)			
	26	36		
	LT	KM		
Superdry	5 (19.2)	0 (0)		
Baseflow	5 (19.2)	0 (0)		
Intermediate	8 (30.8)	11 (20.8)		
Storm	8 (30.8)	25 (47.2)		

Table 4.7 compares nutrient AOF in LT and KM estimated using the six different methods. Figures 4.7 and 4.8 compare mean AOF values for NO₃-N and NH₄-N (2006–2007), respectively, based on Table 4.7. The vertical axes of each figure indicate the AOF values calculated for each watershed. In LT, the NO₃-N AOF values determined using Methods I, II, and V without intensive water sampling during stormflow periods were underrepresented compared with Methods III and VI. In KM, the NH₄-N AOF values estimated by Methods I, II, and V were also underrepresented

4. Water and nutrient balances

compared with Methods III, IV, and VI. This suggests that estimations of NO₃-N AOF made without continuous discharge measurements may be erroneous.

Table 4.7 Comparison of nutrient AOF estimated by six different methods, in LT and KM.

Watershed name	Year		NO ₃ -N	NH ₄ -N	Inorg-N	K	Mg	Ca	Na	Cl	SO ₄ -S
							(kg/ha/year)				
LT	2006	I	0.2	0.8	1.0	9.6	36.5	13.6	13.1	16.8	108.8
		II	0.2	0.3	0.4	6.3	71.5	35.5	12.4	12.1	203.5
		III	0.6	0.2	0.8	39.0	112.0	78.0	13.9	10.1	202.1
		IV	1.5	0.2	1.7	39.0	112.0	78.0	13.9	10.1	202.1
		V	0.2	0.8	1.0	10.0	36.7	12.7	12.7	16.1	106.8
		VI	2.2	0.2	2.4	35.4	34.3	22.3	15.4	10.6	61.4
	2007	I	0.2	0.3	0.5	11.2	28.8	15.9	15.8	18.6	88.0
		II	0.2	0.3	0.5	7.9	89.9	44.5	14.8	14.8	258.6
		III	0.6	0.3	0.9	35.4	134.4	87.9	16.7	12.7	257.0
		IV	1.8	0.3	2.1	35.4	134.4	87.9	16.7	12.7	257.0
		V	0.1	0.4	0.5	11.2	27.6	13.9	15.4	18.1	82.7
		VI	2.3	0.2	2.5	38.1	36.1	24.0	17.5	13.1	67.8
KM	2006	I	0.5	0.2	0.7	8.7	13.2	7.2	6.9	6.5	1.9
		II	0.8	0.4	1.2	7.6	47.4	25.7	5.7	8.6	10.7
		III	0.9	0.6	1.5	9.0	42.3	29.5	5.2	6.1	5.9
		IV	0.9	0.6	1.5	9.0	42.3	29.5	5.2	6.1	5.9
		V	0.7	0.1	0.8	7.8	12.6	7.2	5.5	6.8	2.0
		VI	0.9	0.7	1.6	10.5	9.6	7.8	4.9	5.3	1.1
	2007	I	0.3	0.1	0.4	10.3	14.6	8.3	5.7	6.1	1.6
		II	0.7	0.3	1.1	6.5	40.7	22.1	4.9	7.4	9.3
		III	0.8	0.5	1.3	7.7	36.4	25.3	4.5	5.3	5.7
		IV	0.8	0.5	1.3	7.7	36.4	25.3	4.5	5.3	5.7
		V	0.6	0.0	0.6	7.7	16.0	9.5	4.7	6.4	1.8
		VI	0.7	0.6	1.3	10.1	9.0	7.3	4.0	4.7	0.9

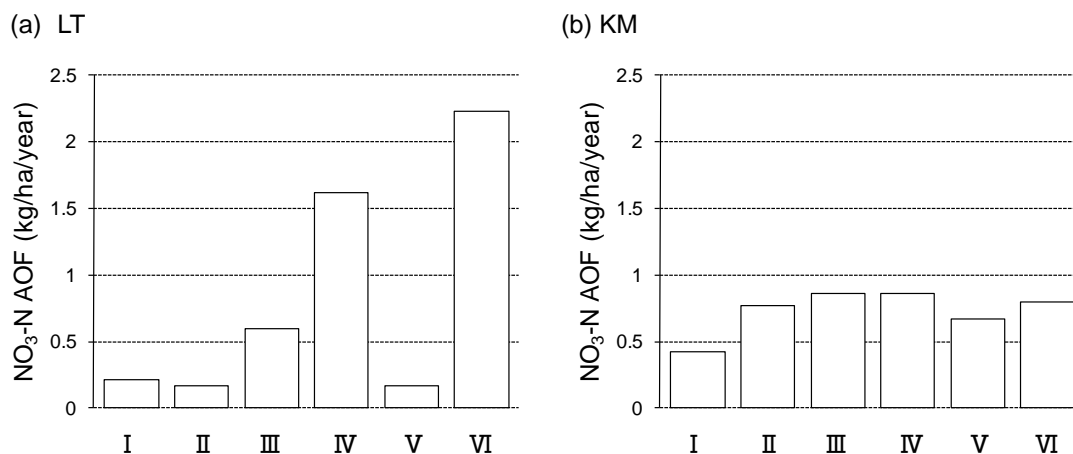


Figure 4.7 Comparison of NO₃-N AOF estimated by six different methods, in (a) LT and (b) KM.

4. Water and nutrient balances

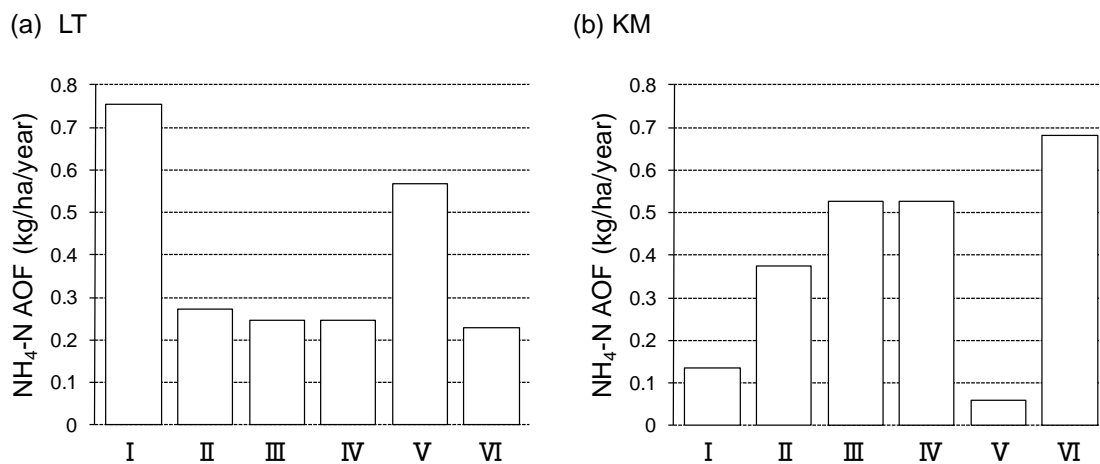


Figure 4.8 Comparison of NH₄-N AOF estimated by six different methods, in (a) LT and (b) KM.

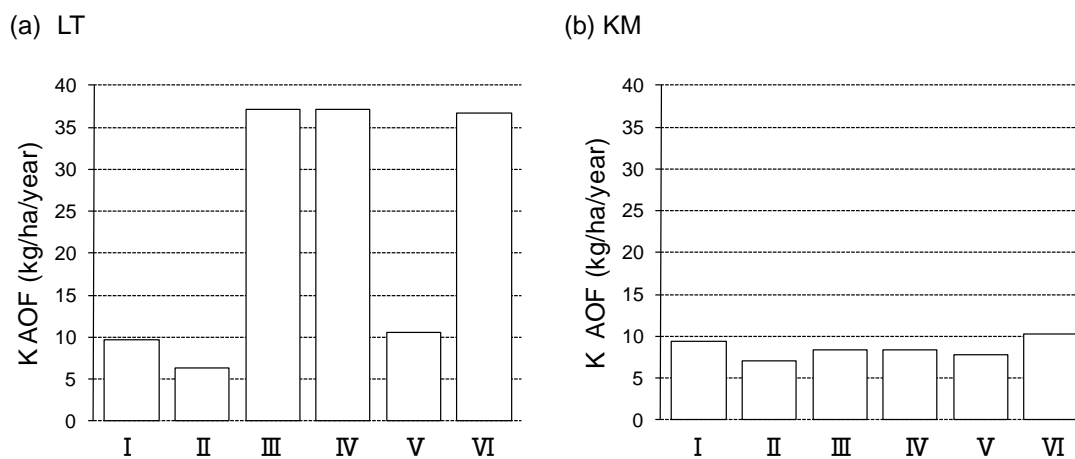


Figure 4.9 Comparison of K AOF estimated by six different methods, in (a) LT and (b) KM.

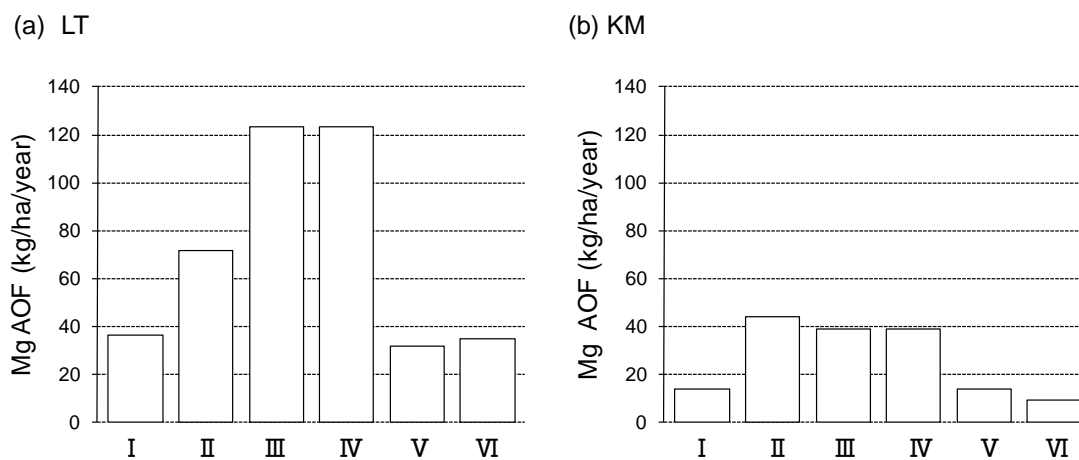


Figure 4.10 Comparison of Mg AOF estimated by six different methods, in (a) LT and (b) KM.

4. Water and nutrient balances

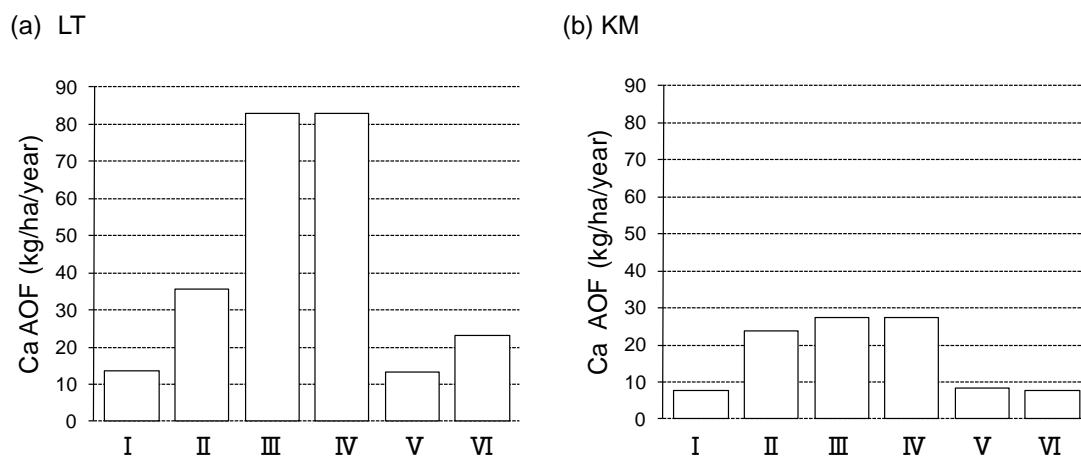


Figure 4.11 Comparison of Ca AOF estimated by six different methods, in (a) LT and (b) KM.

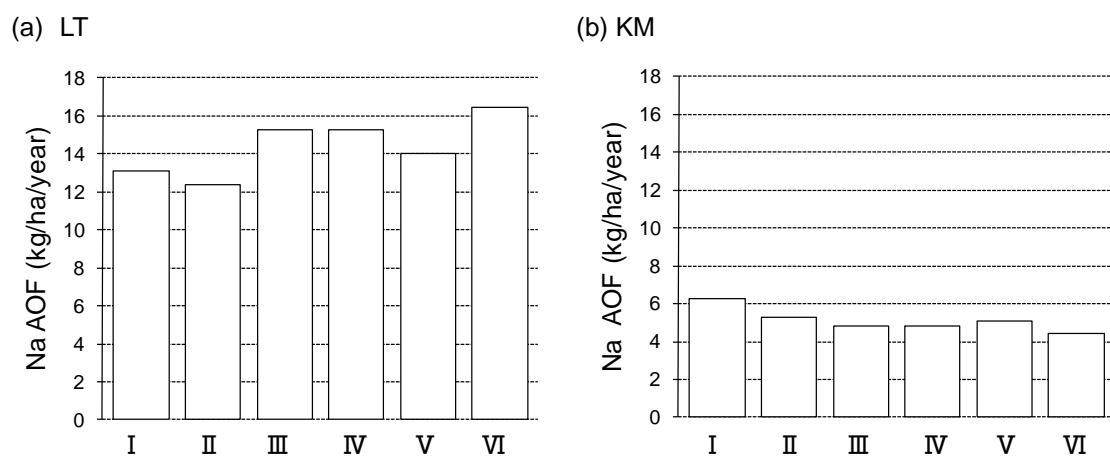


Figure 4.12 Comparison of Na AOF estimated by six different methods, in (a) LT and (b) KM.

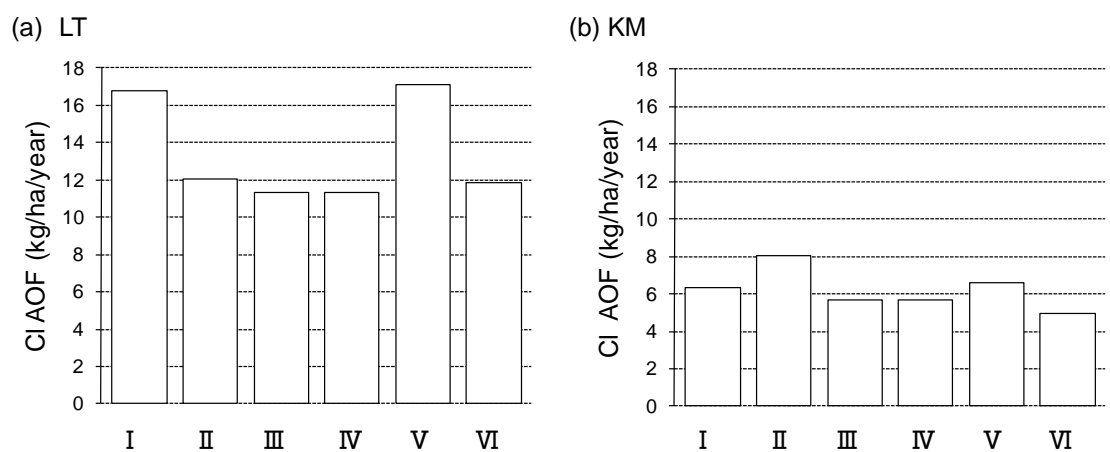


Figure 4.13 Comparison of Cl AOF estimated by six different methods, in (a) LT and (b) KM.

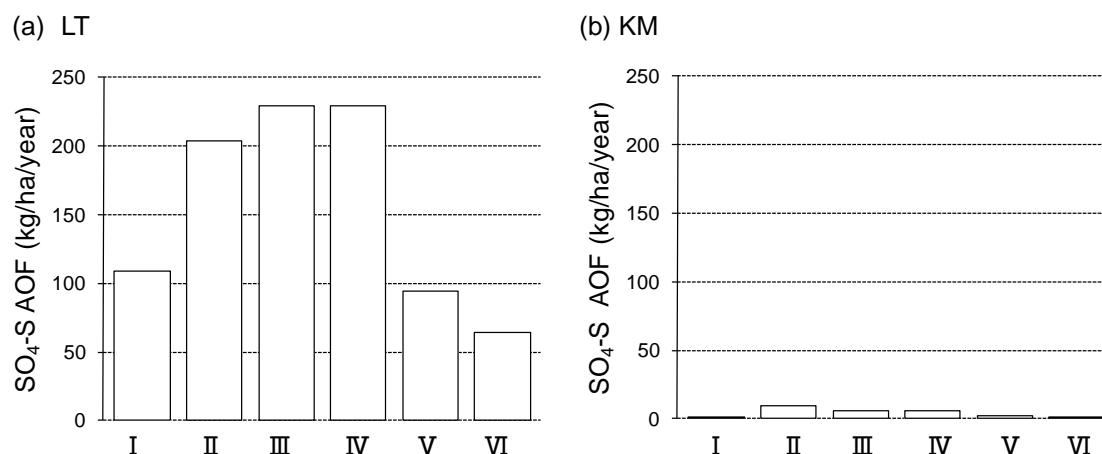


Figure 4.14 Comparison of $\text{SO}_4\text{-S}$ AOF estimated by six different methods, in (a) LT and (b) KM.

Figures 4.9–4.14 compare mean AOF values for K, Mg, Ca, Na, Cl, and $\text{SO}_4\text{-S}$ (2006–2007) based on Table 4.7. The vertical axes of each figure indicate the AOF values calculated for each watershed.

Despite differences in the absolute values, the AOF values for Mg, Ca, and $\text{SO}_4\text{-S}$ estimated by Methods II and III were greater than those determined by the other methods in both LT and KM. The AOF values calculated for Na and Cl showed little variation among the six methods. The AOF values for Mg, Ca, and $\text{SO}_4\text{-S}$ estimated using the C–Q equation were overrepresented compared to those determined by the other methods. After examining all of the data, I decided that the use of Method VI resulted in the most meaningful and accurate values.

4.3.3 Nutrient balance

Table 4.8 shows the annual input fluxes from rainfall (AIF_R) and throughfall (AIF_T) and the AOF values and balances of nutrients and other elements (Na, Cl, and $\text{SO}_4\text{-S}$). The values in parenthesis are the standard deviations of the spatial variation of the input flux from rainfall and throughfall for each element.

The output fluxes were estimated using Method VI. In LT in 2006, inorganic N AIF_R (5.8 kg/ha/year) and AIF_T (5.2 kg/ha/year) were higher than the AOF (2.4 kg/ha/year). In KM, the inorganic N AIF_R (2.4–9.7 kg/ha/year) was greater than the AOF (1.3–2.1 kg/ha/year). In 2008, the AIF_T (9.4 kg/ha/year) was 2.1 times the AIF_R and 4.5 times the AOF.

4. Water and nutrient balances

Table 4.8 AIF_R, AIF_T, and AOF from 2006 to 2008 in the LT and KM watersheds.

Watershed name	Year		NO ₃ -N	NH ₄ -N	Inorg-N	K	Mg	Ca
(kg/ha/year)								
LT	2006	AIF _R	1.9	3.9	5.8	8.1	6.6	22.4
		AIF _T	2.1	3.1	5.2	36.3	15.6	15.7
		AOF	2.2	0.2	2.4	35.4	34.3	22.3
	2007	AOF	2.3	0.2	2.5	38.1	36.1	24.0
KM	2006	AIF _R	1.5 (0.5)	8.2 (6.6)	9.7 (6.0)	13.8 (21.4)	5.0 (3.8)	31.1 (17.7)
		AOF	0.9	0.7	1.6	10.5	9.6	7.8
	2007	AIF _R	0.2 (0.1)	2.2 (1.8)	2.4 (1.5)	13.6 (21.1)	5.1 (3.9)	106.6 (60.6)
		AOF	0.7	0.6	1.3	10.1	9.0	7.3
	2008	AIF _R	1.4 (0.4)	3.0 (2.4)	4.4 (2.7)	10.8 (16.7)	5.4 (4.2)	126.3 (71.7)
		AIF _T	0.1 (-)	9.3 (29.5)	9.4 (29.6)	65.8 (18.3)	10.1 (2.7)	21.9 (8.0)
		AOF	1.1	0.9	2.1	13.9	10.6	10.0

Watershed name	Year		Na	Cl	SO ₄ -S
(kg/ha/year)					
LT	2006	AIF _R	6.8	9.1	6.5
		AIF _T	11.2	21.4	6.1
		AOF	15.4	10.6	61.4
	2007	AOF	17.5	13.1	67.8
KM	2006	AIF _R	5.2 (1.2)	6.5 (5.4)	4.8 (2.4)
		AOF	4.9	5.3	1.1
	2007	AIF _R	5.3 (1.2)	6.1 (5.0)	3.3 (1.6)
		AOF	4.0	4.7	0.9
	2008	AIF _R	4.3 (1.0)	4.1 (3.4)	3.9 (2.0)
		AIF _T	4.0 (1.1)	6.4 (3.1)	6.5 (2.5)
		AOF	5.1	5.8	1.0

Note: AIF_R = Annual Input Flux by Rainfall; AIF_T = Annual Input Flux by Throughfall; AOF = Annual Output Flux; (): Standard deviation

AIF_R = $\sum C_R P_E$ C:Concentration of rainwater ($\mu\text{mol}_e\text{L}^{-1}$); P_E:The volume of rainfall in each sampling interval (mm)

AIF_T = $\sum C_T T_E$ C:Concentration of throughfall ($\mu\text{mol}_e\text{L}^{-1}$); T_E:The volume of throughfall in each sampling interval (mm)

In KM, the K AIF_R was 10.8–13.8kg/ha/year, which was higher than the AOF (10.1–13.9 kg/ha/year). In contrast, the K AIF_R (8.1 kg/ha/year) in LT was 4.6 times smaller than the AOF (35.4 kg/ha/year) in 2006. In 2008, the K AIF_T in KM was 65.8 kg/ha/year, which was more than 4.7 times the AIF_R and AOF, whereas the K AIF_T in LT (36.3 kg/ha/year) was almost the same as the AOF.

The Mg AOF in LT (34.3 kg/ha/year) was 2.2 and 5.2 times the AIF_R (6.6 kg/ha/year) and AIF_T (15.6 kg/ha/year) in 2006, respectively. In KM, the Mg AOF (9.0–10.6 kg/ha/year) was 1.7–2.1 times the AIF_R (5.0–5.4 kg/ha/year). In 2008, the AIF_T was 10.1 kg/ha/year, higher than the AIF_R but almost same as the AOF.

In KM, the values of Ca AIF_R were 31.1, 106.6, and 126.3 kg/ha/year in 2006, 2007, and 2008, respectively, and the respective AOF values were 7.8, 7.3, and 10.0 kg/ha/year. Great

4. Water and nutrient balances

inter-annual variations were observed in AIF_R that were higher than those of the AOF for all three years. The Ca AIF_T in 2008 was 21.9 (kg/ha/year), only 5.8% and 12.6% of the AIF_R and AOF, respectively. In LT, the Ca AOF in 2006 (22.3 kg/ha/year) was 1.0 and 1.4 times the AIF_R (22.4 kg/ha/year) and AIF_T (15.7 kg/ha/year), respectively.

The Na AOF in LT (17.5 kg/ha/year) was 2.3 and 1.4 times the AIF_R (6.8 kg/ha/year) and AIF_T (11.2 kg/ha/year) in 2006, respectively. In KM, the Na AOF (4.0–5.1 kg/ha/year) was almost same values the AIF_R (4.3–5.3 kg/ha/year). In 2008, the AIF_T was 4.0 kg/ha/year, almost same values the AIF_R.

The Cl AOF in LT (10.6 kg/ha/year) was 1.2 times and one-half the AIF_R (9.1 kg/ha/year) and AIF_T (21.4 kg/ha/year) in 2006, respectively. In KM, the Cl AOF (4.7–5.8 kg/ha/year) was almost same values the AIF_R (4.1–6.5 kg/ha/year). In 2008, the AIF_T was 6.4 kg/ha/year, higher than the AIF_R but almost same as the AOF.

The SO₄-S AOF in LT (61.4 kg/ha/year) was 9.4 and 10.1 times the AIF_R (6.5 kg/ha/year) and AIF_T (6.1 kg/ha/year) in 2006, respectively, whereas in KM, the SO₄-S AOF (0.9–1.1 kg/ha/year) was one-five and one-three the AIF_R (3.3–4.8 kg/ha/year). In 2008, the AIF_T was 6.5 (kg/ha/year), higher than the AIF_R.

4.4 Discussion

4.4.1 Water balance

Annual rainfall, discharge and loss (rainfall minus discharge) from 2006 to 2008 had already shown in *Table 4.4*. During this observation period, El Niño or La Niña had not occurred. The annual discharge in KM was approximately twice that in LT because the annual rainfall in KM was 120–670 mm greater than that in LT. Furthermore, annual evapotranspiration may be greater in LT than in KM owing to the higher temperatures in LT.

To compare the annual losses observed in other experimental watersheds throughout Malaysia, *Table 4.9* lists the other watersheds, their elevation, area, observation period, mean annual rainfall, discharge and loss. *Figure 4.15* shows the relationship between (a) rainfall and discharge, (b) rainfall and loss, (c) elevation and loss, and (d) watershed area and loss based on *Table 4.9*. No clear correlation between mean annual rainfall and loss (b) was found, but there was significant

4. Water and nutrient balances

(99%) negative correlation between elevation and mean annual loss (c).

Table 4.9 Water balance in the tropical forested catchments in Malaysia (<100 ha).

No.	Site name	Watershed name	Elevation (m.a.s.l.)	Watershed area (ha)	Observation period (Num. of hydro.year)	Rainfall (mm)	Runoff (mm)	Loss (mm)	References
Malaysia									
1	Ulu Combak		244-548	31.5	1968-1969 (1)	2,500	750	1,750	Kenworthy (1969)
2	Sungai Tekam	C	70	56.2	1977-1986 (9)	1,902	322	1,580	DID (1989)
		sub B	68.5	59.2	1983-1986 (3)	2,148	634	1,514	DID (1989)
		A	72.5	37.7	1983-1986 (3)	2,171	804	1,368	DID (1989)
3	Berebun	C1	168-252	12.9	1980-1983 (3)	1,884	223	1,661	Abdul Raham et al., (1985)
		C2	168-223	4.2	1980-1983 (3)	1,922	275	1,648	Abdul Raham et al., (1985)
		C3	160-293	29.6	1980-1983 (3)	2,003	225	1,778	Abdul Raham et al., (1985)
4	Bukit Tarek	C1	48-175	32.8	1989-1994 (5)	2,700	1,160	1,540	Abdul Raham et al., (1985); Zulkifli et al., (2006)
		C2	53-213	34.3	1989-1994 (5)	2,700	1,132	1,568	Abdul Raham et al., (1985); Zulkifli et al., (2006)
5	Mendolong	W3	650-750	18.2	1985-1990 (5)	3,215	1,962	1,253	Malmer (1992)
		W6	650-750	4.5	1985-1990 (5)	3,490	1,950	1,540	Malmer (1992)
6	Sapulut	SP	515-760	59.4	1991-1992 (2)	2,318	880	1,450	Kuraji and Paul (1995)
7	Ulu Kalumpang	UK	200-275	22.3	1991-1992 (2)	1,851	581	1,206	Kuraji and Paul (1995)
8	Lambir Hills	LT	90-250	23.3	2006-2007 (2)	2,927	1,272	1,655	Gomyo et al., (this study)
9	Kinabalu Park	KM	1,695-1,750	1.8	2006-2008 (3)	3,217	2,368	849	Gomyo et al., (this study)

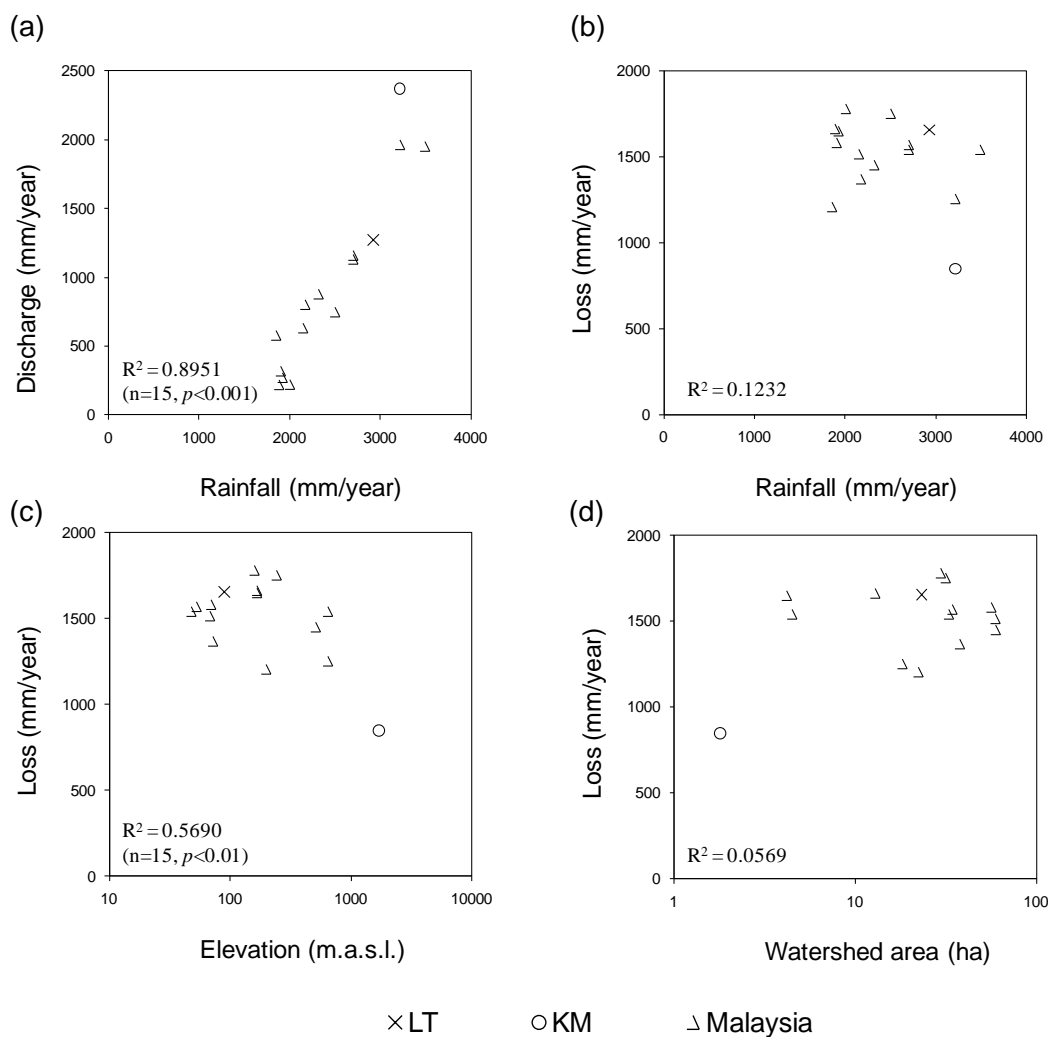
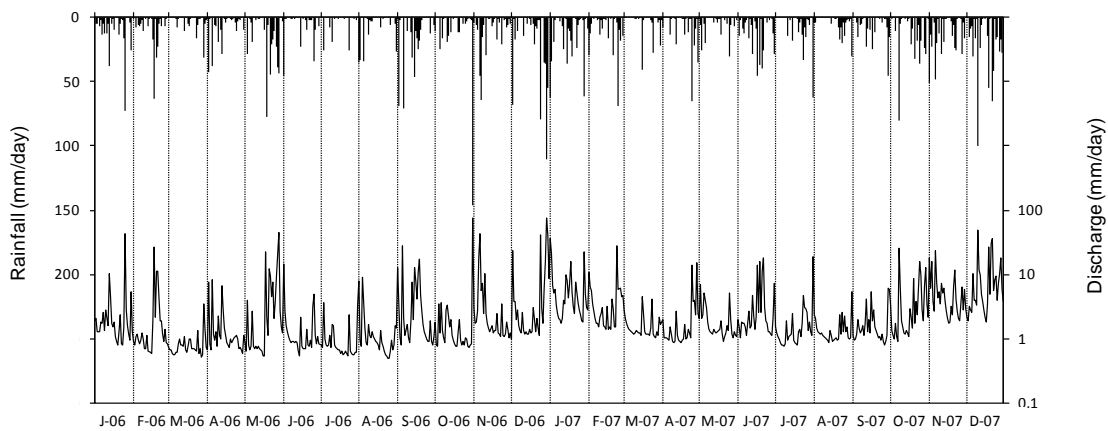


Figure 4.15 Comparison of relationship between (a) rainfall and discharge, (b) loss and rainfall, (c) loss and elevation, and (d) loss and watershed area in the tropical forested catchments in Malaysia. Water balance in the tropical forested catchments in Malaysia (<100 ha).

4.4.2 Rainfall and flow duration curves

Figure 4.16 (a and b) show a time series of daily rainfall and discharge in LT and KM from January 2006 to December 2007, respectively. A series of rainfall events observed at the end of December 2007 are shown in Figure 4.16. One possibility for the greater loss in 2007 compared with that in 2006 is that the discharge of the rainfall at the end of 2007 may have been delayed to early January 2008.

(a) LT



(b) KM

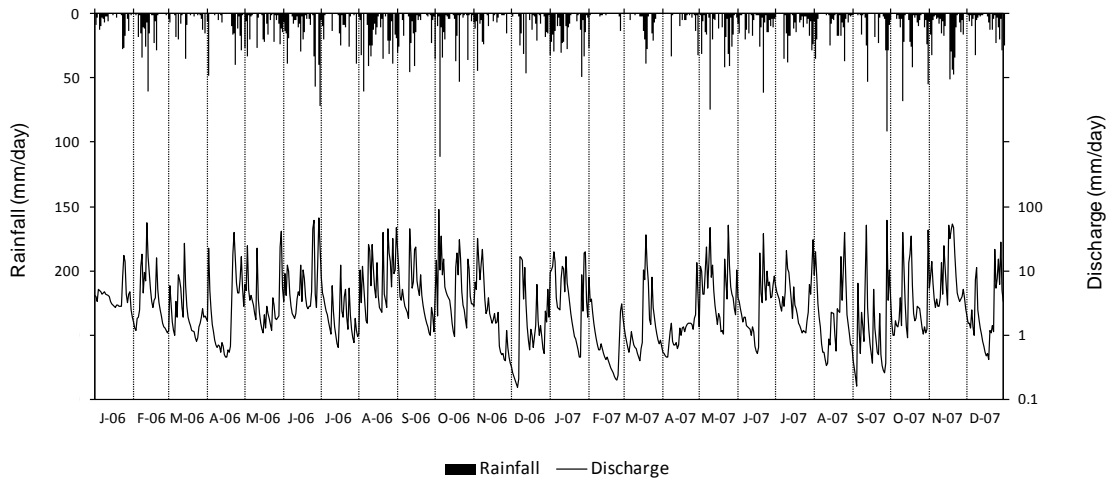


Figure 4.16 Daily rainfall and daily discharge at LT (a) and KM (b) watersheds from January 2006 to December 2007.

4. Water and nutrient balances

Next, rainfall (a) and flow (b) duration curves in LT and KM for 2 years (2006 and 2007) are shown in *Figure 4.17*. Rainfall and flow duration curves observed in two other experimental watersheds in Sabah (SP and UK; Kuraji, 1996) for two years (1991 and 1992) are also shown. The probability of daily rainfall greater than 1 mm in LT, KM, SP and UK was 54%, 60%, 73% and 68%, respectively. The probability of zero daily rainfall in LT, KM, SP and UK was 41%, 33%, 21%, and 26%. The fluctuation of zero daily rainfall was the smallest in SP and the greatest in LT. The probability of daily discharge less than 1 mm in LT, KM, SP and UK was 27%, 20%, 34% and 2.5%, respectively. In LT, KM and UK, there is water flow in the stream throughout a year, whereas in SP the flow frequently ceased. The shape of the flow duration curve in UK looks gentler than those for LT, KM and SP. To compare the gentleness of the curve, the differences of daily discharge when the probability of occurrence exceeds 80% (D80) and 20% (D20) were compared. The differences between D20 and D80 in LT, KM, SP and UK were 2.6, 6.5, 5.6, and 2.2 mm, respectively, showing that the fluctuation of daily discharge was the smallest in UK and the greatest in KM. The difference of the flow duration curve was caused by the difference of rainfall and watershed bedrock geology (Katsuyama et al. 2008). The bedrock geology in KM and SP is Tertiary Sedimentary Rocks, whereas the geology in UK is volcanic ash.

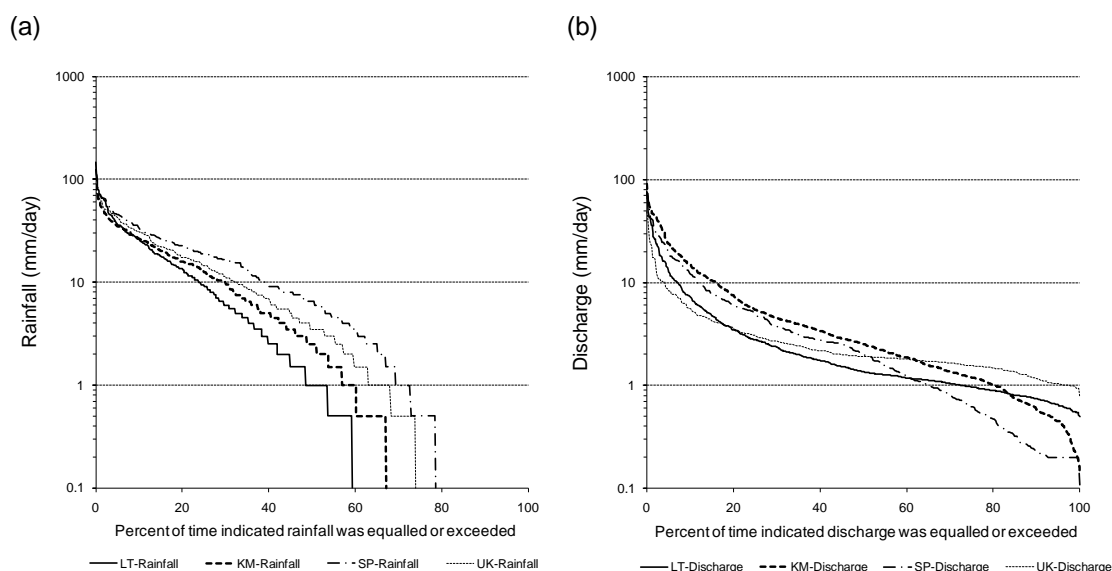


Figure 4.17 (a) Daily rainfall and (b) daily flow duration curves for two years daily rainfall and discharge data (LT and KM = 2006 and 2007, SP and UK = 1991 and 1992).

4.4.3 Output flux estimation methods

Figure 4.18 shows the relationship between discharge and NO_3^- concentration. Nitrate ion concentrations were measured using the six different methods. The relationship between change in NO_3^- concentration and discharge is complex; therefore, the effect of each flow class on NO_3^- concentration was determined. Methods I, II, and V did not account for concentration variations during stormflow; therefore, the output flux values obtained may have been underestimated. Method III did not indicate a relationship between discharge and NO_3^- concentration. Output flux calculated using Method VI may have been overestimated during stormflow. These results suggest that the level of accuracy for each method differs among sites and among nutrient elements. After examining all of the data I decided that Method VI resulted in the most meaningful and accurate values.

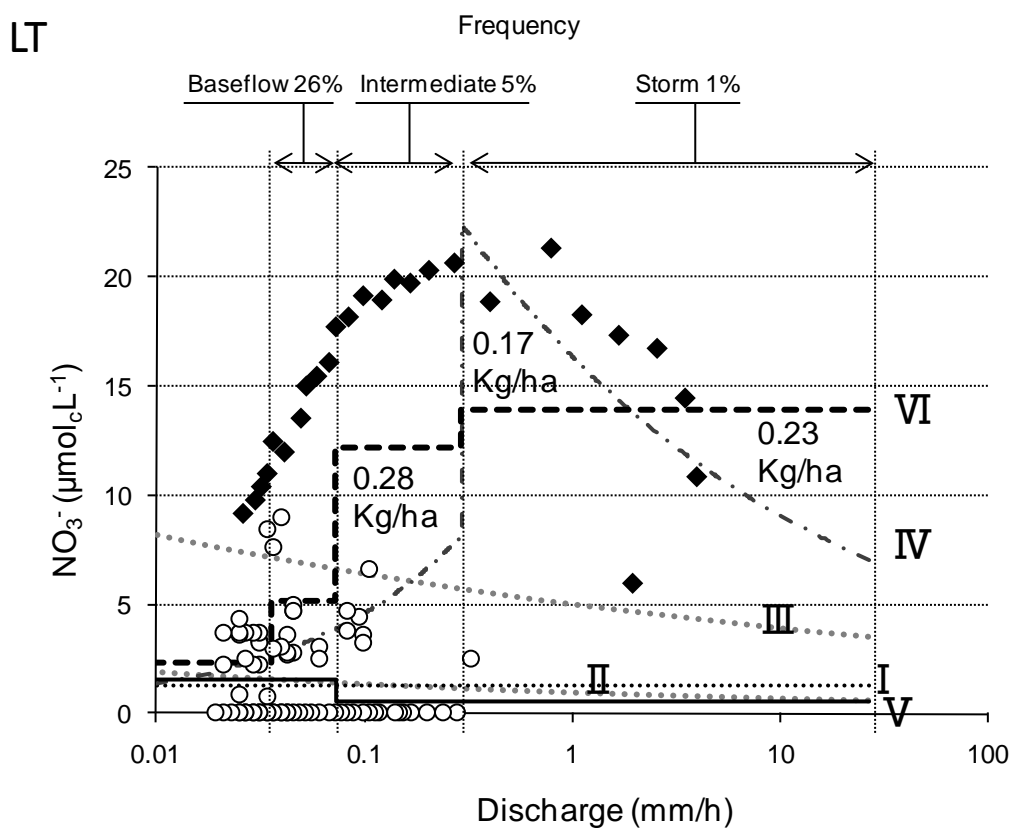


Figure 4.18 Relationship between discharge and NO_3^- concentration, NO_3^- concentration values estimated by used six methods, and frequency of each flow in LT watershed.

4.4.4 Partitioning output flux into in different flow classes

In this study, I estimated nutrients AOF from continuous discharge and output flux data allow annual water and nutrient AOFs to be partitioned into water and nutrient fluxes in different flow classes.

Table 4.10 shows the mean hour, mean discharge and mean AOF by discharge in different flow classes (2006–2007). Percentage values indicate the fraction of total AOF for the corresponding flow class. *Figure 4.19* shows the results of percentage frequencies, discharge, and AOF by discharge in different flow classes (2006-2007) in the LT and KM watersheds based on *Table 4.10*. The flux during storm class was 55.3% and 59.8% of the total discharge, even though the frequency of occurrence was 6.3% and 7.5% in LT and KM, respectively. Zulkifli et al. (2006) reported that the NO₃-N and K AOF values were 73–75% and 62–66% of the total AOF, respectively, during stormflow from two experimental watersheds. Although their definition of stormflow was different from that used in the present study, these ratios are comparable with those obtained in LT (61.4% for NO₃-N and 69.0% for K). Zulkifli et al. (2006) concluded that the leaching of NO₃-N and K from leaves and branches during stormflow produced the relatively higher percentages of NO₃-N and K AOF. Periodic sampling is normally undertaken at times of baseflow, but total AOF cannot be estimated without nutrient concentration data collected during stormflow. In this study, I found that the AOF values of nutrients in KM could be estimated using the Method V of the periodic sampling only, and it was not necessary to conduct water sampling during stormflow. In LT, however, nutrient AOF values (except for NH₄-N, Na, and Cl) were difficult to estimate from the Method I, II and IV without water sampling during stormflow.

4. Water and nutrient balances

Table 4.10 (a) Mean hour (b) Mean discharge and (c) mean AOF by discharge in different flow classes (2006 – 2007). Percentage values indicate the fraction of total AOF for the corresponding flow class.

(a)

Mean (2006-2007)		Superdry		Baseflow		Intermediate		Storm		Total
	Watershed	n	%	n	%	n	%	n	%	n
Hour	LT	2065.0	23.6	3842.0	43.9	2298.5	26.2	554.5	6.3	8760
	KM	3256.00	37.2	2242.0	25.6	2603.0	29.7	659.0	7.5	8760

(b)

Mean (2006-2007)		Superdry		Baseflow		Intermediate		Storm		Total
	Watershed	mm	%	mm	%	mm	%	mm	%	mm
Discharge	LT	61.85	4.9	194.5	15.3	312.60	24.6	702.9	55.3	1271.8
	KM	114.05	5.2	204.1	9.3	561.25	25.7	1307.0	59.8	2186.4

(c)

Mean AOF (2006-2007)		Superdry		Baseflow		Intermediate		Storm		Total
	Watershed	kg/ha/year	%	kg/ha/year	%	kg/ha/year	%	kg/ha/year	%	kg/ha/year
NO ₃ -N	LT	0.03	1.3	0.20	8.8	0.63	28.5	1.37	61.4	2.2
	KM	0.01	0.7	0.02	2.6	0.16	20.0	0.61	76.8	0.8
NH ₄ -N	LT	0.03	12.4	0.05	19.9	0.04	17.0	0.12	50.6	0.2
	KM	0.01	0.9	0.02	2.5	0.07	10.4	0.59	86.2	0.7
Inorg-N	LT	0.06	2.4	0.24	9.9	0.67	27.4	1.48	60.4	2.5
	KM	0.01	0.8	0.04	2.5	0.23	15.5	1.20	81.1	1.5
K	LT	0.63	1.7	2.48	6.8	8.28	22.5	25.38	69.0	36.8
	KM	0.58	5.7	1.08	10.4	2.18	21.2	6.47	62.7	10.3
Mg	LT	2.22	6.3	6.72	19.1	8.73	24.8	17.54	49.8	35.2
	KM	0.86	9.3	1.16	12.5	3.15	34.0	4.10	44.2	9.3
Ca	LT	1.05	4.5	3.81	16.4	5.66	24.4	12.65	54.6	23.2
	KM	0.44	5.8	0.63	8.4	1.88	24.8	4.63	61.0	7.6
Na	LT	0.85	5.1	2.88	17.5	4.29	26.1	8.45	51.3	16.5
	KM	0.41	9.2	0.63	14.1	1.52	34.2	1.89	42.6	4.4
Cl	LT	0.88	7.4	2.45	20.7	3.33	28.1	5.19	43.8	11.8
	KM	0.29	5.9	0.57	11.5	1.58	31.6	2.55	51.1	5.0
SO ₄ -S	LT	5.67	8.8	14.22	22.0	16.33	25.3	28.40	43.9	64.6
	KM	0.08	8.0	0.16	16.4	0.45	45.8	0.29	29.8	1.0

4. Water and nutrient balances

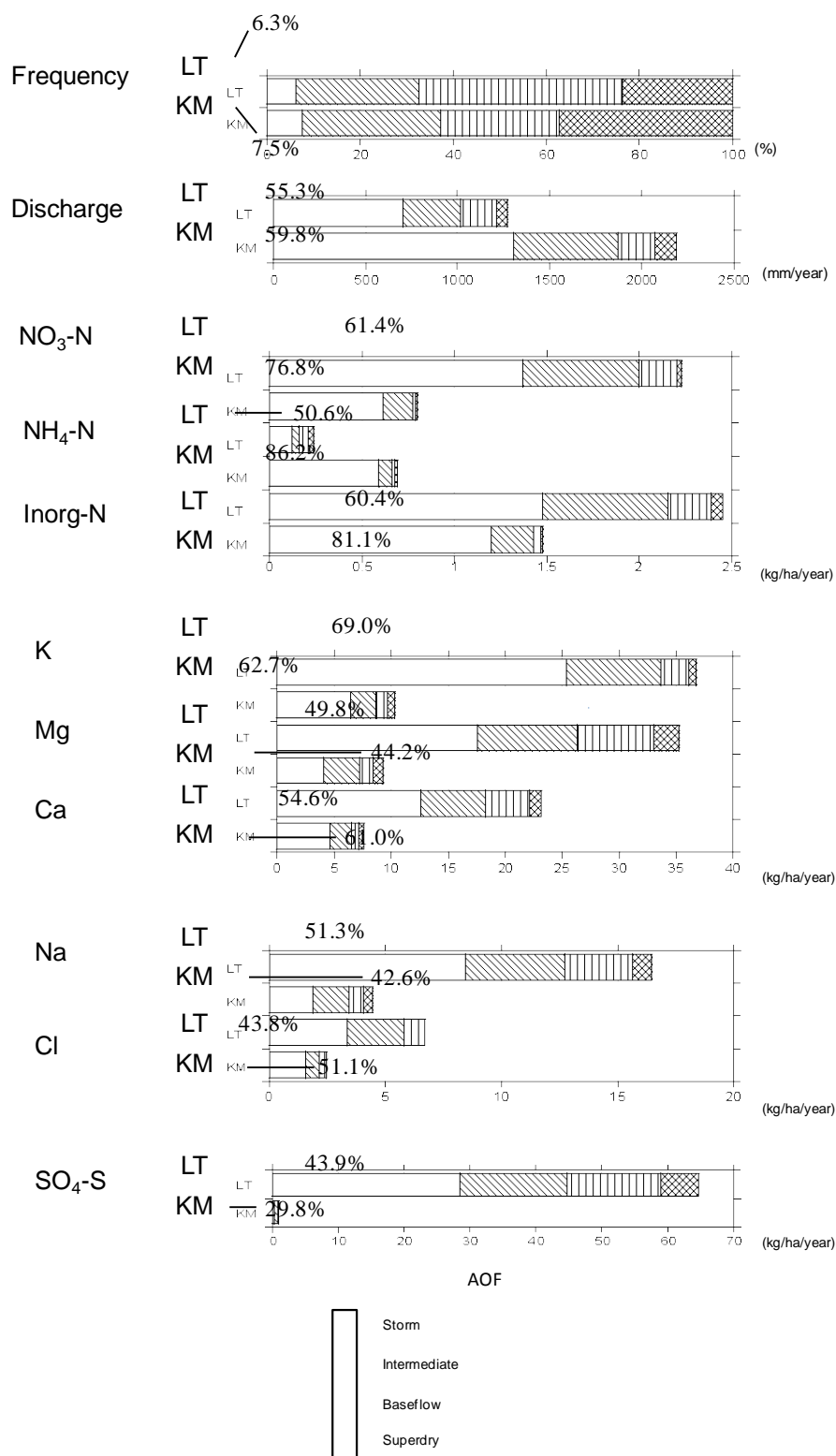


Figure 4.19 Percentage frequencies, discharge, and AOF by discharge in different flow classes (2006-2007) in the LT and KM watersheds.

4.4.5 Nutrient balances in LT and KM

Inorganic Nitrogen

Figure 4.20 compares mean AIF_R , annual input flux through throughfall (AIF_T), and AOF values for NO_3-N , NH_4-N , and inorganic nitrogen from 2006 to 2008 in the LT and KM watersheds based on Table 4.8.

The AIF_R and AIF_T of NH_4-N were greater than those of NO_3-N , and the AOF of NO_3-N was greater than that of NH_4-N in both the LT and KM watersheds. A portion of the NO_3-N in the forest soil might have been reabsorbed by the plants, with the remainder draining through to the streamwater. The following discussion focuses on inorganic N balance without considering the mineralization of organic N.

No distinct differences in terms of inorganic N balance were detected between the tropical lowland forest (LT) and the tropical montane forest (KM). Because of the lack of dissolved organic nitrogen data collected it is difficult to form any conclusions about the differences in nitrogen balance and cycling between LT and KM.

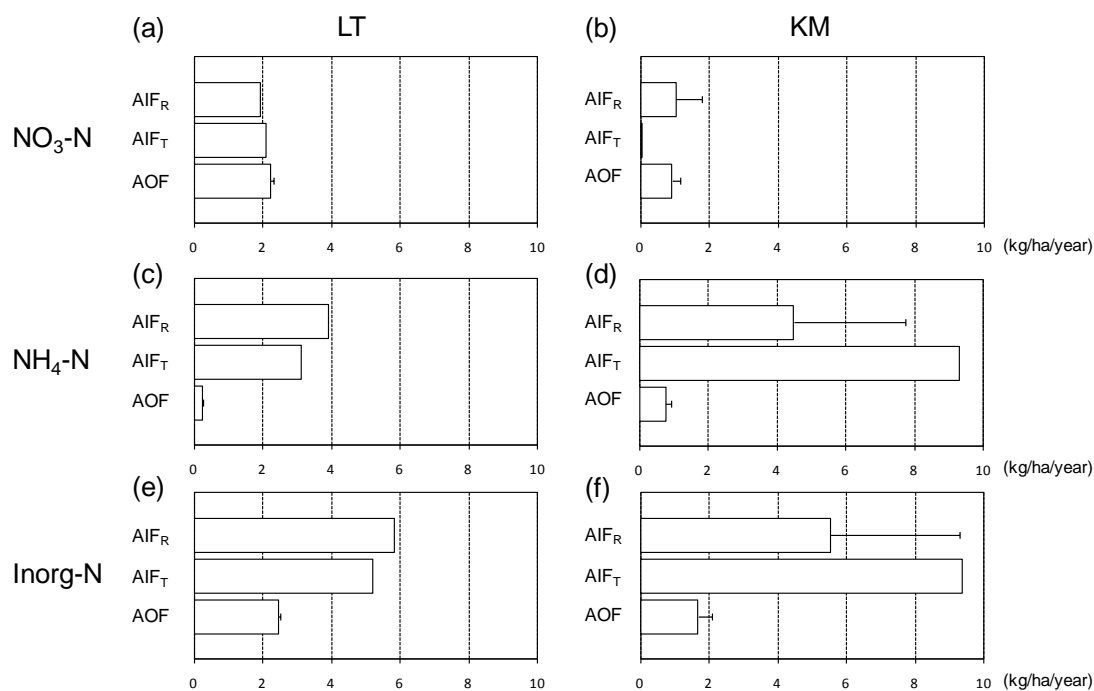


Figure 4.20 AIF_R , AIF_T , and AOF of (a and b) NO_3-N , (c and d) NH_4-N , and (e and f) Inorg-N from 2006 to 2008 in the LT and KM watersheds. The bars are standard

Potassium

The input flux of K to forest ecosystems is mostly via rainfall, dry deposition, and leaching from leaves and branches (Vitousek and Sanford, 1986). The washout of dry deposition on the canopy and leaching from leaves and branches could explain the finding that the AIF_T of K was 4.5–5.2 times higher than the AIF_R in both the KM and LT watersheds. The AIF_T of K was the highest of all nutrients in KM and LT, which is in accordance with previous studies on tropical rain forests.

In KM, the AOF of K (13.9 kg/ha/year) was one fifth of the AIF_T (65.8 kg/ha/year); less of a difference was observed between the AOF (35.4 kg/ha/year) and the AIF_T (36.3 kg/ha/year) of K in LT. Kitayama et al. (2004) reported the annual reabsorption flux of K as 20.3 kg/ha/year in KM and noted that some K supplied by throughfall was absorbed by the trees. *Figure 4.21* compares mean AIF_R , AIF_T , and AOF values for K from 2006 to 2008 in the LT and KM watersheds based on *Table 4.8*. Assuming that K reabsorption by the vegetation occurred in LT and KM, and given that 69% of the AOF in LT occurred during the storm class, it is suggested that other K supply routes exist in LT in addition to rainfall and throughfall. To explain the small difference between AOF and AIF_T in LT, I postulate that K was supplied through chemical weathering of the bedrock. In KM, I expect that chemical weathering contributed minimally to the K supply and that most of the K from rainfall and throughfall was absorbed by the vegetation. This is in accordance with previous reports of the Luquillo Experimental Forest of Puerto Rico (McDowell, 1998).

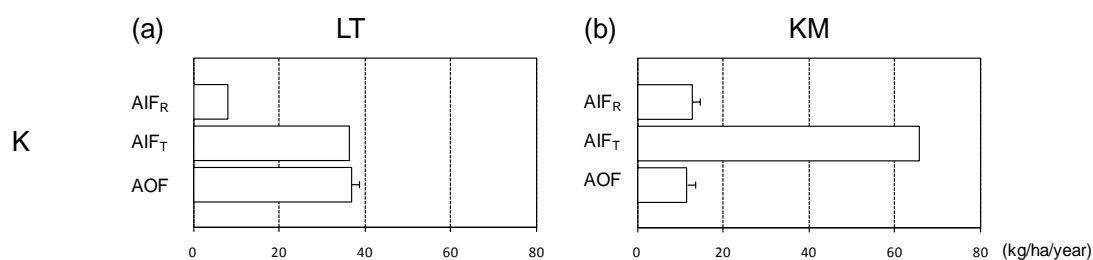


Figure 4.21 AIF_R , AIF_T , and AOF of K from 2006 to 2008 in the (a) LT and (b) KM watersheds. The bars are standard deviation.

Magnesium

The AIF_T of Mg was smaller than that of K or Ca, which is similar to results reported for

4. Water and nutrient balances

other sites. Kitayama et al. (2004) found the leaf litter concentrations of K, Ca, and Mg to be 2.71, 4.26, and 1.70 mg/g, respectively, in KM, suggesting that less Mg than Ca and K was leached from leaves and branches.

Figure 4.22 compares mean AIF_R, AIF_T, and AOF values for Mg from 2006 to 2008 in the LT and KM watersheds based on Table 4.8. The AOF value for Mg was higher than the AIF_R in LT. Input of Mg into forest ecosystems can occur through rainfall, throughfall, and chemical weathering of the bedrock (Grip et al.1994; McDowell, 1998; Bruijnzeel, 1991). In other tropical forests, Mg output was higher than input, something that has been discussed mainly in relation to weathering flux. Although small differences were observed between LT and KM with respect to the AIF_R and AIF_T of Mg, the AOF of Mg in LT was 3.2–4.0 times higher than in KM. This suggests that, like the K input flux, the contribution of chemical weathering to Mg flux was greater in LT than in KM. The high SO₄²⁻ AOF in LT, which might have been produced by FeS₂ oxidization, also supports this hypothesis.

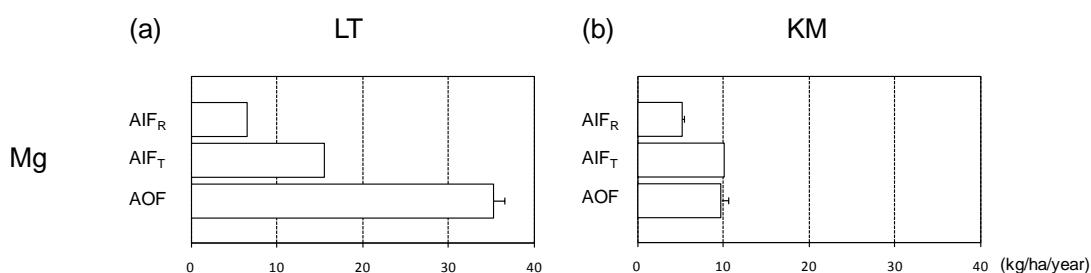


Figure 4.22 AIF_R, AIF_T, and AOF of Mg from 2006 to 2008 in the (a) LT and (b) KM watersheds. The bars are standard deviation.

Calcium

Figure 4.23 compares mean AIF_R, AIF_T, and AOF values for Ca from 2006 to 2008 in the LT and KM watersheds based on Table 4.8.

In KM, the AIF_R of Ca was higher than the AOF, whereas the opposite was found for LT. Berembun in Peninsular Malaysia also had a high AIF_R value for Ca (52.2 kg/ha/year) and a high AIF_R value for Mg (18.6 kg/ha/year) (Zulkifli et al. 1988). Zulkifli et al. (1988) suggested that the high Ca and Mg AIF_R values found in Berembun could be related to sample contamination by local dust. The high Ca input in KM might have been due to aerosols generated by shifting cultivation and

large-scale agriculture around the Kinabalu National Park. These are deposited on leaves and branches and then washed out by rainfall. In LT, the high Ca AOF might have resulted from chemical weathering as for K and Mg. Overall, I postulate that the difference in the K, Mg, and Ca nutrient balance between KM and LT is attributable to differences in chemical weathering.

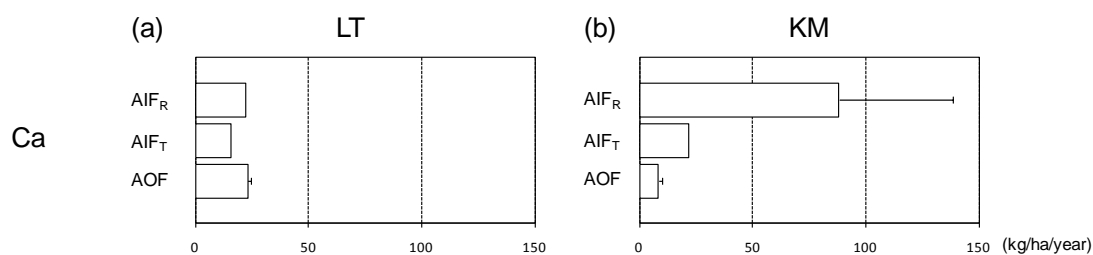


Figure 4.23 AIF_R , AIF_T , and AOF of Ca from 2006 to 2008 in the (a) LT and (b) KM watersheds. The bars are standard deviation.

Sodium and Chloride

Figure 4.24 compares mean AIF_R , AIF_T , and AOF values for Na and Cl from 2006 to 2008 in the LT and KM watersheds based on Table 4.8.

In KM, the AIF_R , AIF_T , and AOF values for Na and Cl showed no distinct differences. In LT, the AIF_R , AIF_T , and AOF values for Na and Cl were higher than in KM. Distance from the sea is the primary factor determining Na and Cl AIF_R . The distance from LT to the coast is only 13.7 km, and the AIF_R of Na and Cl were relatively low compared with values for other sites located less than 20 km from the coast (i.e., four sites in Queensland (Brasell and Gilmour, 1980) and four sites in Fiji (Waterloo et al. 1997)). This may be due to a blocking effect on rainfall from the sea by the Lambir Hills, which are located between the observation site and the nearest coastline. In other tropical rainforests located less than 20 km from the coast (e.g., Turrialba in Costa Rica (Hendry et al. 1984)), strong relationships between Na and Cl AIF_R values have been detected. However, at research sites located more than 20 km from the coast (e.g., Berembun in Malaysia (Zulkifli et al. 1988) and Mt. Kilimanjaro in Tanzania (Schrumpf et al. 2006)), no correlations between Na and Cl AIF_R values have been found.

4. Water and nutrient balances

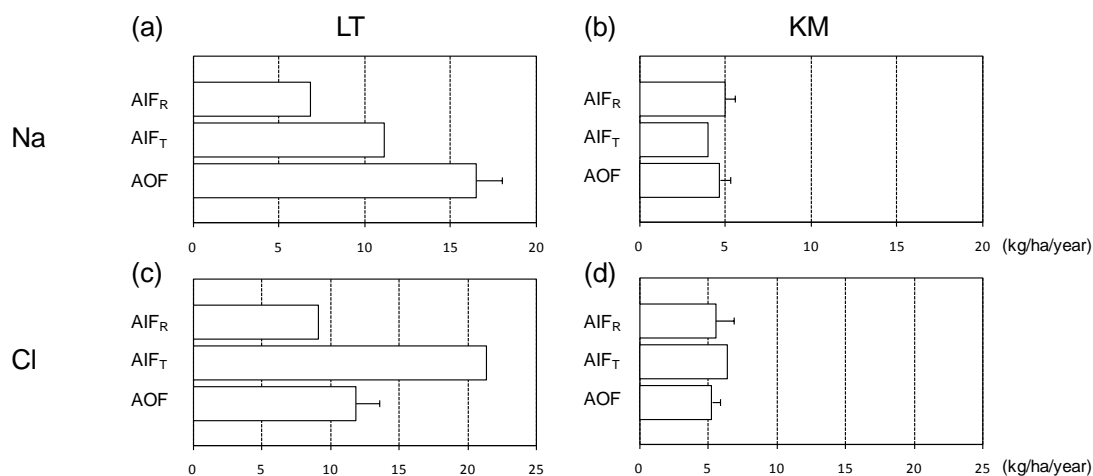


Figure 4.24 AIF_R, AIF_T, and AOF of Na (a and c) and Cl (b and d) from 2006 to 2008 in the LT and KM watersheds. The bars are standard deviation.

Sulfur

Figure 4.25 compares mean AIF_R, AIF_T, and AOF values for SO₄-S from 2006 to 2008 in the LT and KM watersheds based on Table 4.8.

There were no distinct differences in the SO₄-S AIF_R and AIF_T values between KM and LT. However, the mean SO₄-S AOF in LT (64.6 kg/ha/year) was 65 times higher than in KM (1.0 kg/ha/year). In LT, the SO₄-S AOF value was higher than the AIF_R and AIF_T, whereas in KM the SO₄-S AOF was smaller than the AIF_R and AIF_T. There was a greater difference between LT and KM in the absolute AOF values and the estimates of the nutrient balance for SO₄-S than for any other nutrient. It may be that in KM the SO₄-S AIF_R is converted into insoluble sulfate, organic S, and insoluble sulfide in soil S pools or to gaseous S produced by microorganisms (Johnson, 1984; Alewell et al. 1999). The AOF value for SO₄-S obtained in LT was too high to be explained by evapotranspiration of the SO₄-S AIF_R. The AOF of SO₄-S that originates from a terrestrial source within a watershed is released into streamwater. It may be that oxidation of sulfide is the principal source of SO₄-S (e.g., Strauss, 1997; Kohfahl et al. 2008; Fitzhugh et al. 2001). In LT, the high SO₄-S AOF might be a result of sulfide production from chemical weathering.

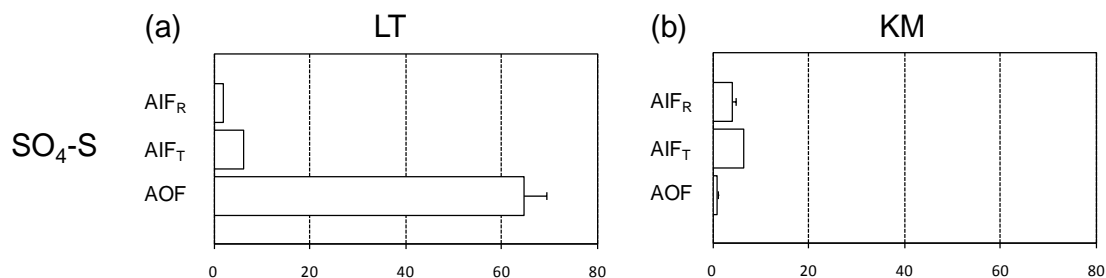


Figure 4.25 AIF_R, AIF_T, and AOF of SO₄-S from 2006 to 2008 in the (a) LT and (b) KM watersheds. The bars are standard deviation.

4.5 Conclusion

The objective of this chapter was to investigate the controversies surrounding three topics. The first concerned the water balance and hydrological characteristics of the LT and KM watersheds. The second involved the perception that there are differences in the nutrient balance of tropical lowland and montane forests. In this case it was essential to conduct comparative watershed-based studies of nutrient input and output estimates through sequential and event-based sampling of rainwater and streamwater as well as with continuous hydrological observations. The third topic involved estimations of nutrient AIF and AOF and the balance between them. To evaluate the accuracy of the AOF values, I tested six estimation methods using continuous discharge data and concentration–discharge relationships for each water sampling event.

(1) Water balance: The annual discharge in KM was approximately twice that in LT because the annual rainfall in KM was 120–670 mm greater than that in LT. No clear correlation was found between mean annual rainfall and loss, but there was a significant (99%) negative correlation between elevation and mean annual loss. **Hydrological characteristics:** The probability of daily rainfall greater than 1 mm in LT and KM was 54% and 60%, respectively. The probability of 0 mm daily rainfall in LT and KM was 41% and 33%, respectively. The fluctuation of daily discharge was smallest in SP and greatest in LT. The probability of daily discharge less than 1

4. Water and nutrient balances

mm in LT and KM was 27% and 20%, respectively. In LT and KM, there is water flow in the stream throughout the year. The differences between the daily discharge when the probability of occurrence exceeded 80% (D80) and 20% (D20) were compared. The differences between D20 and D80 in LT and KM were 2.6 and 6.5 mm, respectively, showing that the fluctuation of daily discharge in LT was smaller than in KM. The differences between D20 and D80 in LT, KM, SP, and UK were 2.6, 6.5, 5.6, and 2.2 mm, respectively, showing that the fluctuation of daily discharge was the smallest in UK and the greatest in KM.

- (2) **Nutrient balance:** The greatest difference in nutrient balance between LT and KM was in the $\text{SO}_4\text{-S}$ balance. There were no distinct differences between $\text{SO}_4\text{-S}$ AIF_R and AIF_T in KM and LT. However, in LT, the mean $\text{SO}_4\text{-S}$ AOF was 65 times that in KM. In LT, the $\text{SO}_4\text{-S}$ AOF was higher than the AIF_R and AIF_T , whereas in KM, the $\text{SO}_4\text{-S}$ AOF was smaller than the AIF_R and AIF_T . The inorganic N balance was smaller than the balance of K, Mg, and Ca in KM and LT. The AIF_R and AIF_T of $\text{NH}_4\text{-N}$ were greater than those of $\text{NO}_3\text{-N}$, and the $\text{NO}_3\text{-N}$ AOF was greater than the $\text{NH}_4\text{-N}$ AOF in both LT and KM. This suggests that most $\text{NH}_4\text{-N}$ and organic N supplied in rainfall was nitrified by microorganisms. The K AOF was one fifth of the AIF_T in KM; less of a difference was observed between the K AOF and AIF_T in LT. To explain the small differences between nutrient AOF and AIF_T in LT, I postulate that K, Mg, and Ca are supplied by chemical weathering of the bedrock and that the differences between KM and LT may be attributable to differences in chemical weathering. There were no differences in the AIF_R , AIF_T , and AOF values for Na and Cl in KM; there was a greater difference in the AIF_R , AIF_T , and AOF values for Na and Cl in LT.
- (3) **Output flux estimation methods:** I estimated the nutrient AOF from a watershed using six methods. First, AOF was calculated by multiplying annual discharge with the volume-weighted mean annual concentration of nutrients (Method I). Second, AOF was calculated from 10-min interval discharge data and the relationship between discharge and concentration (C–Q equation). The exponential equation $\text{Log}(\text{Concentration}) = a + b \text{Log}(\text{Discharge})$ was adopted, and the coefficients of the C–Q equations were obtained from linear regression on log–log plots both without (Method II) and with (Method III) data from samples taken during rainfall-induced stormflow. The only data necessary for Method I were the annual discharge (which could be roughly estimated by subtracting rainfall from evapotranspiration), the concentration of

periodically sampled water, and the simultaneous discharge at sampling times. For Methods II and V, continuously recorded discharge data were necessary. For Methods III and VI, the concentrations of samples during stormflow were added. Methods III or VI may have been more accurate, but they required the highest quality data. As a result of having examined the differences in the methods for AOF estimation, I identified Method VI as the most meaningful and the most accurate of the six methods.

4.7 References

- Abdul. Rahim N., Baharuddin, K., H. Azman, H. 1985. Hydrologic regime of dipterocarp forest catchments in Peninsular Malaysia. In : Saplaco, S. R., Baltazor, E. M., Gorospe, M. V., Cavandang, M. V., Cavand. (Eds.), *Proceedings of the seminar on Watershed Research and Management*, Laguna, Philippines, pp.25-43.
- Alewel, C., Mitchell, M. J., Likens, G. E., Krouse, H. R. 1999. Sources of stream sulfate at the Hubbard Brook Experimental Forest: long-term analysis using stable isotopes. *Biogeochemistry* 44: 281–299.
- Asdak, C., Jarvis, P. G., van Gardingen, P., Fraser, A. 1998. Rainfall interception loss in unlogged and logged forest areas of Central Kalimantan, Indonesia. *Journal of Hydrology* 206: 237–244.
- Ashton, P.S., 1998. Lambir's forest: The world's most diverse known tree assemblage? In: Roubik, D.W., Sakai, S., Abang Hamid, A.K. (Eds.), *Pollination Ecology and the Rain Forest Sarawak Studies*, Ecological Studies 174: 191–216.
- Boy, J. Valarezo, C. Wilcke, W. 2008. Water flow paths in soil control element exports in an Andean tropical montane forest. *European Journal of Soil Science* 59: 1209-1227.
- Brasell, H. M., Gilmour, D. A. 1980. The cation composition of precipitation at four sites in far north Queensland. *Australian Journal of Ecology* 5:397-405.
- Bruijnzeel, L. A. 2001. Hydrology of tropical montane cloud forests: A Reassessment. *Land Use and Water Resources Research* 1:1-18.
- Chappell, N. A., Sherlock, M.D. 2005. Contrasting flow pathways within tropical forest slopes of Ultisol soil. *Earth Surface Processes and Landforms* 30: 735–753.

4. Water and nutrient balances

- Chappell, N. A., Franks, S. W., Larenus, J. 1998. Multi-scale permeability estimation for a tropical catchment. *Hydrological Processes* 12:1507-1523.
- Cuevas, E., Medina, E. 1988. Nutrient dynamics within Amazonian forests II. Fine root growth, nutrient availability and litter decomposition. *Oecologia* 76:222-235.
- Douglas, I., Spencer, T., Greer, T., Bidin, K., Sinun, W., Wong, W.M. 1992. The impact of selective commercial logging on stream hydrology, chemistry and sediment loads in the Ulu Segama rain forest, Sabah. *Philosophical Transactions of the Royal Society* B335: 397–406.
- Drainage and Irrigation Department. 1989. *Sungai Tekam Experimental Basin Final Report from July 1977 to June 1986*. Ministry of Agriculture Malaysia, Water Resources Publication 20: 93pp.
- Dykes, A. P. Thornes, J. B. 2000. Hillslope hydrology in tropical rainforest steplands in Brunei. *Hydrological Processes* 14; 215–235.
- Dykes, A. P. 1997. Rainfall interception from a lowland tropical rainforest in Brunei. *Journal of Hydrology* 200: 260–279.
- Elsenbeer, H. 2001. Hydrologic flowpaths in tropical rainforest soilscaapes-a review. *Hydrological Processes* 15:1751-1759.
- Elsenbeer, H., Newton, B. E., Dunne, T., de Moraes, J. M. 1999. Soil hydraulic conductivities of latosols under pasture, forest, and teak in Rondonia, Brazil. *Hydrological Processes* 13:1417-1422.
- Fitzhugh, R.D., Furman, T., Korsak, A.K., 2001. Sources of stream sulphate in headwater catchments in Otter Creek Wilderness, West Virginia, USA. *Hydrological Processes* 15: 541–556.
- Fleischbein, K., Wilcke, W., Valarezo, C., Zech, W., Knoblich, K. 2006. Water budgets of three small catchments under montane forest in Equador : experimental and modeling approach. *Hydrological Processes* 20:2491-2507.
- Fleischbein, K., Wilcke, W., Goller, R., Boy, J., Valarezo, C., Zech, W. 2005. Rainfall interception in a lower montane forest in Equador : effects of canopy properties. *Hydrological Processes* 19:1355-1371.
- Godsey, S., Elsenbeer, H., Stallard, R. 2004. Overland flow generation in two lithologically distinct rainforest catchments. *Journal of Hydrology* 295:276-290.
- Goller, R., Wilcke, W., Fleischbein, K., Valarezo, C., Zech, W. 2006. Dissolved nitrogen, phosphorus,

4. Water and nutrient balances

- and sulfur forms in the ecosystem fluxes of a montane forest in Ecuador. *Biogeochemistry* 77:57-89.
- Grip, H., Malmer, A., Wong, F. K. 1994. Converting tropical rain forest to forest plantation in Sabah, Malaysia. Part I. Dynamics and net losses of nutrients in control catchments in control catchment streams. *Hydrological Processes* 8: 179-194.
- Grubb, P. J. 1989. The role of mineral nutrients in the tropics: a plant ecologist's view. In: Proctor, J. (Eds.). *Mineral Nutrients in Tropical Forest and Savanna Ecosystems*, Special publications series of the British ecological society 9, pp.417-437.
- Hafkenscheid, R. L. L. J. 2000. *Hydrology and biogeochemistry of tropical montane rain forests of contrasting stature in the Blue Mountains, Jamaica*. PhD Thesis, VU University Amsterdam, Amsterdam, The Netherlands. 302pp.
- Hazebroek, H.P., Abang Kashim, A.M. 2001. National Parks of Sarawak. Natural History Publications (Borneo), Kota Kinabalu, 502pp.
- Hendry, C. D., Berish, C. W., Edgerton, E. S. 1984. Precipitation chemistry at Turrialba, Costa Rica. *Water Resources Research* 20:1677-1684.
- Jacobson, G., 1970. *Gunung Kinabalu Area, Sabah, Malaysia*. Geological Survey Malaysia, Report 8 (with a colored geological map on a scale of 1:500,000). Kuching (Malaysia): Geological Survey Malaysia, 111pp.
- Johnson, D.W., 1984. Sulfur cycling in forests. *Biogeochemistry* 1: 29-43.
- Katsuyama, M., Fukushima, K., Tokuchi, N. 2008. Comparison of rainfall-runoff characteristics in forested catchments underlain by granitic and sedimentary rock with various forest age. *Hydrological Research Letters* 2: 14-17.
- Kenworthy, J. B. 1969. Water balance in the tropical rain forest: a preliminary study in the Ulu Combak Forest Reserve. *Malaysian Nature Journal* 22: 129-135.
- Kitayama, K., Aiba, S., Takyu, M., Majalap, N., Wagai, R. 2004. Soil phosphorus fractionation and phosphorus-use efficiency of a Bornean tropical montane rain forest during soil aging with podzolization. *Ecosystems* 7: 259-274.
- Kitayama, K., Mueller-Dombois, D., Vitousek, P. M. 1995. Primary succession of Hawaiian montane rain forest on a chronosequence of eight lava flows. *Journal of Vegetation Science* 6:211-222.
- Kohfahl, C., Brown, P. L., Linklater, C. M., Mazur, K., Irannejad, P., Pekdeger, A., 2008. The impact

4. Water and nutrient balances

- of pyrite variability, dispersive transport and precipitation of secondary phases on the sulphate release. *Applied Geochemistry* 23: 3783–3798.
- Kumagai, T., Saitoh, T. M., Sato, Y., Takahashi, Y., Manfroi, O. J., Morooka, T., Kuraji, K., Suzuki, M., Yasunari, T., Komatsu, H. 2005. Annual water balance and seasonality of evapotranspiration in a Borneo tropical rainforest. *Agricultural and Forest Meteorology* 128 : 81-92.
- Kume, T., Manfroi, O. J., Kuraji, K., Tanaka, N., Horiuchi, T., Suzuki, M., Kumagai, T. 2008. Estimation of canopy water storage capacity from sap flow measurements in a Bornean tropical rainforest. *Journal of Hydrology* 352: 288–295.
- Kuraji, K. 2004. Hydrological characteristics of small watersheds in Sabah: hill dipterocarp forest in Sapulut and Macaranga forest in Ulu Kalumpang. In: Sidle, R. C., Tani, M., Abdul Rahim, A.N., Twodros (Eds.), *Forests and Water in Warm, Humid Asia, Proceedings, 2004 IUFRO Forest Hydrology Workshop (Kota Kinabalu), IUFRO, Malaysia*, pp: 57–60.
- Kuraji, K. 1996. Hydrological characteristics of moist tropical forests. *Bulletin of the University of Tokyo* 95: 93-208. (in Japanese, with English abstract) .
- Kuraji, K., Paul, L. L. 1995. Observational studies on water balance in two tropical rainforest catchments, Sabah, Malaysia. *Proceedings of the Second International Study Conference on GEWEX in Asia and GAME, Pattaya, Thailand*: 403-406.
- Lesack, L. F. W. 1993. Export of nutrients and major ionic solutes from a rain forest catchment in the central Amazon basin. *Water Resources Research* 29: 743–758.
- Malmer, A. 2004. Streamwater quality as affected by wild fires in natural and manmade vegetation in Malaysian Borneo. *Hydrological Processes* 18: 853–864.
- Malmer, A. 1992. Water-yield changes after clear-felling tropical rainforest and establishment of forest plantation in Sabah, Malaysia. *Journal of Hydrology* 134:77-94.
- Manfroi, O. J., Kuraji, K., Suzuki, M., Tanaka, N., Kume, T., Nakagawa, M., Kumagai, T., Nakashizuka, T. 2006. Comparison of conventionally observed interception evaporation in a 100-m² subplot with that estimated in a 4-ha area of the same Bornean lowland tropical forest. *Journal of Hydrology* 329: 329-349.
- Manfroi, O.J., Kuraji, K., Tanaka, N., Suzuki, M., Nakagawa, M., Nakashizuka, T., Chong, L. 2004. The stemflow of trees in a Bornean lowland tropical forest. *Hydrological Processes*

4. Water and nutrient balances

- 18:2455-2474.
- Markewitz, D., Resende, J. C. F., Parron, L., Bustamante, M., Klink, C. A., Figueiredo, R. de O., Davidson, E. A. 2006. Dissolved rainfall inputs and streamwater outputs in an undisturbed watershed on highly weathered soils in the Brazillian cerrado. *Hydrological Processes* 20:2615–2639.
- Martinelli, L. A., Piccolo, M. C., Townsend, A. R., Vitousek, P. M., Cuevas, E., McDowell, W. 1999. Nitrogen stable isotopic composition of leaves and soil : tropical versus temperature forests. *Biogeochemistry* 46:45-65.
- McDowell, W. H. 1998. Internal nutrient fluxes in a Puerto Rican rain forest. *Journal of Tropical Ecology* 14: 521-536.
- McDowell, W. H., Asbury, C. E. 1994. Export of carbon, nitrogen, and major ions from three tropical montane watersheds. *Limnology and Oceanography* 39:111-125.
- Nortcliff, S., Thornes, J. B. 1989. Variations in soil nutrients in relation to soil moisture status in a tropical forested ecosystem. In: Proctor, J. (ed.) *Mineral Nutrients in Tropical Forest and Savanna Ecosystems*. Blackwell, Oxford. pp.43-54.
- Potts, M. D., Ashton, P. S., Kaufman, L. S., Plotkin, J. B. 2002. Habitat patterns in tropical rain forests: A comparison of 105 plots in northwest Borneo. *Ecology* 83: 2782-2797.
- Proctor, J. 2005. Rainforest mineral nutrition: the 'black box' and a glimpse inside it. In: Bonell, M., Bruijnzeel, L. A. (Eds). *Forest, Water and People in the Humid Tropics*, Cambridge University Press, pp.422-446.
- Saunders, T. J., McClain, M. E., Llerena, C. A. 2006. The biogeochemistry of dissolved nitrogen, phosphorus, and organic carbon along terrestrial-aquatic flowpaths of a montane headwater catchment in the Peruvian Amazon. *Hydrological Processes* 20:2549-2562.
- Schrumpf, M., Zech, W., Axmacher, J. C., Lyaruu, H. V. M. 2006. Biogeochemistry of an afrotropical montane rain forest on Mt. Kilimanjaro, Tanzania. *Journal of Tropical Ecology* 22:77-89.
- Schuur, E. A. G. 2001. The effect of water on decomposition dynamics in mesic to wet Hawaiian montane forests. *Ecosystems* 4:259-273.
- Shiraki, K., Wakahara, T. 2005. Runoff characteristics and water balance at Lambir hills catchment. In: Proceedings of International Symposium on Forest Ecology, Hydrometeorology and Forest

4. Water and nutrient balances

- Ecosystem Rehabilitation in Sarawak (Malaysia), pp.133–136.
- Strauss, H. 1997. The isotopic composition of sedimentary sulfur through time. *Palaeogeography, palaeoclimatology, palaeoecology* 132: 97–118.
- Vernimmen, R. R. E., Bruijnzeel, L.A., Romdoni, A., Proctor, J. 2007. Rainfall interception. I. Three contrasting lowland rain forest types in Central Kalimantan, Indonesia. *Journal of Hydrology* 340: 217–232.
- Vitousek, P. M., Sanford, R. L. 1986. Nutrient cycling in moist tropical forest. *Annual Review of Ecology and Systematics* 17: 137-167.
- Walsh, R. P. D., Newberry, D. M. 1999. The ecoclimatology of Danum, Sabah, in the context of the world's rainforest regions with particular reference to dry periods and their impact. In : Newbery, D. M., Clutton-Brock, T. H., Prance, G. T. (Eds.). *Changes and Disturbance in Tropical Rainforest in South-East Asia*, Philosophical Transactions of the Royal Society London B354 : 1869-1883.
- Waterloo, M. J., Schelleken, J., Bruijnzeel, L. A., Vugts, H. F., Assenberg, P. N., Rawaqa, T. T. 1997. Chemistry of bulk precipitation in southwestern Viti Levu, Fiji. *Journal of Tropical Ecology* 13: 427-447.
- Wilcke, W., Gunter, S., Alt, F., Geissler, C., Boy, J., Knuth, J., Oelmann, Y., Weber, M., Valarezo, C., Mosandl, R. 2009. Response of water and nutrient fluxes to improvement fellings in a tropical montane forest in Ecuador. *Forest Ecology and Management* 257:1292-1304.
- Wilcke, W., Yasin, S., Valarezo, C., Zech, W. 2001. Change in water quality during the passage through a tropical montane rain forest in Ecuador. *Biogeochemistry* 55:45-72.
- Wilford, G.E. 1961. *The Geology and Mineral Resources of Brunei and Adjacent Parts of Sarawak*. Memoir 10. Geology Survey Department, British Territories in Borneo, 319pp.
- Zulkifli, Y., Douglas, I., Nik, A. R. 2006. Export of dissolved and undissolved nutrients from forested catchments in Peninsular Malaysia. *Forest Ecology and Management* 224: 26–44.
- Zulkifli, Y., Nik, A. R., Suki, A., Zakaria, M. F., 1988. Rainfall chemistry and nutrient loading in a peninsular Malaysia forest site. *Journal of Tropical Forest Science* 1: 201–214.

Chapter 5

Factors controlling pH and ion concentrations of streamwater

5.1 Introduction

The change of land use has resulted in physical and chemical weathering due to soil surface loss and mineral oxidation by supplied oxygen and water. The conversion of tropical forest may affect streamwater hydrology and chemistry directly and indirectly through the land cover change itself and through the changes in physical and chemical weathering processes. However, assessment of the impacts of such land use changes is constrained by the lack of knowledge of the hydrology, hydrochemistry, and chemical weathering in tropical forests.

Recently, a number of small watershed studies with a comprehensive approach including ecology, hydrology, and geochemistry have been conducted in tropical forests. The details of those studies are described in Chapter 1. Of such studies, however, few have been conducted in sedimentary rock watersheds.

The pioneering study by Grip et al. (1994) in Mendolong, Malaysian Borneo, may be the first comprehensive study of two tropical forest watersheds with sedimentary rock. They examined the streamwater chemistry of two soil types and found local differences in the nutrient content of the bedrock, explained by weathering rates. However, they did not compare their data with findings from other locations in the tropics to interpret their results. Zulkifli et al. (2006) conducted another study in Bukit Tarek in Peninsular Malaysia. They mainly examined the pattern of nutrient export in relation to streamflow regimes. Thus, the results of these studies are too diverse to explain the factors determining the streamwater chemistry of tropical forests on sedimentary rock.

In Chapter 5, the overall goal of my study was to examine the relationship between bedrock type and chemical weathering in tropical forest watersheds. To approach this goal and examine generality of the streamwater chemistry, I established the LT watershed and another experimental watershed (LC) next to LT in LHNP, and KM watershed and another experimental watershed (KB)

in MKNP, and conducted hydrological and hydrochemical observations. In this Chapter 5, I describe the characteristics of streamwater inorganic ion concentrations in a tropical lowland forest and a tropical montane forest in Malaysian Borneo and present possible factors determining the differences between the two sites through comparisons with data reported at a number of other tropical locations.

5.2 Methods

5.2.1 Watersheds description

In this chapter, LT watershed and another experimental watershed (LC) next to LT in LHNP, and KM watershed and another experimental watershed (KB) in MKNP were used to examine generality of the streamwater chemistry. The details of the watersheds are described in Chapter 2.

5.2.2 Rainfall and discharge observation

The details of rainfall and discharge observation are described in 4.2.2 (Chapter 4).

5.2.3 Intensive observation of streamwater and rainwater during rainfall-induced stormflow.

Streamwater for chemical analysis was collected at discharge observation points in the four watersheds (LT, LC, KM, and KB) twice a week in 100-mL polyethylene bottles. The details of intensive streamwater sampling during rainfall-induced stormflow events and rainwater for chemical analysis are described in 4.2.3 (Chapter 4).

All observations and water samplings were conducted for two years from January 2006 until December 2007. The results reported in the following section are based on the data obtained during that study period.

5.2.4 Chemical analysis

Bottles containing samples were brought to the field laboratory within 30 min of sampling and immediately refrigerated at 2°C. All samples were filtered using a 0.2- μm filter (Minisart RC15, Hydrophilic regenerated cellulose) within 2 months of sampling. The details of chemical analysis of the concentrations of cations (Na^+ , NH_4^+ , K^+ , Mg^{2+} , and Ca^{2+}) and anions (Cl^- , NO_3^- , and SO_4^{2-}) are

5. Factors controlling pH and ion concentrations of streamwater

described in 4.2.4 (Chapter 4). The concentrations of Fe, Al, and Si in KM and KB were analyzed using inductively coupled plasma mass spectrometry (ICPS-7000 Shimadzu Co., Kyoto, Japan). The precision of the inductively coupled plasma mass spectrometer was also confirmed to be within -5% to +5% of standard solution. The Fe and Al concentrations in LT and LC were analyzed by flame atomic absorption spectrometry, and the SiO₂ concentration was analyzed according to the 8-anilinoanthralene sulfonic acid spectroscopic method following standard methods (APHA, 1998). The pH was measured using a pH meter (D-54 HORIBA Co., Kyoto, Japan). The precision of the pH meter was confirmed by checking readings of standard solution (pH 4 and 7).

5.3 Results

5.3.1 Streamwater and rainwater chemistry

Table 5.1 shows the volume-weighted mean (VWM) concentrations of the ions studied for streams in the four watersheds and rainwater at the two sites. As discharge data were unavailable for KB and LC, separation of flow class for calculating VWM concentrations for KB and LC was performed using discharge data for KM and LT, respectively.

Table 5.1 Volume-weighted mean (VWM) concentrations of ions from January 2006 to December 2007 for (a) streamwater in 4 watersheds and (b) rainwater in 2 sites.

Flow class	(a)																(b)						
	Superdry				Baseflow				Intermediate				Storm				Total				Rain		
	LT	LC	KM	KB	LT	LC	KM	KB	LT	LC	KM	KB	LT	LC	KM	KB	LT	LC	KM	KB	LT, LC	KM, KB	
n	66	89	71	71	16	13	54	50	7	17	66	64	0	4	3	3	89	123	194	188	140	152	
pH	4.2	4.8	5.8	6.3	4.3	4.4	5.7	6.3	4.0	4.4	5.6	6.5	-	4.5	4.9	6.5	4.2	4.7	5.7	6.3	5.6	5.9	
VWM																							
Cl ⁻	40.8	44.2	7.3	8.1	37.2	42.7	7.8	7.3	36.9	47.5	8.4	8.6	-	52.2	8.6	8.1	23.9	48.3	5.8	8.1	12.7	6.1	
NO ₃ ⁻	1.6	0.6	0.3	0.0	1.6	0.9	0.8	2.7	0.5	1.1	1.6	2.2	-	3.1	2.8	0.0	12.5	1.8	3.1	2.2	4.0	2.1	
SO ₄ ²⁻	505.8	124.5	4.3	5.2	421.8	148.7	4.8	3.1	370.9	172.9	5.1	4.9	-	143.5	5.6	5.2	287.4	147.8	1.8	4.5	14.4	8.6	
OH ⁻	0.0	0.0	0.0	0.0	0.0	0.0	0.0	0.1	0.0	0.0	0.0	0.0	-	0.0	0.0	0.0	0.0	0.0	0.0	0.0	0.0	0.1	
H ⁺	70.1	48.7	2.2	0.3	73.5	66.8	2.8	1.1	95.6	72.7	3.1	0.4	-	47.1	63.5	0.3	12.2	56.2	1.8	0.6	3.2	2.5	
Na ⁺	51.1	47.7	15.5	26.7	48.6	47.3	13.4	27.5	48.5	51.0	12.5	27.6	-	52.5	8.0	26.7	53.4	50.5	7.0	27.3	18.1	7.9	
NH ₄ ⁺	2.5	3.2	0.4	0.0	1.6	1.0	0.7	0.4	2.2	0.2	0.5	0.2	-	0.0	0.0	0.0	1.3	0.8	2.9	0.2	5.8	12.7	
K ⁺	21.6	22.9	13.0	7.5	20.0	15.2	13.1	11.3	20.9	14.5	10.2	12.1	-	12.1	7.7	7.5	81.2	15.5	12.4	11.2	9.3	12.0	
Mg ²⁺	215.8	66.5	62.0	83.0	189.3	77.3	45.2	61.6	163.0	77.1	52.9	82.9	-	57.0	47.8	83.0	211.1	66.4	28.5	76.2	17.5	14.4	
Ca ²⁺	64.2	14.3	19.4	72.9	55.8	15.2	14.8	39.8	48.9	10.6	18.0	66.7	-	8.9	17.6	72.9	87.8	11.2	17.6	58.9	35.3	118.7	
TA	548.2	169.3	12.0	13.3	460.6	192.3	13.4	13.2	408.4	221.5	15.1	15.7	-	198.8	17.0	13.3	323.8	237.5	1.6	14.9	31.2	16.9	
TC	425.3	203.2	112.6	190.4	388.8	222.8	90.0	141.7	379.1	226.1	97.3	189.9	-	177.6	144.5	190.4	446.9	200.6	11.0	174.3	89.3	168.2	

Note: Ion concentration (μmolL⁻¹), TA = Total anion ([Cl⁻] + [NO₃⁻] + [SO₄²⁻] + [OH⁻]), TC = Total cation ([H⁺] + [Na⁺] + [NH₄⁺] + [K⁺] + [Mg²⁺] + [Ca²⁺])

5. Factors controlling pH and ion concentrations of streamwater

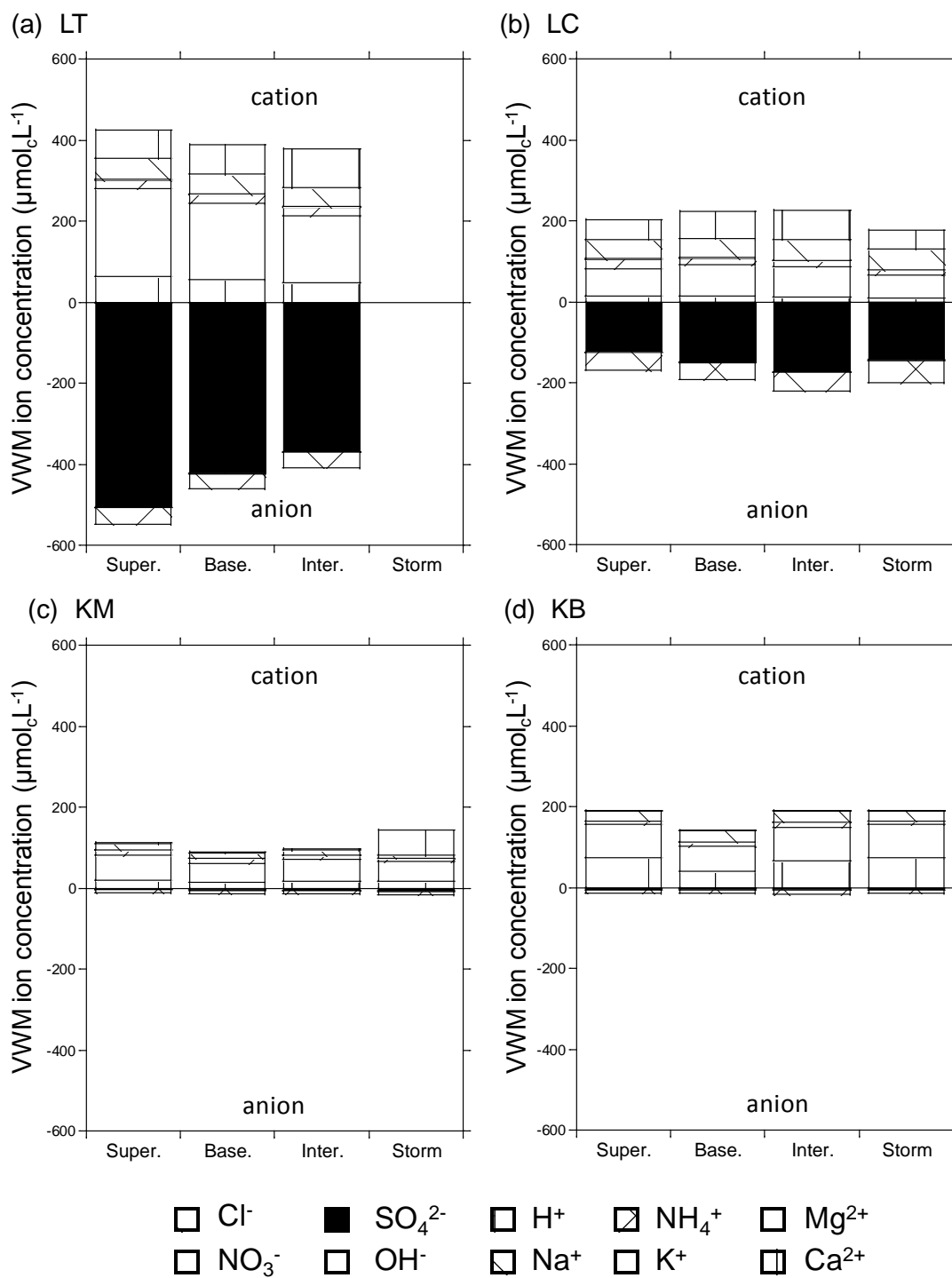


Figure 5.1 Relationship between anions and cations based on Table 5.1.

Figure 5.1 and 5.2 show the VWM concentration of anions and cations based on the data given in Table 5.1. The SO₄²⁻ concentrations at LT and LC were extremely high, approximately 100 times larger than were those at KM and KB (Table 5.1). The concentrations of basic cations were higher at

5. Factors controlling pH and ion concentrations of streamwater

LC and LT than at KM and KB (Table 5.1). At KM and KB, the concentrations of ions in streamwater were higher than were those in rainwater, except for Na^+ and Mg^{2+} . At LT and LC, the ion concentrations in streamwater were higher than were those in rainwater, except for the concentrations of NO_3^- and NH_4^+ .

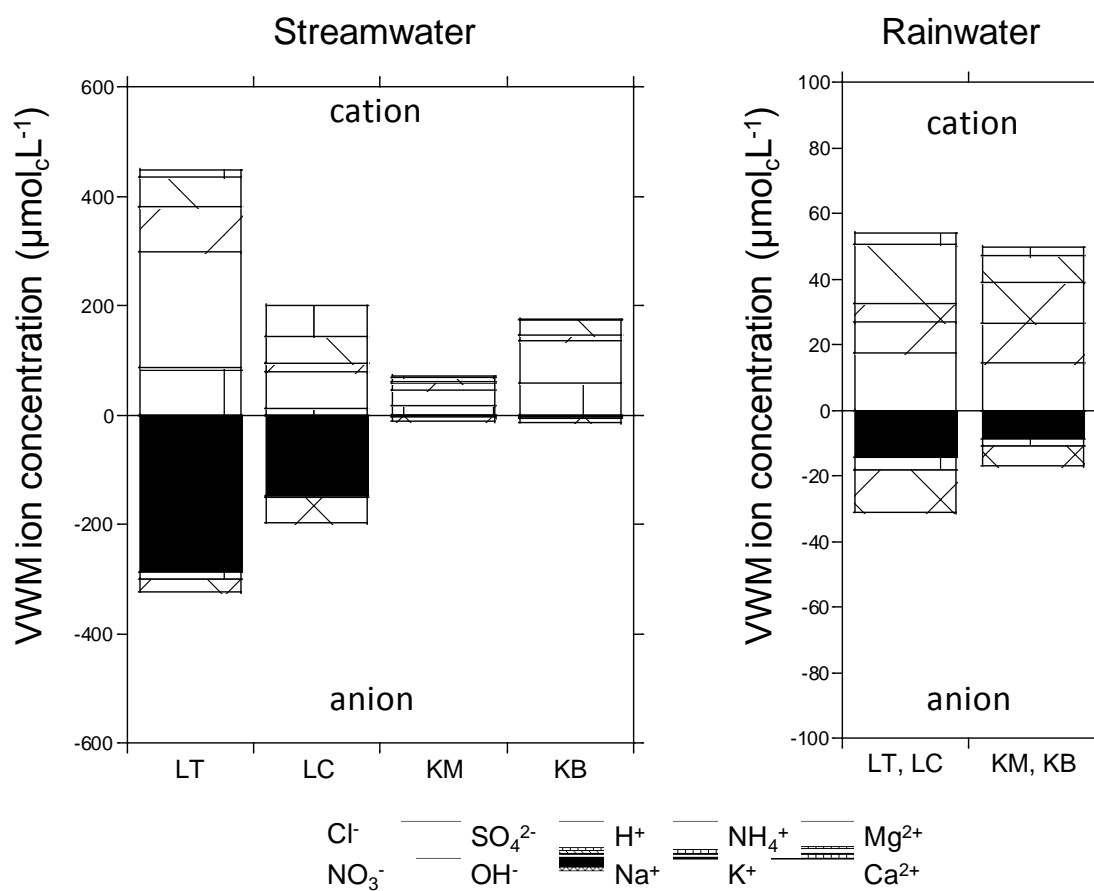


Figure 5.2 Relationship between anions and cations of rainwater based on Table 5.1. The legends in this figure are the same as in Figure 5.1.

Table 5.2 shows the significant differences between sites revealed by analysis of variance. Except for KM-KB and LT-LC, the significant differences were greater between sites (*t-test*, $p < 0.001$). The streamwater at LT and LC was acidic, with pH values ranging from 4.0 to 4.8. The

5. Factors controlling pH and ion concentrations of streamwater

streamwater pH values for KM and KB were higher than were those for LT and LC. Except for LT–LC, the significant differences were greater between sites (*t*-test, $p < 0.001$, $p < 0.01$ and $p < 0.05$).

Table 5.2 Significance level of difference between sites tested by *t*-test. Data used were volume-weighted mean concentrations of ions except ‘storm’.

	Cl ⁻	NO ₃ ⁻	SO ₄ ²⁻	H ⁺	Na ⁺	NH ₄ ⁺	K ⁺	Mg ²⁺	Ca ²⁺
LT-LC			***					***	***
LT-KM	*	***	***	***			***		
LT-KB	**	***	***	***	***	*	***	**	***
LC-KM	***	***	***	***			***	***	***
LC-KB	***	***	***	***	***		***	***	***
KM-KB		***		***	***			**	***

Note: *** $P < 0.001$, ** $P < 0.01$, * $P < 0.05$

Table 5.3 shows the volume-weighted mean concentrations of Fe, Si, and Al for streamwater in the four watersheds. The Fe concentration in streamwater at LT (3.89 mgL⁻¹) was higher than were those of LC, KM, and KB. The statistical significance of the difference between sites was not tested by *t*-test because fewer samples were available for Fe, Si and Al than for the other ions.

Table 5.3 Volume-weighted mean concentrations of Fe, Si, and Al from January 2006 to December 2007 for streamwater in four watersheds.

VWM	Fe	Si	Al
LT	3.89 (42)	2.69 (6)	0.75 (3)
LC	0.36 (16)	1.92 (15)	0.74 (1)
KM	0.05 (34)	1.47 (34)	0.05 (34)
KB	0.06 (31)	1.67 (31)	0.02 (31)

Note: Metal concentration (mgL⁻¹), The number of samples is shown in parentheses.

5.4 Discussion

5.4.1 Characteristics of streamwater chemistry in LHNP and MKNP

Table 5.4 shows tropical rainforest watersheds for which both anion and cation concentrations in streamwater have been reported. One of the objectives of this paper was to determine the ion concentrations of streamwater at MKNP and LHNP, compare them with those of other tropical rainforests, and evaluate the influence of geological disparities on the streamwater ion

5. Factors controlling pH and ion concentrations of streamwater

concentrations. To determine factors that bring about differences in anion compositions in streamwater at the four watersheds, all studies in sedimentary, granitic, ultrabasic, and volcanoclastic watersheds that reported data for anions (Cl^- , NO_3^- , SO_4^{2-}) and cations (Na^+ , NH_4^+ , K^+ , Mg^{2+} , Ca^{2+}) were selected. Research papers on streamwater properties that did not contain information on all the ion concentrations reported here were not considered. Data used in LT, LC, KM, and KB were volume-weighted mean concentrations of ions obtained by all sample.

Table 5.4 Ion concentrations of streamwater in tropical rainforests worldwide, as reported in the literature. The metal concentrations are shown for reference.

Geology type	Watershed name	Code	Country	pH	Cl ⁻	NO ₃ ⁻	SO ₄ ²⁻	Na ⁺	NH ₄ ⁺	K ⁺	Mg ²⁺	Ca ²⁺	H ⁺	TA	TC	TC-TA
Teriary sedimentary (mudstone and sandstone)	Bukit Tarek C1	B1	Malaysia	5.4	121	22.1	1.2	13.0	7.2	15.3	25.5	24.5	4.0	35.5	89.5	54.0
	Bukit Tarek C2	B2		5.3	13.8	24.3	1.0	10.0	5.0	15.6	28.0	14.5	5.0	39.1	78.1	38.9
	Mendolong W3	M1		6.3	10.2	0.7	142.8	114.0	1.6	27.1	128.3	84.8	0.5	153.6	356.3	202.7
	Mendolong W6	M2		4.9	7.1	0.2	11.8	25.2	0.8	7.9	19.7	11.0	12.6	19.1	77.2	58.1
	Lambir Tower Large	LT		4.2	23.9	12.5	287.4	53.4	1.3	81.2	211.1	87.8	12.2	323.8	446.9	123.1
	Lambir Crane Large	LC		4.7	48.3	1.8	147.8	50.5	0.8	15.5	66.4	11.2	56.2	197.9	200.6	2.7
	Kinabalu Menpening	KM		5.7	5.8	3.1	1.8	7.0	2.9	12.4	28.5	17.6	1.8	10.8	70.3	59.5
Granite	Kinabalu Bukit Ular	KB	6.3	8.1	2.2	4.5	27.3	0.2	11.2	76.2	58.9	0.6	14.9	174.3	159.4	
	Berembun BC1	Malaysia	6.3	63.2	4.1	13.0	172.2	3.5	109.3	129.2	148.5	0.5	80.3	563.2	482.9	
Berembun BC2	6.2		59.8	2.7	12.9	139.2	3.0	101.0	118.5	139.8	0.6	75.4	502.2	426.7		
Ultrabasic	Rio Icacos	Puerto Rico	6.8	176.0	50.0	70.4	222.0			13.0	98.0	166.0	0.2	296.4	499.2	202.8
	Quebrada Gnaaba		6.5	193.0	2.5	31.7	250.0			11.5	88.8	146.0	0.3	227.2	496.6	269.4
	Tributary Quebrada		6.5	177.0	2.9	39.8	261.0			18.1	94.4	214.0	0.3	219.7	587.8	368.1
Voicaniclastic	Gumung Silam	Malaysia	7.5	149.5	50.0	16.6	87.0	3.5	2.6	1028.4	25.4	0.0	216.1	1146.9	930.7	
	El Verde Quebrada Sonadora	Puerto Rico		206.8	6.1	74.5	172.7	1.4	6.6	92.1	91.8		287.4 *	364.7 *	77.3	
	El Verde Quebrada Toronja			242.0	4.0	71.7	286.2	1.3	7.9	292.9	259.0		317.7 *	847.3 *	529.6	
	Bisley Puente Roto Maneyes			241.7	5.2	129.0	295.8	1.6	19.7	334.8	474.1		376.0 *	1125.9 *	750.0	
	Bisley Quebradas 1			240.1	6.5	113.7	301.9	2.3	25.8	222.1	220.6		360.3 *	772.7 *	412.4	
	Bisley Quebradas 2			230.7	8.7	106.6	276.2	1.4	26.1	224.6	262.0		346.0 *	790.3 *	444.2	
	Bisley Quebradas 3			246.5	7.4	73.2	282.3	1.1	20.7	245.2	205.1		327.2 *	754.4 *	427.2	
	La Seva		Costa Rica		72.0	15.0	94.0	0.0	16.0	108.0	72.0		87.0 *	290.0 *	203.0	
	Lake Calado, Upper Brago		Brazil	4.6	13.0	50.9	5.8	6.3	0.7	0.6	1.4	1.5	25.1	69.7	35.6	-34.1
	Lake Calado, Mota Brook			4.7	11.9	36.3	35.6	10.6	0.3	1.3	5.6	2.6	20.0	83.8	40.4	-43.5
Serra do navio	6.2			75.4	28.8	19.8	83.5	2.3	15.4	80.8	140.0	0.6	124.0	322.6	198.6	
Vigario	1.7	215.1		0.8	2.5	135.0	0.2	0.5	0.5	0.5		217.6 *	138.7 *	-78.9		
Ubatuba	0.8	66.8		0.8	1.1	24.2	0.1	0.2	0.3			68.4 *	25.9 *	-42.5		
Caranguço	0.5	19.9		0.9	0.6	5.1	0.1	0.2	0.2			21.3 *	6.2 *	-15.1		
Corrego Roncador	5.8	8.5	4.2	0.8	9.3	1.5	2.1	9.3	27.0	1.6	13.5	50.7	37.2			

Geology type	Watershed name	Code	Country	Fe	Si	Al	References
Teriary sedimentary (mudstone and sandstone)	Bukit Tarek C1	B1	Malaysia		4.07		Zulkifli et al., 2006
	Bukit Tarek C2	B2		3.59			Zulkifli et al., 2006
	Mendolong W3	M1		0.11	3.51	0.04	Grip et al., 1994
	Mendolong W6	M2		0.40	0.48	0.28	Grip et al., 1994
	Kinabalu Menpening	KM		0.05 **	1.47 **	0.05 **	This study
	Kinabalu Bukit Ular	KB		0.06 **	1.67 **	0.02 **	This study
	Lambir Crane Large	LC		0.36 **	1.92 **	0.74 **	This study
Granite	Lambir Tower Large	LT	3.89 **	2.69 **	0.75 **	This study	
	Berembun BC1	Malaysia		17.56		Zulkifli et al., 1988	
Berembun BC2			16.28		Zulkifli et al., 1988		
Ultrabasic	Rio Icacos	Puerto Rico		8.57		White et al., 1998	
	Quebrada Gnaaba		0.02	9.07		White et al., 1998	
	Tributary Quebrada			11.91	0.01	White et al., 1998	
Voicaniclastic	Gumung Silam	Malaysia				Bruijnzeel et al., 1993	
	El Verde Quebrada Sonadora	Puerto Rico				Schaefer et al., 2000	
	El Verde Quebrada Toronja					Schaefer et al., 2000	
	Bisley Puente Roto Maneyes					Schaefer et al., 2000	
	Bisley Quebradas 1					Schaefer et al., 2000	
	Bisley Quebradas 2					Schaefer et al., 2000	
	Bisley Quebradas 3					Schaefer et al., 2000	
	La Seva		Costa Rica				Genereux and Jordan 2006
	Lake Calado, Upper Brago		Brazil				Lesack 1993
	Lake Calado, Mota Brook				0.04		Williams and Melack 1997
Serra do navio						Forti et al., 2000	
Vigario		3.81			Figueiredo and Ovalff 1998		
Ubatuba		2.89			Figueiredo and Ovalff 1998		
Caranguço		2.10			Figueiredo and Ovalff 1998		
Corrego Roncador		0.02	2.50	0.04	Markewitz et al., 2006		

Note: Ion concentration ($\mu\text{mol L}^{-1}$), TA = Total anion ($[\text{Cl}^-] + [\text{NO}_3^-] + [\text{SO}_4^{2-}] + [\text{OH}^-]$), TC = Total cation ($[\text{H}^+] + [\text{Na}^+] + [\text{NH}_4^+] + [\text{K}^+] + [\text{Mg}^{2+}] + [\text{Ca}^{2+}]$), Fe, Al and Si (mg L^{-1}). Blanks are no data. *: estimated with an assumption that the value of all blanks regard as zero. **: volume-weighted mean of less sample than the other ions.

Figure 5.3 (a) shows the relationship between total anion concentration ([TA]) and total cation concentration ([TC]). Like MKNP and LHNP, the two watersheds in Bukit Tarek (Zulkifli et al.

5. Factors controlling pH and ion concentrations of streamwater

2006) (hereafter B1 and B2) and the other two watersheds in Mendolong (Grip et al. 1994) (hereafter M1 and M2) in Malaysia were underlain by sedimentary rocks. The two watersheds in Berembun (Zulkifli et al. 1988) and those in Rio Icacos, Quebrada Guaba, and Tributary Quebrada in Puerto Rico (White et al. 1998) were granitic watersheds. The total cation concentrations for the granitic watersheds ($499.2\sim 587.8\ \mu\text{mol}_c\text{L}^{-1}$) were higher than the total cation concentrations for the sedimentary rock watersheds ($70.3\sim 446.9\ \mu\text{mol}_c\text{L}^{-1}$). This result supports the suggestion that granitic watersheds have higher total dissolved solids (TDS) than do sedimentary watersheds (Berner and Berner, 1995). Similarly, the variance in the total anion concentrations for the granitic watersheds ($75.4\sim 296.4\ \mu\text{mol}_c\text{L}^{-1}$) was smaller than that for the sedimentary watersheds ($10.8\sim 323.8\ \mu\text{mol}_c\text{L}^{-1}$). The highest total anion concentration was observed in LT ($323.8\ \mu\text{mol}_c\text{L}^{-1}$), as shown in Table 5.4, and was 30 times greater than the smallest total anion concentration, which was observed in KM ($10.8\ \mu\text{mol}_c\text{L}^{-1}$).

Figure 5.3 (b) shows the relationship between the concentrations of total anions and those of SO_4^{2-} . When the plot approaches the 1:1 line, the proportion of SO_4^{2-} in the total anions approaches 100. When the plot moves down from the 1:1 line, anions other than SO_4^{2-} become the principal anions. At LHNP, the SO_4^{2-} concentration in rainwater ($14.4\ \mu\text{mol}_c\text{L}^{-1}$) was 5–10% of that in streamwater.

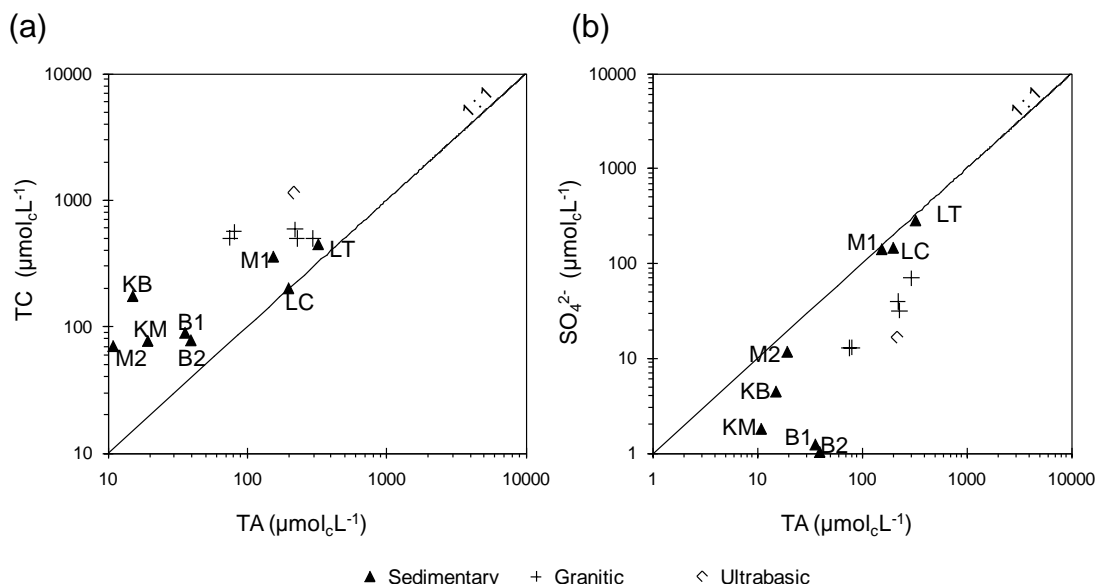


Figure 5.3 (a) Scatter graph of the ion balance of streamwater chemistry in watersheds in tropical rainforest. (b) Scatter graph of the relationship between anion and SO_4^{2-} concentration. KM = Kinabalu Mempening, KB = Kinabalu Bukit Ular, LC = Lambir Crane Large, LT = Lambir Tower Large, M1 = Mendolong W3, M2 = Mendolong W6, B1 = Bukit Tarek C1, B2 = Bukit Tarek C2.

5. Factors controlling pH and ion concentrations of streamwater

Possible causes for the elevated concentration in streamwater in comparison to that in rainwater are evapotranspiration and release of SO_4^{2-} within the watershed (Fitzhugh et al. 2001). Rough estimates of the concentrations due to evapotranspiration, calculated from the annual rainfall and annual loss shown in *Table 4.4* (Chapter 4), give values 1.4 times greater than the actual value for MKNP and 2.0 times greater than the actual value for LHNP. The SO_4^{2-} concentrations in streamwater at KM ($1.8 \mu\text{mol}_c\text{L}^{-1}$) and KB ($4.5 \mu\text{mol}_c\text{L}^{-1}$) were too low to be explained by evapotranspiration of rainwater ($8.6 \mu\text{mol}_c\text{L}^{-1}$). It may be that the SO_4^{2-} from rainwater at KM and KB is converted into insoluble sulfate, organic S, and insoluble sulfide in soil S pools or to gaseous sulfur produced by microorganisms (Johnson, 1984; Alewell et al. 1999). The SO_4^{2-} concentrations in streamwater at LT ($287.4 \mu\text{mol}_c\text{L}^{-1}$) and LC ($147.8 \mu\text{mol}_c\text{L}^{-1}$) were too high to be explained by evapotranspiration of rainwater ($14.4 \mu\text{mol}_c\text{L}^{-1}$). The SO_4^{2-} that originates from a terrestrial source within a watershed is released into streamwater. It may be that oxidation of sulfide is the principal source of SO_4^{2-} (e.g., Strauss, 1997; Kohfahl et al. 2008; Fitzhugh et al. 2001). *Figure 5.4(b)* shows a high concentration of SO_4^{2-} at M1 ($142.8 \mu\text{mol}_c\text{L}^{-1}$), as well as at LT and LC. However, the SO_4^{2-} concentration in rainwater at Mendolong ($1.17 \mu\text{mol}_c\text{L}^{-1}$) (Grip et al. 1994) was 122 times smaller than that in streamwater. In contrast, the SO_4^{2-} concentration at M2 ($11.8 \mu\text{mol}_c\text{L}^{-1}$) was 12 times smaller than that at M1. This difference may have been the result of a high S concentration in the soil and bedrock at M1; weathering would thus produce a greater supply of SO_4^{2-} at M1 than at M2 (Grip et al. 1994). Accordingly, it may be that the high concentrations of SO_4^{2-} at LT and LC were affected by the degree of weathering of sulfide at those locations.

The total anion concentrations in streamwater at KM and KB were 0.03 to 0.07 times those at LT and LC, the SO_4^{2-} concentration at KM ($1.8 \mu\text{mol}_c\text{L}^{-1}$) represented 17% of the anion concentration ($10.8 \mu\text{mol}_c\text{L}^{-1}$) at KM, whereas the SO_4^{2-} concentration at KB ($4.5 \mu\text{mol}_c\text{L}^{-1}$) represented 30% of that watershed's total anion concentration ($14.9 \mu\text{mol}_c\text{L}^{-1}$). The component rates of SO_4^{2-} at KM and KB were not as high as were those at LT (89%) and LC (75%) and. In contrast, the Cl^- concentrations at KM ($5.8 \mu\text{mol}_c\text{L}^{-1}$) and KB ($8.1 \mu\text{mol}_c\text{L}^{-1}$) represented 54% and 54% of the total anion concentration in each watershed. Because the component ratio of Cl^- for all anions was twice that of SO_4^{2-} , the principal anion at KM and KB was Cl^- , not SO_4^{2-} . *Figure 5.4 (b)* shows that the smallest SO_4^{2-} concentrations in streamwater were observed at B1 and B2; at these sites, the principal anion was Cl^- (Zulkifli et al. 2006). The SO_4^{2-} concentration in rainwater was not reported

5. Factors controlling pH and ion concentrations of streamwater

by Zulkifli et al. (2006).

Figure 5.4 presents a schematic diagram of input, pool, gases, and runoff data for SO_4^{2-} for LT, LC, KM, and KB. The SO_4^{2-} concentrations in streamwater were higher than those of rainwater at LC and LT. The oxidation of sulfide is the principal source of SO_4^{2-} at these sites (e.g., Strauss 1997; Kohfahl et al. 2008; Fitzhugh et al. 2001). The differences in SO_4^{2-} concentrations depend not only on whether the rock that underlies the watershed area is granitic or sedimentary rock; even when comparing two watersheds underlain by sedimentary rock, great variations can occur in SO_4^{2-} concentrations. This may be attributable to the degree to which the sulfides from which the SO_4^{2-} originates are present in sedimentary rock (e.g., the almost total absence of sulfides from which SO_4^{2-} can originate in sedimentary rocks or the extremely low concentrations of sulfides in rocks) and the weathering that takes place in those rocks that contain sulfides. The SO_4^{2-} concentrations in streamwater were lower than were those of rainwater at KM and KB. The SO_4^{2-} transfers from rainwater to soil at KM and KB by conversion into insoluble sulfate, organic S, and insoluble sulfide or to the atmosphere by conversion to gaseous sulfur produced by microorganisms (Johnson, 1984; Alewell et al. 1999).

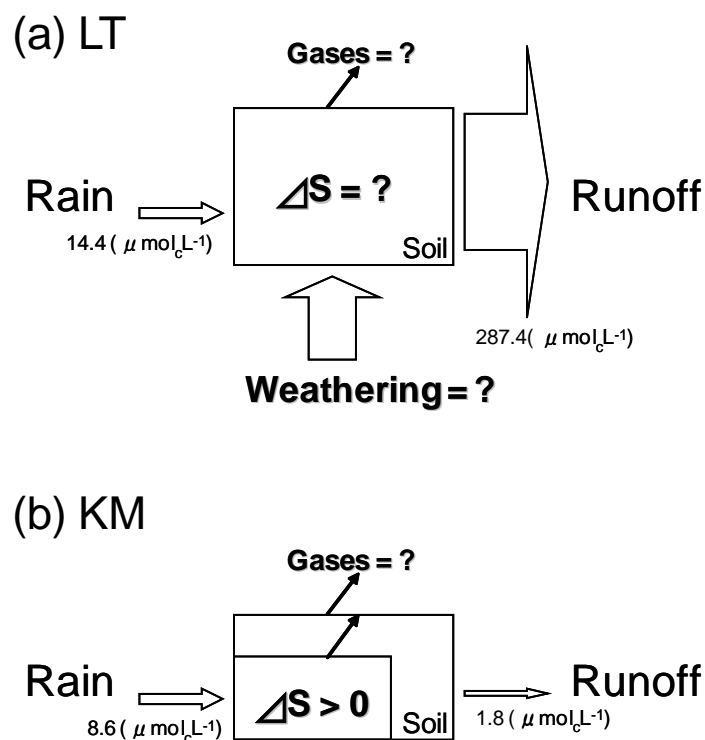


Figure 5.4 Schematic diagram of the input, pool, and runoff of SO_4^{2-} for (a) LT and (b) KM.

5. Factors controlling pH and ion concentrations of streamwater

To assess the relative importance of pyrite or gypsum for the systems, *Figure 5.5 (a)* shows a ternary diagram of the composite rates of $[\text{Cl}^-]$, $[\text{SO}_4^{2-}]$, and other anions such as HCO_3^- or an organic anion, calculated by the difference of total cations and total anions ($[\text{TC}] - [\text{TA}]$). When $([\text{TC}] - [\text{TA}])$ is negative, the value is regarded as zero. Pyrite oxidation along with the concomitant weathering of carbonate (through the generation of sulfuric acid) would result in data points falling along the $([\text{TC}] - [\text{TA}])$ axis of the diagram (Galy and France-Lanord, 1999; Moon et al. 2007). Where carbonates are present, the soils tend not to be acidic, and gypsum is a prominent product (Potter et al. 2005). The rocks consist of mudstones or shales in LT and LC. Mud and mudstone are the most abundant of all sediments and sedimentary rocks (Potter et al. 2005). From *Table 5.4*, the Fe concentration in streamwater at LT ($3.89 \mu\text{mol}\cdot\text{L}^{-1}$) was notably higher than that at KM and KB, possibly due to a significant amount of pyrite, which could subsequently contribute substantial portions of SO_4^{2-} to the systems via oxidation. The chemical equation for that process is as follows:

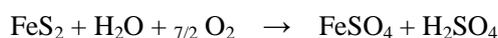


Figure 5.5 (b) shows a ternary diagram of cations ($([\text{Na}^+] + [\text{K}^+]) - [\text{Mg}^{2+}] - [\text{Ca}^{2+}]$). This diagram provides insight into the overall input of cations in these systems from either silicate or carbonate weathering (Galy and France-Lanord, 1999; Moon et al. 2007). The plots in *Figure 5.5 (b)* are determined by geology type. Except in ultrabasic rocks, Mg^{2+} was included in the watersheds of the sedimentary rocks. If gypsum ($\text{CaSO}_4 \cdot 2\text{H}_2\text{O}$) is present in a watershed, the SO_4^{2-} concentration is higher than concentrations of other anions, and the Ca^{2+} concentration is higher than that of other cations. If limestone is present in a watershed, the concentration of $([\text{TC}] - [\text{TA}])$ is likely higher than that of Cl^- or SO_4^{2-} , and the concentration of Ca^{2+} is likely higher than that of other cations. *Figures 5.6 (a)* and *(b)* indicate that those types of watersheds were not included in this study. Also, the origin of higher SO_4^{2-} in LC and LT may not be provided by gypsum, but by pyrite oxidization.

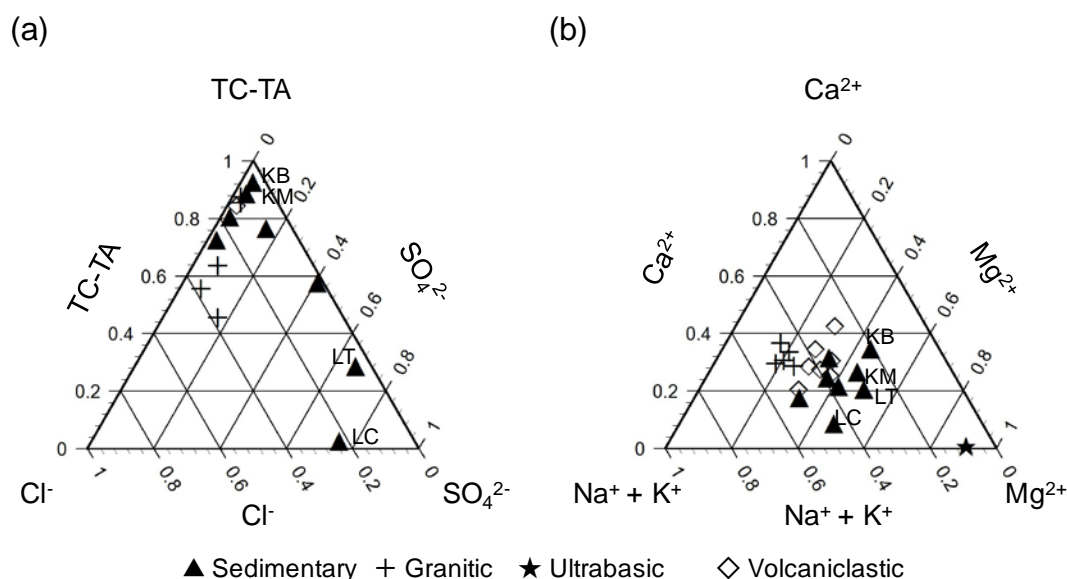


Figure 5.5 Ternary diagram of (a) $\text{Cl}^- - \text{SO}_4^{2-} - ([\text{TC}] - [\text{TA}])$ and (b) cations ($[\text{Na}^+] + [\text{K}^+] - \text{Mg}^{2+} - \text{Ca}^{2+}$). The labels LT, LC, KM, M1, M2, B1, and B2 are the same as in Figure 5.3.

5.4.2 Effects of SO_4^{2-} concentration on pH

In section 5.4.1, the streamwater properties at MKNP and LHNP are strikingly different in their SO_4^{2-} concentrations. To investigate the influence of SO_4^{2-} on the pH values of LT and LC where SO_4^{2-} is the principal anion, the relationship between SO_4^{2-} and pH is shown in Figure 5.6(a). Solid lines represent the relationship between H^+ and SO_4^{2-} when the solution contains only H_2SO_4 and no other anions or cations. The degree to which the plot lies to the upper right of the solid line represents the amount of buffering anions; the degree to which the plot lies to the lower left of the solid line represents the amount of acids other than H_2SO_4 . The plots of KB, LT, and LC are to the upper right of the solid line, suggesting that the pH values of streamwater from these watersheds are determined by acid buffering of the SO_4^{2-} . Because the pH at M1 is between 6 and 6.5, despite the high SO_4^{2-} concentration, acid buffering may be particularly prominent in this sample.

To test this hypothesis, the relationship between $[\text{SO}_4^{2-}]$ and $[\text{Na}^+] + [\text{K}^+] + 2[\text{Mg}^{2+}] + 2[\text{Ca}^{2+}]$ is shown in Figure 5.6 (b). A higher correlation between $[\text{SO}_4^{2-}]$ and $[\text{Na}^+] + [\text{K}^+] + 2[\text{Mg}^{2+}] + 2[\text{Ca}^{2+}]$ than between SO_4^{2-} and granitic may be evidence in support of this hypothesis. In the granitic watersheds, no significant correlation ($r = 0.166$) is seen between $[\text{SO}_4^{2-}]$ and $[\text{Na}^+] + [\text{K}^+] +$

5. Factors controlling pH and ion concentrations of streamwater

$2[\text{Mg}^{2+}] + 2[\text{Ca}^{2+}]$; however, a positive significant correlation ($r = 0.8802$, $p < 0.05$) is seen between the $[\text{SO}_4^{2-}]$ and $[\text{Na}^+] + [\text{K}^+] + 2[\text{Mg}^{2+}] + 2[\text{Ca}^{2+}]$ in the sedimentary rock watersheds. From *Figure 5.6 (b)*, the level of acid buffering in KM and M2 is lower than that in LT, LC, KB, and M1.

These figures indicate that the first factors determining the pH of streamwater may be whether the SO_4^{2-} concentration is lower or higher than that of rainwater and whether the major anion is SO_4^{2-} or not. The second factor may be whether the cation runoff is sufficient to buffer SO_4^{2-} when the major anion in streamwater is SO_4^{2-} and the concentration is higher than that of rainwater. Even if the concentration of SO_4^{2-} is higher than that of rainwater, the pH is not lower when sufficient cations are present to buffer the SO_4^{2-} in watershed M1. On the other hand, if the SO_4^{2-} concentration is higher than that of rainwater and not enough cations are present for buffering, the pH of streamwater in LT and LC is lower than that of rainwater.

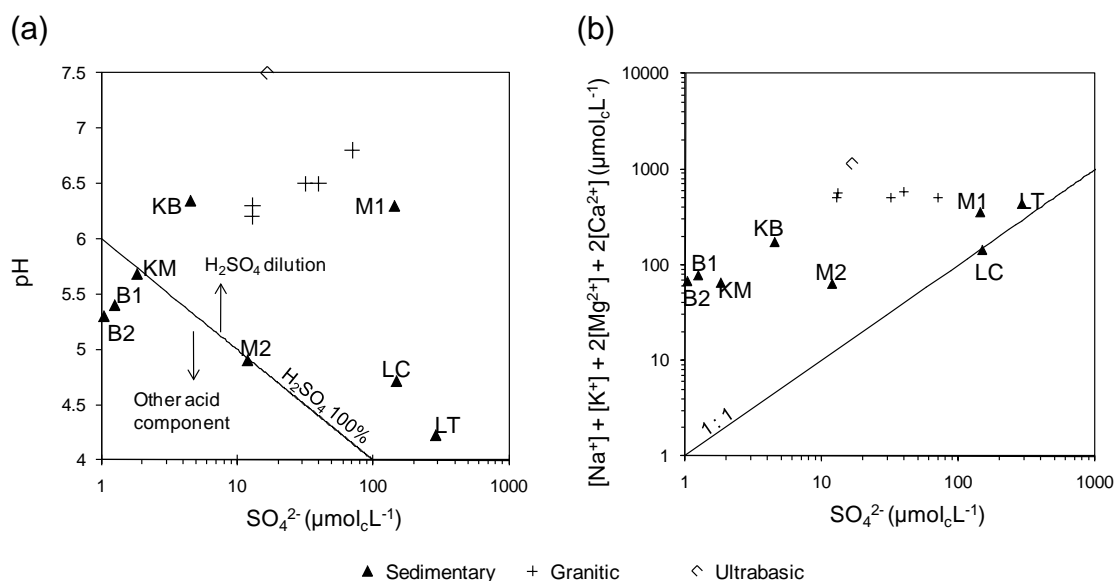


Figure 5.6 (a) Scatter graph of the relationship between the SO_4^{2-} concentration and pH. The solid line depicts when the ion composition is 100% H_2SO_4 . (b) Scatter graph of the relationship between SO_4^{2-} concentration and cations ($[\text{Na}^+] + [\text{K}^+] + 2[\text{Mg}^{2+}] + 2[\text{Ca}^{2+}]$).

The labels LT, LC, KM, M1, M2, B1, and B2 are the same as in *Figure 5.3*.

5.5 Conclusion

To understand characteristics of hydrology, biogeochemistry, and chemical weathering in tropical rainforests, four experimental watersheds were established in Malaysian Borneo. Two of the four experimental watersheds (KM and KB) were located in tropical montane forest in Mount Kinabalu National Park, and the other two (LT and LC) were located a lowland tropical rainforest in Lambir Hills National Park. Hydrological and biogeochemical observation was conducted at the four watersheds for 2 years.

Watersheds LT and LC had acidic streamwater, with pH values ranging from 4.0 to 4.8, and extremely high SO_4^{2-} concentrations that were approximately 100 times higher than those at KM and KB and those of other tropical watersheds.

To understand the relationship between bedrock type and chemical weathering in tropical forest watersheds, I compared our watersheds with other watersheds and with data reported in the literature with regard to a number of other locations in the tropics. The absolute concentrations of total cations varied among sites with different bedrock. The component rate of cations is likely explained by bedrock geology. On the other hand, both the absolute concentrations and component rates of anions varied even among sites on the same type of geology. Because the main anion was SO_4^{2-} at LT and LC, the origin of SO_4^{2-} may be attributable to which sulfide is present in sedimentary rock and to the chemical weathering that takes place in sulfide-containing rocks.

The first factor determining the pH of streamwater is likely whether the SO_4^{2-} concentration is lower or higher than that of rainwater. The second factor is whether the major anion is SO_4^{2-} and whether the cation runoff is sufficient to buffer SO_4^{2-} .

5.6 References

- Alewell, C., Mitchell, M. J., Likens, G. E., Krouse, H. R. 1999. Sources of stream sulfate at the Hubbard Brook Experimental Forest: long-term analysis using stable isotopes. *Biogeochemistry* 44: 281–299.
- Fitzhugh, R.D., Furman, T., Korsak, A.K., 2001. Sources of stream sulphate in headwater catchments in Otter Creek Wilderness, West Virginia, USA. *Hydrological Processes* 15: 541–556.

5. Factors controlling pH and ion concentrations of streamwater

- Golley, F. B., McGinnis, J. T., Clements, R. G., Child, G. I., Duever, M. J. 1983. *Mineral Cycling in a Tropical Moist Forest Ecosystem*. University of Georgia Press, Athens, 248pp.
- Grip, H., Malmer, A., Wong, F. K. 1994. Converting tropical rain forest to forest plantation in Sabah, Malaysia. Part I. Dynamics and net losses of nutrients in control catchments in control catchment streams. *Hydrological Processes* 8: 179-194.
- Johnson, D.W., 1984. Sulfur cycling in forests. *Biogeochemistry* 1: 29–43
- Kohfahl, C., Brown, P. L., Linklater, C. M., Mazur, K., Irannejad, P., Pekdeger, A., 2008. The impact of pyrite variability, dispersive transport and precipitation of secondary phases on the sulphate release. *Applied Geochemistry* 23: 3783–3798.
- Moon, S., Huh, Youngsook., Qin, Jianhua., van Pho, N., 2007. Chemical weathering in the Hong (Red) river basin: rates of silicate weathering and their controlling factors. *Geochimica et Cosmochimica Acta* 71: 1411–1430.
- Potter, P.E., Maynard, J.B., Deoetris, P.J. 2005. *Mud and mudstones: introduction and overview*. Springer, 297pp.
- Strauss, H. 1997. The isotopic composition of sedimentary sulfur through time. *Palaeogeography, palaeoclimatology, palaeoecology* 132: 97–118.
- White, A. F., Blum, A. E., Schulz, M. S., Vivit, D. V., Stonestron, D. A., Larsen, M., Murphy, S. F., Eberl, D. 1998. Chemical weathering in a tropical watershed, Luquillo Mountains, Puerto Rico, I: Long-term versus short-term weathering fluxes. *Geochimica Cosmochimica Acta* 62: 209–226.
- Zulkifli, Y., Douglas, I., Nik, A. R. 2006. Export of dissolved and undissolved nutrients from forested catchments in Peninsular Malaysia. *Forest Ecology and Management* 224: 26–44.
- Zulkifli, Y., Nik, A. R., Suki, A., Zakaria, M. F., 1988. Rainfall chemistry and nutrient loading in a peninsular Malaysia forest site. *Journal of Tropical Forest Science* 1: 201–214.

Chapter 6

Sources and possible generation mechanism for controlling ion concentrations of streamwater

6.1 Introduction

Acid sulfur soils are distributed widely around the world, particularly in the coastal lowlands of Southeast Asia, western Africa, eastern Australia, and Latin America, with a total extent of 17 million ha (Andriessse and van Mensvoort, 2006). In Southeast Asia, most acid sulfur soils occur in tidal swampland covered by mangrove swamps, where pyrite (FeS_2) is formed (Arkesteyn, 1980; Attanandana and Vacharotayan, 1986). When these soils are exposed to air during reclamation projects such as irrigation and drainage canal construction, the pyrite oxidizes to produce ferric ions and sulfuric acid in the drainage water. Acid sulfate soils develop where the production of acid exceeds the neutralizing capacity of the parent material, and the pH value falls to 4 (MacKinnon et al. 1996). Pyrite oxidation after peatland development has been found to cause not only acidification of soil but also acidification of the canals ($\text{pH} = 2.0\text{--}3.0$) and connecting rivers (Haraguchi, 2007).

In the tropics, peat swamps as well as hills and valleys include areas of underlying marine sediments uplifted by plate tectonic activities in the Tertiary Age. These marine sedimentary rocks on land are generally covered by terrestrial sedimentary rocks and are rarely exposed on the land surface. However, when exposed by agricultural, industrial, or residential development, these marine sedimentary rocks may chemically react with atmospheric oxygen and rainwater to produce acid sulfate soils.

The objective of this chapter was to identify the major source and generation process of high SO_4^{2-} concentrations in stream water in a small watershed in a national park in Malaysian Borneo. I have been monitoring stream water quality in this park and obtained a volume-weighted mean annual SO_4^{2-} concentration of $448 \mu\text{mol}_c\text{L}^{-1}$ except “storm”, one of the highest concentrations reported in the literature for tropical forested catchments (Gomyo et al. 2009). Atmospheric deposition (Likens et al. 1990), mineralization of organic matter (Megonigal et al. 2005), and

chemical weathering of gypsum and pyrite (Berner and Berner, 1995) are the main possible generation mechanisms explaining a high sulfate ion concentration in stream water. Since the 1990s, land conversion from tropical rainforests to oil palm plantations has expanded from the flatlands to include hills and valleys in Borneo. Identifying the major sources and generation mechanisms of the high sulfate concentrations in stream flow in natural forests is essential for assessing the impact of agricultural transformation of tropical rain forests. Similar studies have been conducted in coastal plain forests (Morgan et al. 1988), floodplain fens (Loeb et al. 2007) and hilly watersheds (Mitchell et al. 2008) in temperate regions. However, no previous studies on this matter have been conducted in natural rainforests on non-swampy land in the tropics.

6.2 Methods

6.2.1 Study watershed

Figure 6.1 shows the location and topography of the experimental watershed (Lambir Micro; hereafter abbreviated as LM). The watershed was located in Lambir Hills National Park (LHNP), 25 km southwest of the city of Miri in the state of Sarawak, Malaysian Borneo. The longitude, latitude, elevation, and watershed area were 4°12'22"N, 144°01'58"E, 190 –212 m above sea level, and 0.59 ha, respectively. For the 8 years from 2000 to 2007, the mean annual temperature and rainfall were 25.9°C and 2649 mm, respectively. This area has a humid tropical maritime climate and no distinct seasonal change in either rainfall or temperature. Micrometeorological and hydrological research studies, including studies of rainfall interception (Manfroi et al. 2006), transpiration (Kumagai et al. 2004), and water balance (Kumagai et al. 2005), have been conducted in LHNP. Based on the continuous observation of rainfall and rainwater chemistry, the atmospheric SO₄-S input in LHNP was 6.5 kg/ha/year in 2006 (Gomyo et al. 2009).

The geology of LM is Lambir formation sandstone, between 6 and 13 million years old (Middle and Late Miocene) (Ashton, 1998; Hutchison, 2005). The sea probably reached its greatest depth near Lambir about 12.8 million years ago, as shown by the concentration of fossils in massive blue claystones, which are thought to represent a peak in the abundance and biodiversity of the animals living in, on, and above the sea bed (Hazebroek and Abang Kashim, 2001). Sandstone and mudstone accumulated and consolidated to form a considerable thickness of about 2100 m of rocks,

6. Sources and possible generation mechanism for controlling ion concentrations of streamwater

resulting in the Lambir Formation. The rocks of Lambir Hills may include pyrite, because they were uplifted and gently folded from the seabed at the onset of the Pleistocene (Wilford, 1961). The soils of LM are sandy humult ultisols (Baillie et al. 2006). Organic matter content measured at a site 100 m away from the study site was only high in the surface layer (0–5 cm), where a root mat had developed (Ishizuka et al. 1998). Below the surface layer, the soils of the study watershed were mostly organic-poor soils. The vegetation of LM is undisturbed tropical lowland mixed dipterocarp forest (Yamakura et al. 1995; Ashton, 1998; Potts et al. 2002).

6.2.2 Sampling Design and Chemical Analysis

Water

I sampled soil water at five different sites along the main stream (*Figure 6.1*). LM1 represents the lowest point near the watershed outlet (LMS1), and LM4 represents the point just above the spring (stream source, LMS4). At all sites, I sampled the soil water using a suction soil water sampler (DIK-8392; Daiki Rika Kogyo Co., Ltd., Japan), which consisted of a ceramic porous cup (18 × 95 mm), a lead pipe, and a syringe buried in the soil to extract the soil water from three different depths (20, 60, and 100 cm), except at LM2 (20 and 60 cm only). A groundwater well made from a PVC pipe (diameter, 10 cm) was installed at LM4 for groundwater sampling. The average groundwater depth for 2 years (January 2007 to December 2008) was 170 cm (Wakahara, unpublished data). Stream water was sampled at LMS1 and LMS4. Water sampling was performed on 6 days: 30 and 31 December 2007 and 3, 4, 11, and 13 January 2008. During this period, the mean volumetric soil water contents at depths of 10, 30, and 60 cm at LM4, observed continuously by thermo-time domain reflectometry sensors (CS616; Campbell Scientific, Inc., USA), were 0.35, 0.32, and 0.34 %, respectively, which were slightly more than the 2-year averages from January 2007 to December 2008 (0.33, 0.31, and 0.33 %, respectively) (Wakahara, unpublished data). The pH was measured on site using the glass electrode of a pH meter (D-54; Horiba Co., Kyoto, Japan). The precision of the pH meter was confirmed with standard solutions (pH 4 and 7).

Bottles containing the samples were brought to the field laboratory within 30 min of sampling and immediately stored at 2°C. All samples were filtered through a 0.2-µm hydrophilic regenerated cellulose filter (Minisart RC15; Sartorius Stedim Japan Co., Ltd., Japan). The

6. Sources and possible generation mechanism for controlling ion concentrations of streamwater

concentrations of cations (Na^+ , NH_4^+ , K^+ , Mg^{2+} , and Ca^{2+}) and anions (Cl^- , NO_3^- , and SO_4^{2-}) were analyzed using an ion chromatograph analyzer (HIC-6A; Shimadzu Co., Kyoto, Japan). The bulk dissolved Fe concentration was analyzed with inductively coupled plasma emission spectrometry (SPS 1500VR; Seiko Instruments, Inc., Japan). In this report, I define the total anion concentration (TA) ($\mu\text{mol}_e\text{L}^{-1}$) as $([\text{Cl}^-] + [\text{NO}_3^-] + 2[\text{SO}_4^{2-}] + [\text{OH}^-])$ and the total cation concentration (TC) ($\mu\text{mol}_e\text{L}^{-1}$) as $([\text{Na}^+] + [\text{NH}_4^+] + [\text{K}^+] + 2[\text{Mg}^{2+}] + 2[\text{Ca}^{2+}] + [\text{H}^+])$.

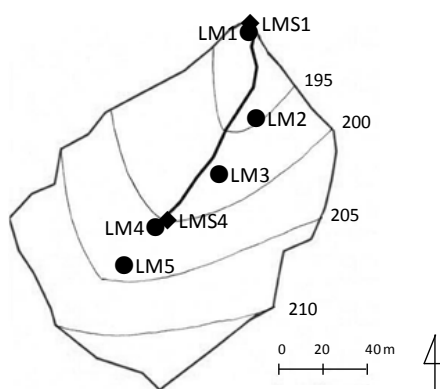


Figure 6.1 Location and topography of the LM watershed showing locations of soil water, groundwater, and streamwater sampling sites.

Soil

Soils were sampled on 18 June 2009 at LM1, LM4, and LM5 (Figure 6.1). The depths of sampling were 10 and 30 cm at LM1; 10, 30, 60, and 100 cm at LM4; and 30 and 60 cm at LM5. All soil samples were filtered through a 2-mm mesh sieve, immediately followed by pH (H_2O), pH (KCl), and pH (H_2O_2) measurements in the field laboratory. The pH was measured with a glass electrode pH meter (D-54; Horiba Co., Japan) using a soil-to-solution (H_2O or 1M KCl) ratio of 1:5. The pH (H_2O_2), which can be used as a semi-quantitative indicator of oxidizable sulfur in soils (Murakami, 1961; Tange and Yagi, 1995), was measured by mixing 2 g of soil and 20 ml of 30% hydrogen peroxide.

6.3 Results

6.3.1 Spatial and Vertical Distribution

Table 6.1 shows the arithmetic mean concentrations of soil water, groundwater, and streamwater sampled at five sites and various depths.

Table 6.1 Arithmetic mean concentration of soil water, groundwater, and streamwater sampled at five sites and various depths

	n	Cl ⁻	NO ₃ ⁻	SO ₄ ²⁻	OH ⁻	H ⁺ (μmolL ⁻¹)	Na ⁺	NH ₄ ⁺	K ⁺	Mg ²⁺	Ca ²⁺	
LM5	Soil water 100cm	6	73.3 (10.1)	0.0 (-)	420.5 (55.7)	0.0 (0)	39.9 (17.9)	86.7 (5.0)	2.5 (3.2)	14.3 (11.0)	168.9 (11.0)	16.5 (10.3)
	Soil water 60cm	5	76.4 (1.7)	0.0 (-)	395.1 (15.6)	0.0 (0)	59.3 (13.2)	78.6 (2.3)	0.0 (-)	4.4 (1.2)	171.5 (6.7)	4.2 (4.0)
	Soil water 20cm	5	71.9 (4.5)	0.0 (-)	250.4 (12.1)	0.0 (0)	39.4 (8.6)	73.6 (2.0)	6.0 (0.9)	13.9 (4.3)	131.9 (7.0)	10.3 (5.1)
LM4	Groundwater	2	65.6 (1.3)	0.0 (-)	173.8 (27.2)	0.0 (0)	44.7 (3.4)	65.7 (1.1)	0.0 (-)	14.5 (15.4)	106.4 (10.3)	13.8 (1.3)
	Soil water 100cm	6	69.0 (0.9)	0.0 (-)	161.4 (7.1)	0.0 (0)	18.2 (4.3)	67.1 (1.0)	0.4 (1.0)	5.3 (0.6)	115.7 (2.9)	12.0 (2.1)
	Soil water 60cm	4	53.3 (0.9)	0.0 (-)	123.0 (68.9)	0.0 (0)	21.8 (6.3)	55.5 (31.1)	0.0 (-)	3.7 (2.4)	86.9 (48.8)	9.1 (5.5)
LM3	Soil water 20cm	6	63.1 (2.6)	0.0 (-)	140.2 (8.9)	0.0 (0)	39.2 (32.0)	67.4 (1.5)	0.6 (1.4)	9.6 (4.9)	129.4 (14.7)	18.8 (6.0)
	Soil water 100cm	5	55.1 (3.8)	0.3 (0.6)	103.6 (5.0)	0.0 (0)	12.6 (10.3)	77.5 (15.1)	2.4 (2.4)	12.4 (5.2)	90.5 (8.3)	61.8 (35.0)
	Soil water 60cm	5	61.5 (10.2)	0.0 (-)	77.8 (6.9)	0.0 (0)	8.1 (5.3)	95.5 (39.8)	3.9 (2.4)	20.9 (8.7)	82.3 (19.8)	78.7 (47.8)
LM2	Soil water 20cm	5	107.8 (9.1)	0.0 (-)	46.8 (6.8)	0.0 (0)	12.9 (7.8)	57.6 (4.2)	11.2 (3.9)	51.2 (27.3)	77.3 (22.2)	50.4 (30.1)
	Soil water 60cm	6	70.1 (7.0)	0.3 (0.6)	2.3 (2.8)	0.0 (0)	4.7 (3.0)	65.0 (16.7)	2.2 (2.6)	12.2 (5.6)	69.5 (9.0)	68.8 (26.4)
	Soil water 20cm	6	50.5 (4.2)	0.0 (-)	0.5 (1.3)	0.0 (0)	10.7 (4.3)	47.4 (2.7)	2.3 (2.7)	10.8 (2.8)	80.8 (7.2)	45.1 (11.7)
LM1	Soil water 100cm	6	18.2 (1.4)	17.1 (1.4)	9.0 (0.7)	0.0 (0)	5.7 (2.6)	33.8 (2.4)	3.1 (5.4)	44.0 (4.9)	60.6 (2.6)	33.8 (15.3)
	Soil water 60cm	6	15.2 (1.7)	23.4 (2.5)	5.4 (2.6)	0.0 (0)	6.1 (3.3)	33.1 (1.7)	0.0 (-)	47.4 (2.7)	60.5 (4.4)	30.7 (15.1)
	Soil water 20cm	6	26.7 (5.9)	29.6 (2.8)	15.2 (9.0)	0.0 (0)	7.3 (3.8)	31.9 (3.6)	0.0 (-)	45.7 (1.0)	54.5 (3.4)	37.4 (15.5)
LMS4	Streamwater	6	65.1 (4.7)	0.3 (0.6)	259.7 (64.9)	0.0 (0)	68.5 (38.9)	68.3 (4.7)	0.6 (1.5)	4.7 (1.7)	128.1 (25.7)	1.9 (2.2)
LMS1	Streamwater	6	57.5 (1.4)	1.5 (1.1)	175.0 (1.3)	0.0 (0)	65.1 (33.6)	60.8 (1.3)	1.9 (1.6)	9.9 (4.0)	83.4 (4.7)	5.1 (2.8)

	n	[TA]	[TC]	[TC] - [TA]	
LM5	Soil water 100cm	6	493.8 (65.7)	328.8 (34.6)	-165.1 (90.1)
	Soil water 60cm	5	471.5 (17.0)	318.0 (27.4)	-153.5 (33.8)
	Soil water 20cm	5	322.2 (15.9)	275.2 (25.8)	-47.0 (19.0)
LM4	Groundwater	2	239.4 (28.5)	245.1 (34.3)	5.8 (62.9)
	Soil water 100cm	6	230.4 (7.8)	218.6 (7.5)	-11.8 (8.5)
	Soil water 60cm	4	176.3 (98.6)	177.0 (96.5)	0.7 (4.8)
LM3	Soil water 20cm	6	203.3 (11.1)	264.9 (32.7)	61.5 (38.4)
	Soil water 100cm	5	159.0 (8.6)	257.2 (56.6)	98.2 (48.1)
	Soil water 60cm	5	139.3 (16.6)	289.4 (108.3)	150.1 (91.8)
LM2	Soil water 20cm	5	154.5 (13.9)	260.5 (77.1)	106.0 (73.0)
	Soil water 60cm	6	72.7 (10.1)	222.3 (57.8)	149.6 (48.0)
	Soil water 20cm	6	51.0 (4.2)	197.1 (20.3)	146.0 (23.8)
LM1	Soil water 100cm	6	44.3 (3.9)	180.9 (23.1)	136.6 (19.2)
	Soil water 60cm	6	44.0 (3.7)	177.8 (14.7)	133.8 (15.8)
	Soil water 20cm	6	71.5 (5.5)	176.8 (18.1)	105.3 (22.1)
LMS4	Streamwater	6	325.2 (71.7)	272.1 (48.7)	-52.8 (67.0)
LMS1	Streamwater	6	233.9 (9.9)	226.2 (34.1)	-6.3 (37.6)

	n	Fe (μmolL ⁻¹)	(Fe ³⁺) (μmolL ⁻¹)	
LM5	Soil water 100cm	2	53.8	161.5
	Soil water 60cm	2	34.5	103.5
	Soil water 20cm	2	6.8	20.5
LM4	Groundwater	2	0.2	0.5
	Soil water 100cm	2	7.1	21.4
	Soil water 60cm	2	2.2	6.7
LM3	Soil water 20cm	2	4.9	14.6
	Soil water 100cm	2	0.1	0.2
	Soil water 60cm	2	0.7	2.2
LM2	Soil water 20cm	2	11.3	34.0
	Soil water 60cm	2	0.8	2.4
	Soil water 20cm	2	0.1	0.4
LM1	Soil water 100cm	2	0.0	0.1
	Soil water 60cm	2	0.0	0.1
	Soil water 20cm	2	0.1	0.2
LMS4	Streamwater	2	0.4	1.3
LMS1	Streamwater	2	0.9	2.7

Note: [TA] = [Cl⁻] + [NO₃⁻] + 2[SO₄²⁻] + [OH⁻], [TC] = [Na⁺] + [NH₄⁺] + [K⁺] + 2[Mg²⁺] + 2[Ca²⁺] + [H⁺], (): Standard deviation

SO₄²⁻ concentration

Figure 6.2 shows the SO₄²⁻ concentrations of soil water, groundwater, and streamwater sampled at the five sites and various depths.

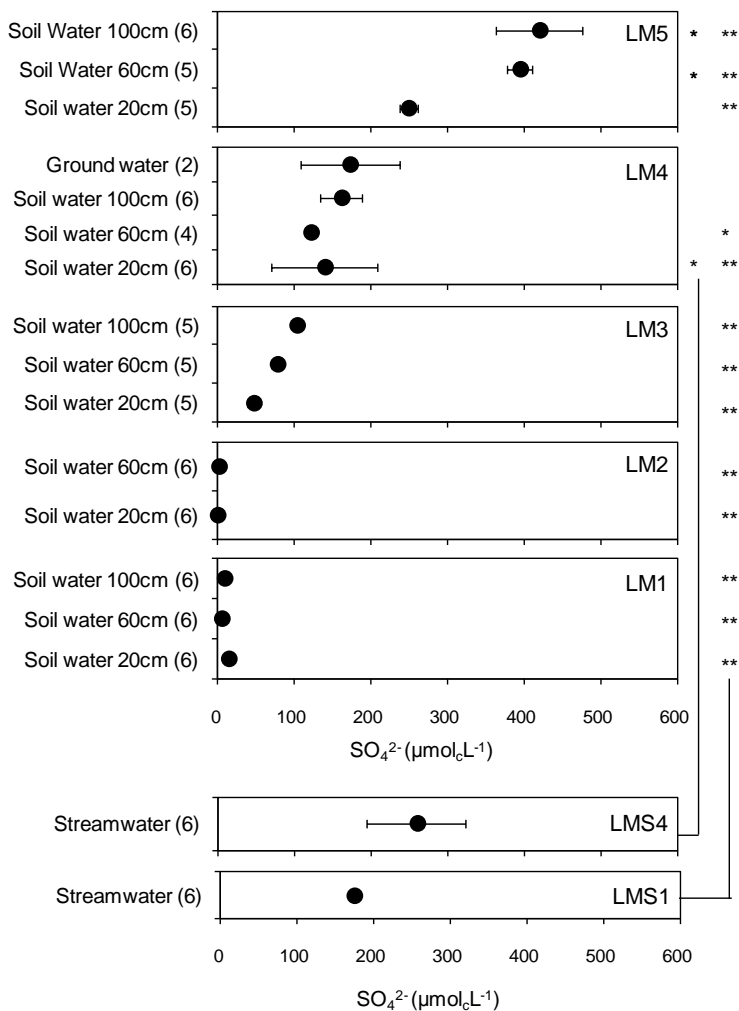


Figure 6.2 Arithmetic mean concentrations of SO₄²⁻ for soil water, groundwater, and streamwater in the LM watershed. The numbers in parentheses indicate the number of samples, and the bars are standard deviation. Significant differences between LM1 streamwater and all soil water, groundwater, and LM4 streamwater, and between LM4 streamwater and soil water at LM4 and LM5 and groundwater are indicated by *'s on the right side of the figure (t-test, **: *p* < 0.001; *: *p* < 0.01).

The SO₄²⁻ concentration in soil water was lowest at LM2 (minimum 0.5 μmol_cL⁻¹), followed by LM1. The concentration increased from LM3 to the upstream sites. The highest value, 420.5 μmol_cL⁻¹, observed at LM5, was 782 times greater than the lowest value observed at LM2. The concentrations of SO₄²⁻ in groundwater and soil water at LM4 did not differ significantly.

6. Sources and possible generation mechanism for controlling ion concentrations of streamwater

The concentration of SO_4^{2-} in streamwater at LMS1 was significantly higher than that of soil water at LM1, LM2, and LM3, but significantly lower than that of soil water at LM5. The concentration of SO_4^{2-} in streamwater at LMS4 was significantly higher than that of soil water at LM4 from a depth of 20 cm, but significantly lower than that of soil water at LM5 from depths of 60 and 100 cm.

Total anion concentration

Figure 6.3 shows the [TA] ($= [\text{Cl}^-] + [\text{NO}_3^-] + 2[\text{SO}_4^{2-}] + [\text{OH}^-]$) concentrations of soil water, groundwater, and streamwater sampled at five sites and various depths.

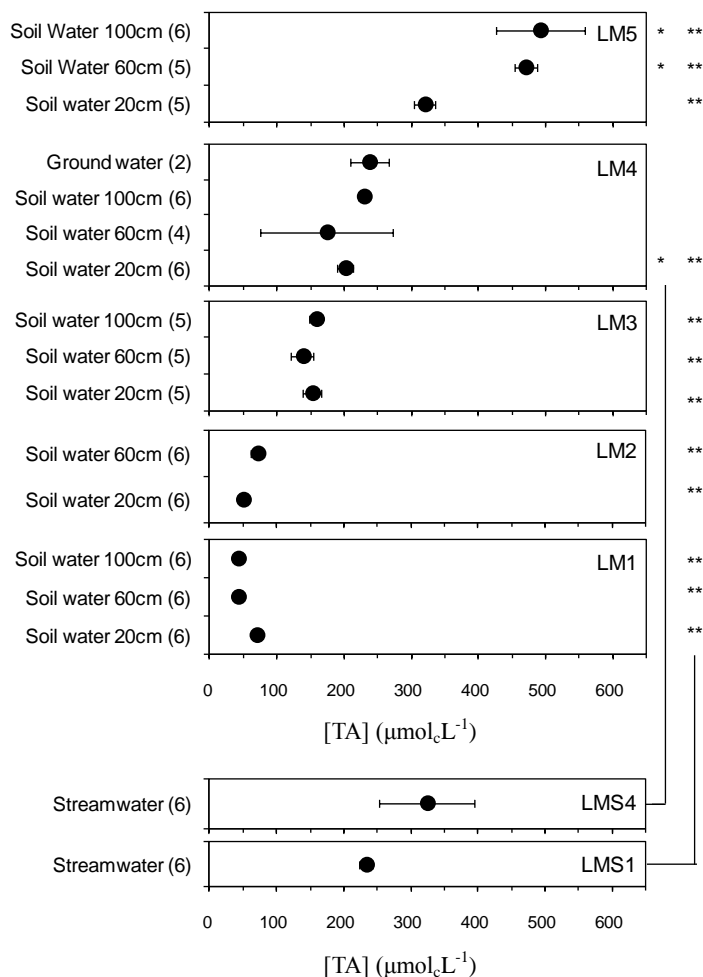


Figure 6.3 Arithmetic mean concentrations of [TA] for soil water, groundwater, and streamwater in the LM watershed. The numbers in parentheses indicate the number of samples, and the bars are standard deviation. Significant differences are the same as in Figure 6.2.

6. Sources and possible generation mechanism for controlling ion concentrations of streamwater

The [TA] concentration in soil water was lowest at LM1 60cm (minimu 44.0 $\mu\text{mol}_e\text{L}^{-1}$). The concentration increased from LM3 to the upstream sites.

NO₃⁻ concentration

Figure 6.4 shows the NO₃⁻ concentrations of soil water, groundwater, and streamwater sampled at five sites and various depths.

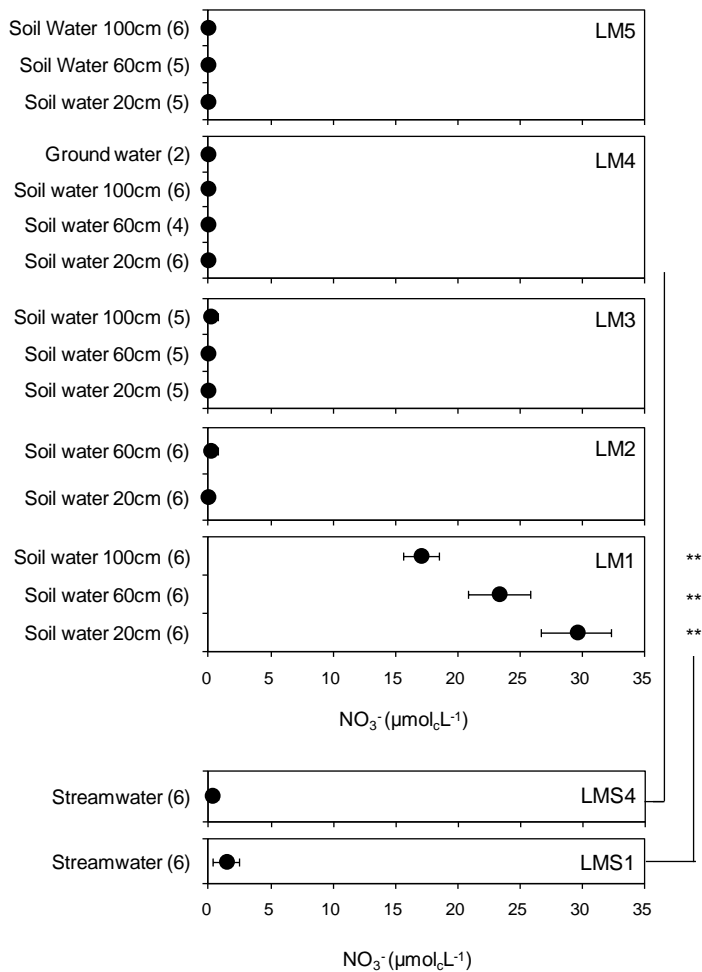


Figure 6.4 Arithmetic mean concentrations of NO₃⁻ for soil water, groundwater, and streamwater in the LM watershed. The numbers in parentheses indicate the number of samples, and the bars are standard deviation. Significant differences are the same as in Figure 6.2.

The NO₃⁻ concentration in soil water was almost zero at LM2, LM3, LM4, and LM5. At LM1, the NO₃⁻ concentration increased from 100cm to 20cm depths.

The concentration of NO₃⁻ in streamwater at LMS1 was significantly lower than that of soil water at LM1.

Cl⁻ concentration

Figure 6.5 shows the Cl⁻ concentrations of soil water, groundwater, and streamwater sampled at five sites and various depths.

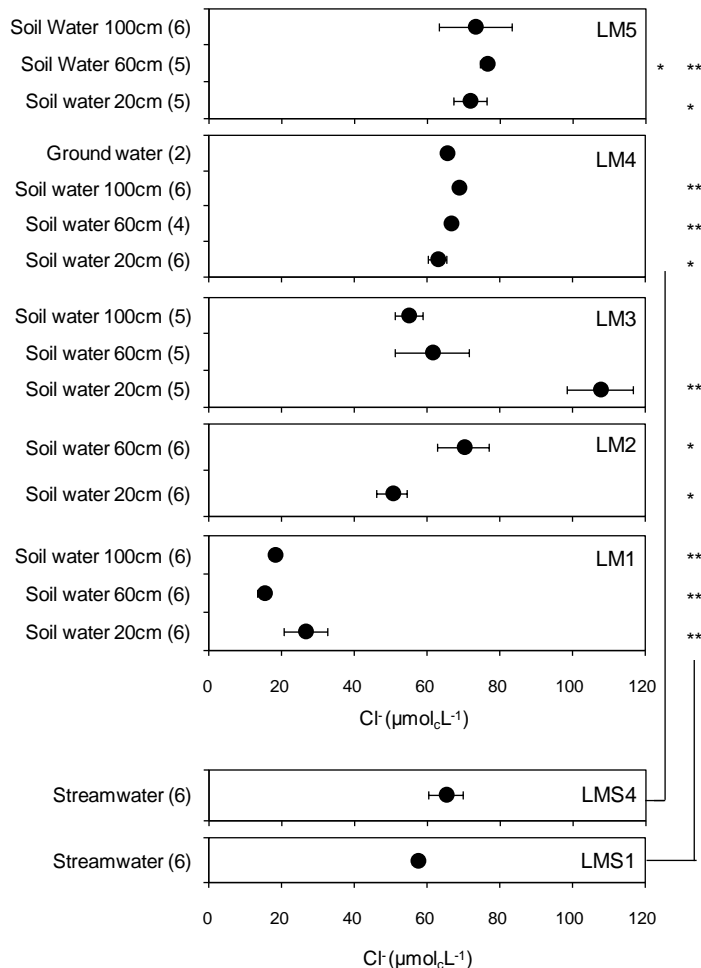


Figure 6.5 Arithmetic mean concentrations of Cl⁻ for soil water, groundwater, and streamwater in the LM watershed. The numbers in parentheses indicate the number of samples, and the bars are standard deviation.

Significant differences are the same as in Figure 6.2.

The Cl⁻ concentration in soil water was lowest at LM1 (minimum 15.2 μmolcL⁻¹). The concentration increased from LM2 to the upstream sites.

Ca²⁺ concentration

Figure 6.6 shows the Ca²⁺ concentrations of soil water, groundwater, and streamwater sampled at five sites and various depths.

The Ca²⁺ concentration in soil water was highest at LM3. The concentration increased from

6. Sources and possible generation mechanism for controlling ion concentrations of streamwater

LM2 to the upstream sites. The concentration of Ca^{2+} in streamwater at LMS1 and LMS4 were significantly lower than that of soil water at LM1, LM2, and LM3.

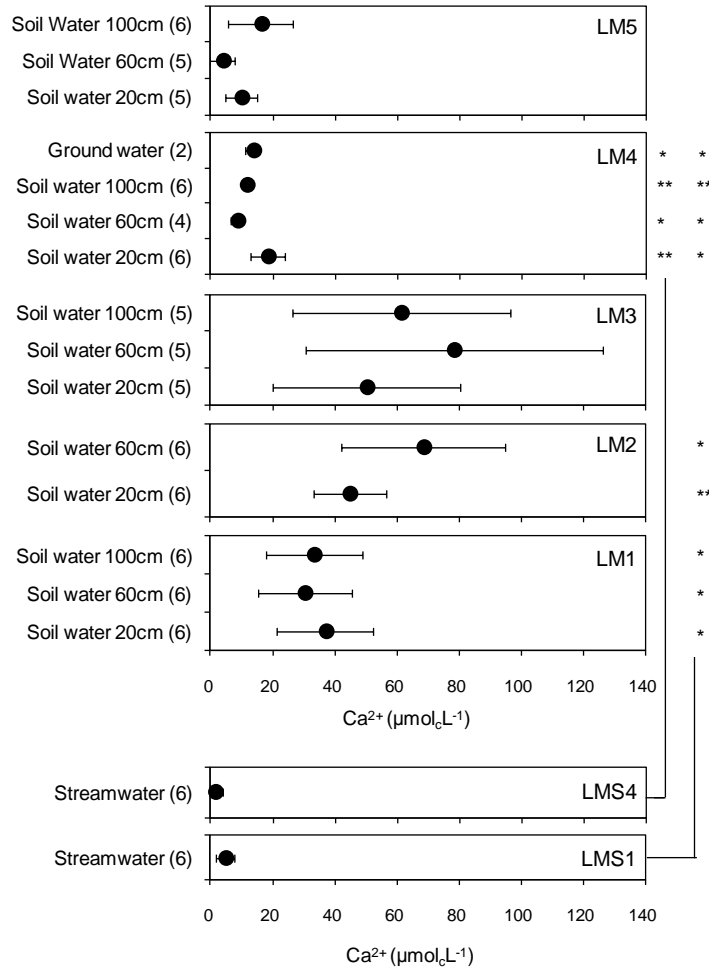


Figure 6.6 Arithmetic mean concentrations of Ca^{2+} for soil water, groundwater, and streamwater in the LM watershed. The numbers in parentheses indicate the number of samples, and the bars are standard deviation. Significant differences are the same as in Figure 6.2.

Mg^{2+} concentration

Figure 6.7 shows the Mg^{2+} concentrations of soil water, groundwater, and streamwater sampled at five sites and various depths.

6. Sources and possible generation mechanism for controlling ion concentrations of streamwater

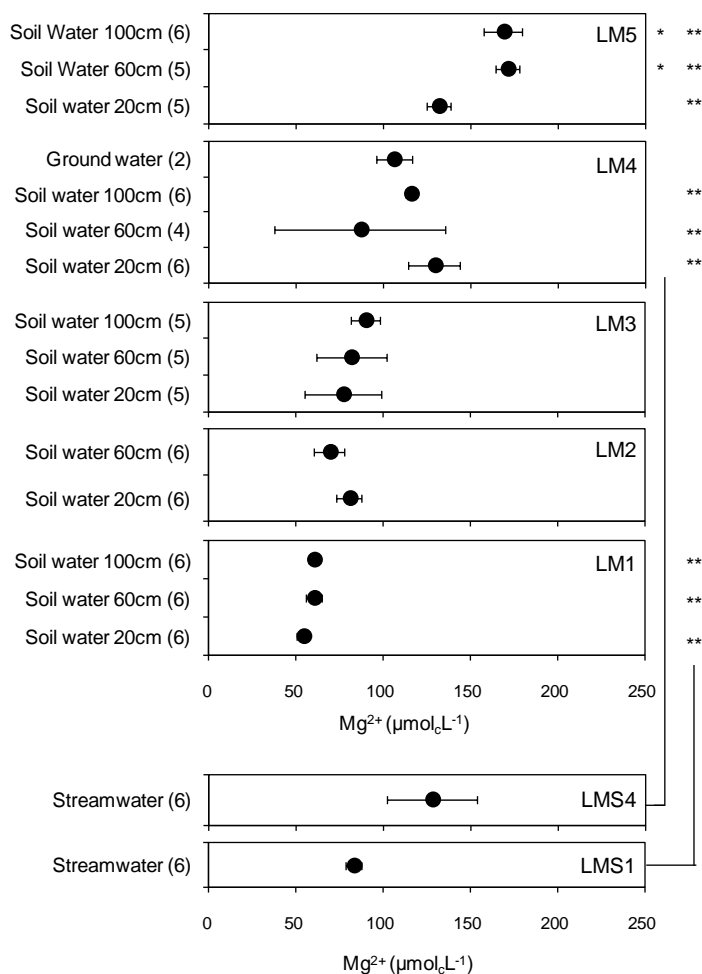


Figure 6.7 Arithmetic mean concentrations of Mg^{2+} for soil water, groundwater, and streamwater in the LM watershed. The numbers in parentheses indicate the number of samples, and the bars are standard deviation. Significant differences are the same as in Figure 6.2.

The Mg^{2+} concentration in soil water was lowest at LM1 (minimum $54.5 \mu\text{mol}_c\text{L}^{-1}$), followed by LM2. The concentration increased from LM3 to the upstream sites. The highest value, $171.5 \mu\text{mol}_c\text{L}^{-1}$, observed at LM5, was 3.3 times greater than the lowest value observed at LM2. The concentrations of Mg^{2+} in groundwater and soil water at LM4 did not differ significantly.

The concentration of Mg^{2+} in streamwater at LMS1 was significantly higher than that of soil water at LM1, LM2, and LM3, but significantly lower than that of soil water at LM4 and LM5 as same as SO_4^{2-} concentration.

Total cation concentration

Figure 6.8 shows the [TC] ($=[\text{Na}^+]+[\text{NH}_4^+]+[\text{K}^+]+2[\text{Mg}^{2+}]+2[\text{Ca}^{2+}]+[\text{H}^+]$) concentrations of

6. Sources and possible generation mechanism for controlling ion concentrations of streamwater

soil water, groundwater, and streamwater sampled at five sites and various depths.

The [TC] concentration in soil water was no distinct difference during depths.

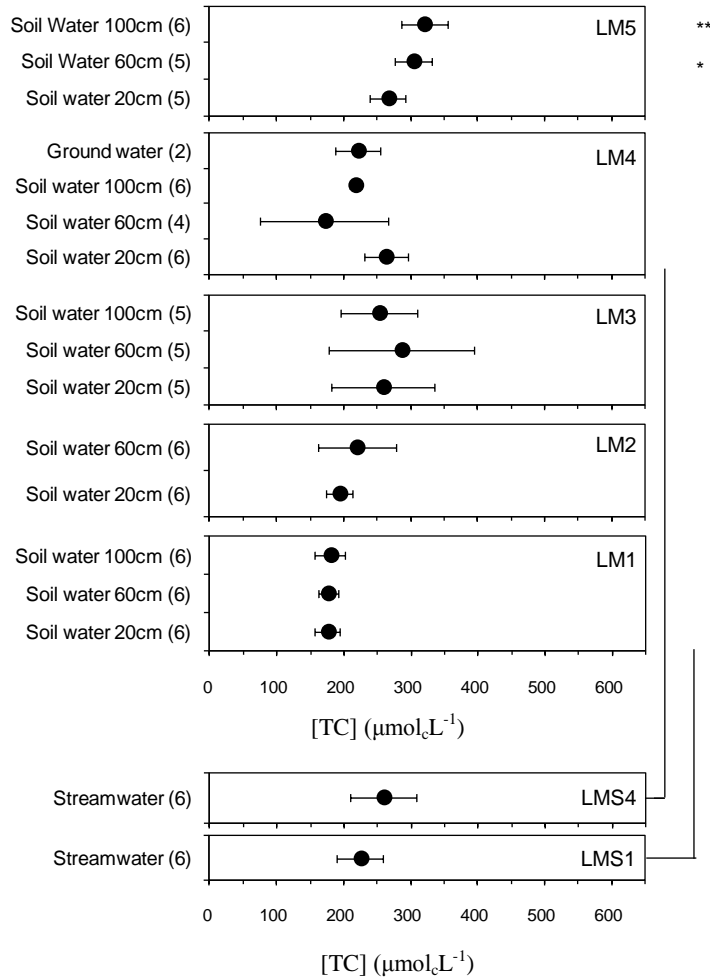


Figure 6.8 Arithmetic mean concentrations of [TC] for soil water, groundwater, and streamwater in the LM watershed. The numbers in parentheses indicate the number of samples, and the bars are standard deviation. Significant differences are the same as in Figure 6.2.

pH

Figure 6.9 shows the pH values of soil water, groundwater, and streamwater sampled at the five sites and various depths. The average pH values of streamwater at LMS4 and LMS1 were 4.26 and 4.35, respectively. Unlike with SO_4^{2-} concentration, no statistical difference was detected between streamwater pH at LMS4 and soil water pH at LM5, or between streamwater pH at LMS1 and soil water pH at LM3, LM2 (20 cm), and LM1 (20 cm). This finding suggests that the SO_4^{2-}

6. Sources and possible generation mechanism for controlling ion concentrations of streamwater

concentrations of soil water, groundwater, and streamwater do not determine the pH. The high SO_4^{2-} concentration of soil water at LM5 may be buffered by some cations, and the acidity in the soil water at LM2 and LM1 may be controlled by anions other than SO_4^{2-} , such as organic anions.

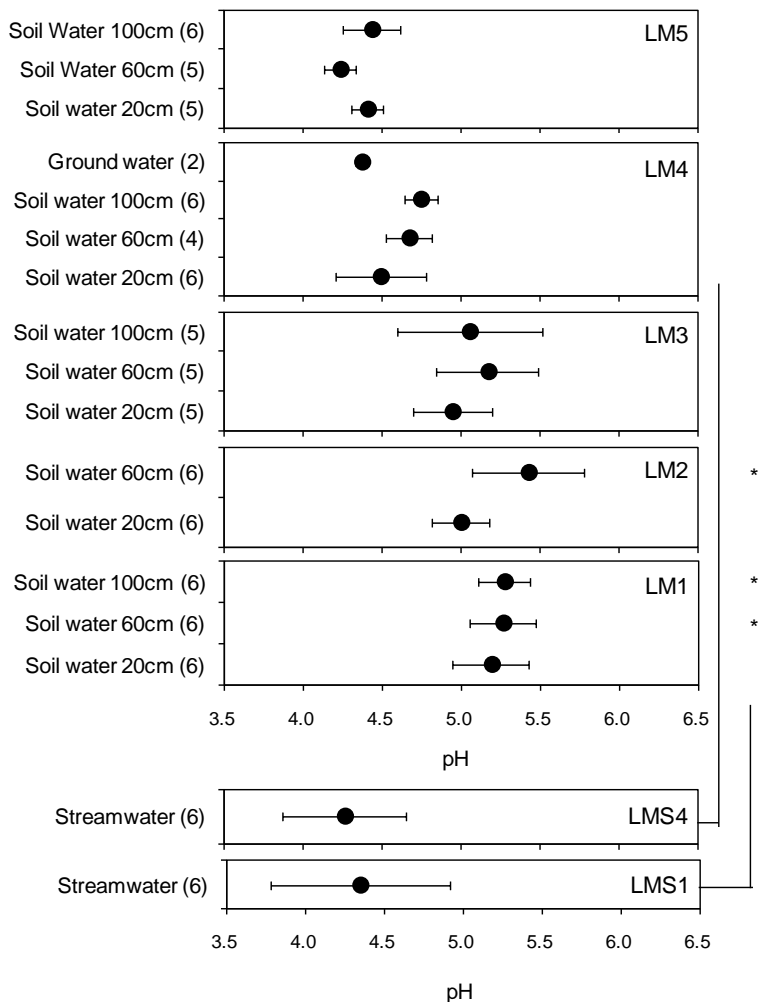


Figure 6.9 The pH for soil water, groundwater, and streamwater in the LM watershed. The numbers in parentheses indicate the number of samples, and the bars are standard deviation. Significant differences are the same as in Figure 6.2.

[TC]-[TA] and Fe concentration

Figure 6.10 shows the [TC]-[TA] concentrations of soil water, groundwater, and streamwater sampled at five sites and various depths.

6. Sources and possible generation mechanism for controlling ion concentrations of streamwater

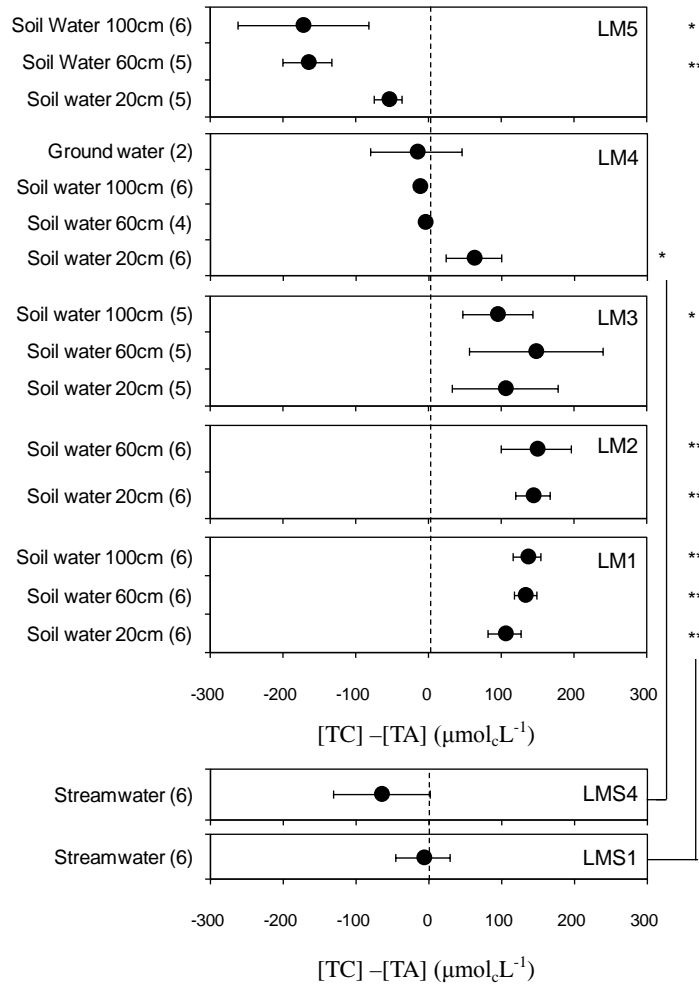


Figure 6.10 Arithmetic mean concentrations of $[TC]-[TA]$ for soil water, groundwater, and streamwater in the LM watershed. The numbers in parentheses indicate the number of samples, and the bars are standard deviation. Significant differences are the same as in Figure 6.2.

Figure 6.11 shows the Fe concentrations of soil water, groundwater, and streamwater sampled at five sites and various depths. Figure 6.10 and Figure 6.11 show that $[TC]$ exceeds $[TA]$ indicates some contributions from organic anions because no contributions from $[HCO_3^-]$ are present due to the low pH. It may be that the imbalance ($[TC]-[TA]$) can be explained by Fe supply etc.

6. Sources and possible generation mechanism for controlling ion concentrations of streamwater

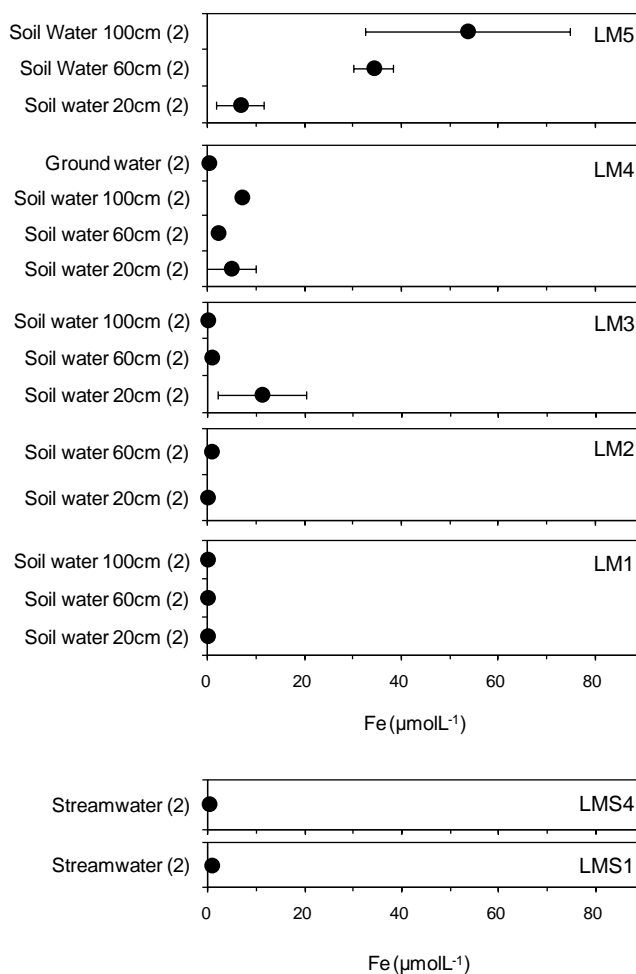


Figure 6.11 Arithmetic mean concentrations of Fe for soil water, groundwater, and streamwater in the LM watershed. The numbers in parentheses indicate the number of samples, and the bars are standard deviation. Significant differences are the same as in Figure 6.2.

6.4 Discussion

6.4.1 Spatial and Vertical Distributions of SO_4^{2-} Concentration and pH

Table 6.1 shows the mean cation and anion concentrations in soil water, groundwater, and stream water. Figure 6.2 shows the SO_4^{2-} concentrations in soil water, groundwater, and stream water sampled at the five sites and at various depths. The SO_4^{2-} concentration in soil water was lowest at LM2 (minimum, $0.5 \mu\text{mol}_c\text{L}^{-1}$), followed by LM1. The concentration increased from LM3 to the upstream sites. The highest value, $420.5 \mu\text{mol}_c\text{L}^{-1}$ was observed at LM5 and was 782 times the lowest value observed at LM2. At LM4, the concentration of SO_4^{2-} did not differ significantly between groundwater and soil water. The high concentrations of SO_4^{2-} cannot be explained by the

condensation of rainwater, which had a volume-weighted mean concentration of about $14.4 \mu\text{mol}_c\text{L}^{-1}$ (Gomyo et al. 2009). The concentration of SO_4^{2-} in stream water at LM1 was significantly higher than that in soil water at LM1, LM2, and LM3, but was significantly lower than that in soil water at LM5. The concentration of SO_4^{2-} in stream water at LMS4 was significantly higher than that in soil water from a depth of 20 cm at LM4, but was significantly lower than that in soil water from depths of 60 and 100 cm at LM5.

6.4.2 Balance: The Ratio of Ca and Fe Concentrations

Figure 6.12 (a, b, and c) shows the relationship between $[\text{SO}_4^{2-}]$ and $(\text{TC} - \text{TA})$, and the ratio of $[\text{Ca}^{2+}]$ to $([\text{Mg}^{2+}] + [\text{Ca}^{2+}])$ and to $[\text{Fe}]$, respectively. In the lower part of the LM watershed (LM1 through LM3), $(\text{TC} - \text{TA})$ was positive (Figure 6.12a) and Ca^{2+} -rich (Figure 6.12b), whereas in the upper part of the watershed (LM4 through LM5), $(\text{TC} - \text{TA})$ was zero or negative (Figure 6.12a), except at a depth of 20 cm at LM4, and Ca^{2+} -poor (Figure 6.12b). To explain these differences, I postulate that there may be a large gap in the bedrock geology between the lower and upper watershed. The lower part of the watershed may consist of calcium carbonate (CaCO_3)-rich and pyrite (FeS_2)-poor bedrock, while the bedrock of upper part of the watershed may be CaCO_3 -poor and FeS_2 -rich. The positive $(\text{TC}-\text{TA})$ values in the lower part of the watershed (Figure 6.12a) could be explained by HCO_3^- produced by chemical weathering of CaCO_3 -rich rocks (Ohte et al. 1995). Similar to the results shown in Figure 6.2, $(\text{TC} - \text{TA})$ and the $[\text{Ca}^{2+}]$ ratios of stream water at LMS1 and LMS4 were similar to those of soil water at depths of 60 and 100 cm at LM4 and soil water at a depth of 20 cm at LM5, respectively. The soil water at depths of 60 and 100 cm at LM5 was rich in sulfate and low in Ca^{2+} , with a negative $(\text{TC} - \text{TA})$, suggesting that some cations had not been included in the TC calculation. One possibility is that Fe^{3+} might have been produced along with SO_4^{2-} by pyrite oxidation, as in the following equation (Calmels et al. 2007):



As shown in Figure 6.12c, although the concentration of dissolved iron was less than $15 \mu\text{mol}_c\text{L}^{-1}$ in most cases, exceptionally high concentrations (34.5 and $53.8 \mu\text{mol}_c\text{L}^{-1}$) were measured at LM5 at depths of 60 and 100 cm, respectively. If all of the dissolved iron were to be in

6. Sources and possible generation mechanism for controlling ion concentrations of streamwater

the form of Fe^{3+} (which would be possible under conditions of low pH and high Eh), the electric charge concentration of Fe^{3+} at LM5 at 60 and 100 cm would be 103.5 and 161.5 $\mu\text{mol}_e\text{L}^{-1}$, respectively. These levels are comparable to the ion imbalance (153.5 and 165.1 $\mu\text{mol}_e\text{L}^{-1}$), suggesting that the high concentrations of SO_4^{2-} and dissolved Fe may be the result of FeS_2 oxidation. Unlike $[\text{SO}_4^{2-}]$, the dissolved iron concentration in the stream water was relatively low. The normal procedure for removing iron from a solution is to precipitate it as ferric hydroxide, $\text{Fe}(\text{OH})_3$. When iron exists as Fe^{3+} in an acidic leaching solution, precipitation is accomplished by increasing the pH with the addition of an alkali such as CaCO_3 , which may exist in the lower part of the watershed.

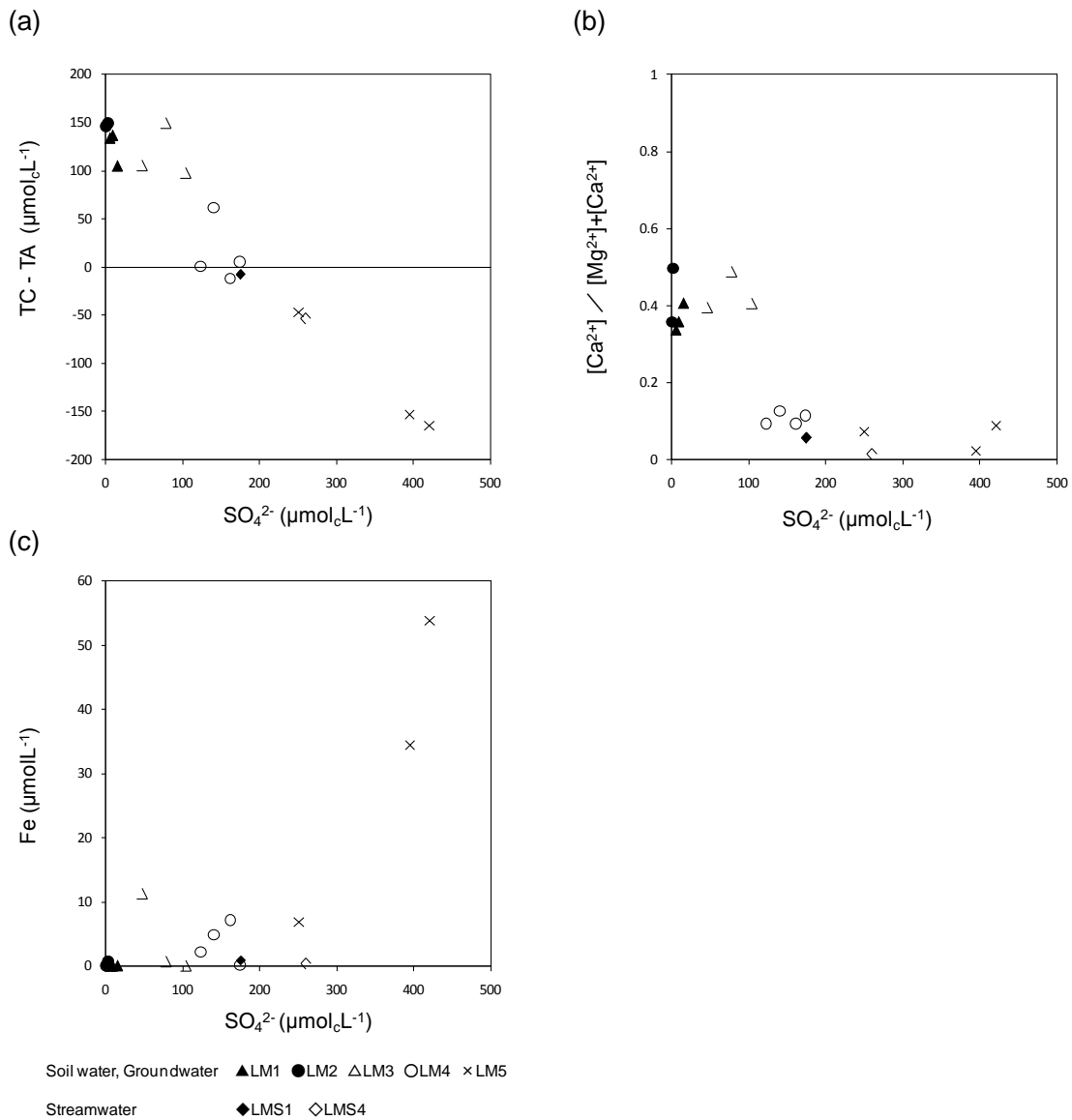


Figure 6.12 Scatter graph showing the relationship between $[\text{SO}_4^{2-}]$ and (a) $(\text{TC} - \text{TA})$ (b) $[\text{SO}_4^{2-}]$ and the ratio of $[\text{Ca}^{2+}]$ and $/([\text{Ca}^{2+}] + [\text{Mg}^{2+}])$, and (c) $[\text{SO}_4^{2-}]$ and $[\text{Fe}]$ for soil water, groundwater, and streamwater.

6. Sources and possible generation mechanism for controlling ion concentrations of streamwater

Table 6.2 lists the pH (H₂O), pH (KCl), and pH (H₂O₂) in the soil at LM1, LM4, and LM5. The soil pH (H₂O) was measured in the laboratory. The pH (H₂O) and pH (KCl) values were similar to those measured in an 8-ha permanent vegetation plot in LHNP (Ishizuka et al. 1998; 4.03–5.16 and 3.03–4.18, respectively). The pH (H₂O₂) values at LM1, LM4, and LM5 were less than 3, indicating that the soils were acid sulfate soils (Murakami, 1961) with high concentrations of SO₄²⁻.

Figure 6.2 The pH of soil samples.

Soil	pH (H ₂ O)	pH (KCl)	pH (H ₂ O ₂)
LM1 10cm	5.64	3.99	2.98
LM1 30cm	5.52	4.17	
LM4 10cm	4.61	3.62	2.49
LM4 30cm	4.81	3.63	
LM4 60cm	4.62	3.55	
LM4 100cm	4.57	3.80	
LM5 10cm	4.42	3.67	2.63
LM5 30cm	4.41	3.57	
LM5 60cm	4.34	3.65	

6.5 Conclusion

To determine the source and generation mechanism of high SO₄²⁻ concentrations in stream water in natural tropical rainforests, sampling and chemical analysis of soil, soil water, groundwater, and stream water were conducted in a small experimental watershed in Lambir Hills National Park, Malaysian Borneo. I found that (1) the SO₄²⁻ concentration of soil water exhibited great spatial heterogeneity; (2) the SO₄²⁻ concentration of stream water at the watershed outlet was dissimilar to that of soil water in both the lower and upper parts of the catchment, but was similar to that of soil water, groundwater, and stream water at the spring (stream source); and (3) at the points where the SO₄²⁻ concentration of soil water was the highest (around 400 μmol_cL⁻¹), high dissolved iron concentrations were detected, which may explain the ion and mass balance of FeS₂, Fe³⁺, and SO₄²⁻. From these findings, I conclude that the high SO₄²⁻ concentrations in stream water may be generated by chemical and bacterial weathering of inorganic FeS₂ unevenly distributed in the watershed.

6.6 References

- Andriessse, W., van Mensvoort, M. E. F. 2006. Acid sulfate soils: distribution and extent. In: Lai, R. (Eds.) *Encyclopedia of Soil Science*, 2nd ed. Taylor & Francis, New York, pp. 4-19.
- Arkesteyn, G.J.M.W. 1980. Pyrite oxidation in acid sulphate soils: the role of microorganisms. *Plant and Soil* 54: 119-134.
- Ashton, P.S., 1998. Lambir's forest: The world's most diverse known tree assemblage? In: Roubik, D.W., Sakai, S., Abang Hamid, A.K. (Eds.), *Pollination Ecology and the Rain Forest Sarawak Studies*, Ecological Studies 174: 191–216.
- Attanandana, T., Vacharotayan, S. 1986. Acid sulfate soils: Their characteristics, genesis, amelioration and utilization. *Southeast Asian Studies* 24:154-180.
- Baillie, I. C., Ashton, P. S., Chin, S. P., Davies, S. J., Palmiotto, P. A., Russo, S. E., Tan, S., 2006. Spatial associations of humus, nutrients and soils in mixed dipterocarp forest at Lambir, Sarawak, Malaysian Borneo. *Journal of Tropical Ecology* 22: 543–553.
- Berner, E. K., Berner, R. A. 1995. *Global environment: water, air and geochemical cycles*. Prentice Hall, USA, 376pp.
- Calmels, D., Gaillardet, J., Brenot, A. and France-Lanord, C. 2007 Sustained sulfide oxidation by physical erosion processes in the Mackenzie River basin: climate perspectives. *Geology* 35: 1003-1006.
- Gomyo, M., Wakahara, T., Shiraki, K., Kuraji, K., Kitayama, K., and Suzuki, M. 2009. Characteristics of streamwater concentrations of inorganic ions in a montane forest and a tropical lowland forest in Malaysian Borneo. In: Proceeding of the Second international conference on forests and water in a changing environment. (Eds.), Raleigh, North Carolina, pp.47-48.
- Haraguchi, A. 2007. Effect of sulfuric acid discharge on river water chemistry in peat swamp forests in central Kalimantan, Indonesia. *Limnology* 8:175-182.
- Hazebroek, H.P., Abang Kashim, A.M. 2001. National Parks of Sarawak. Natural History Publications (Borneo), Kota Kinabalu, 502pp.
- Hutchison, C. S. 2005. *Geology of North-West Borneo Sarawak, Brunei and Sabah*. Elsevier, London. 421pp.

6. Sources and possible generation mechanism for controlling ion concentrations of streamwater

- Ishizuka, S., Tanaka, S., Sakurai, K., Hirai, H., Hirotsu, H., Ogino, K., Lee, H. S., Kendawang, J. J., 1998. Characterization and distribution of soils at Lambir Hills National Park in Sarawak, Malaysia, with special reference to soil hardness and soil texture. *Tropics* 8: 31–44.
- Kumagai, T., Saitoh, T. M., Sato, Y., Takahashi, Y., Manfroi, O. J., Morooka, T., Kuraji, K., Suzuki, M., Yasunari, T., Komatsu, H. 2005. Annual water balance and seasonality of evapotranspiration in a Borneo tropical rainforest. *Agricultural and Forest Meteorology* 128 : 81-92.
- Kumagai, T., Saitoh, T., Sato, Y., Morooka, T., Manfroi, O.J., Kuraji, K. and Suzuki, M. 2004. Transpiration, canopy conductance and the decoupling coefficient of a lowland mixed Dipterocarp forest in Sarawak, Borneo: dry spell effects. *Journal of Hydrology* 287: 237-251.
- Likens, G. E., Bormann, F. H., Hedin, L. O., Driscoll, C. T., and Eaton, J. E. 1990. Dry deposition of sulfur: A 23 year record for the Hubbard Brook Forest ecosystem. *Tellus* 42:319-329.
- Loeb, R., van Daalen, E., Lamers, L.P.M. and Roelofs, J.G.M. 2007 How soil characteristics and water quality influence the biogeochemical response to flooding in riverine wetlands. *Biogeochemistry* 85: 289-302.
- MacKinnon, K., Hatta, G., Halim, H., Mangalik, A. 1996. *The ecology of Kalimantan*. Periplus Editions, Singapore, 802pp.
- Manfroi, O. J., Kuraji, K., Suzuki, M., Tanaka, N., Kume, T., Nakagawa, M., Kumagai, T., Nakashizuka, T. 2006. Comparison of conventionally observed interception evaporation in a 100-m² subplot with that estimated in a 4-ha area of the same Bornean lowland tropical forest. *Journal of Hydrology* 329: 329-349.
- Megonigal, J.P., Hines, M.E., and Visscher, P. T. 2005. Anaerobic metabolism: linkages to trace gases and aerobic processes. In: Schlesinger, W.H. (Eds.) *Biogeochemistry*. Elsevier-Perigamon, Oxford. pp.317-424.
- Mitchell, M., Bailey, S.W., Shanley, J.B and Mayer, B. 2008 Evaluating sulfur dynamics during storm events for three watersheds in the northeastern USA: a combined hydrological, chemical and isotopic approach. *Hydrological Processes* 22: 4023-4034.
- Morgan, M.D., Good, R.E., Spratt, J., Henry, G. 1988 Acidic deposition impacts mediated by sulfur cycling in a coastal plain forest ecosystem. *GeoJournal* 17.2: 183-187.
- Murakami, H. 1961. A Method of Semi-quantitative Determination of Oxidizable Sulfur in Polder

6. Sources and possible generation mechanism for controlling ion concentrations of streamwater

Soils by Hydrogen Peroxide. *Journal of the science of soil and manure, Japan* 32:276-279 (in Japanese).

- Ohte, N., Tokuchi, N., and Suzuki, M. 1995 Biogeochemical influences on the determination of water chemistry in a temperate forest basin: Factors determining the pH value. *Water Resources Research* 11:2823-2834.
- Potts, M. D., Ashton, P. S., Kaufman, L. S., Plotkin, J. B. 2002. Habitat patterns in tropical rain forests: A comparison of 105 plots in northwest Borneo. *Ecology* 83: 2782-2797.
- Tange, T., Yagi, H. 1995. Iron sulfide contained in the tertiary stratum in the Kiyosumi mountain area, the Boso peninsula, Japan. *Pedologist* 38:83-86.
- Wilford, G.E. 1961. *The Geology and Mineral Resources of Brunei and Adjacent Parts of Sarawak*. Memoir 10. Geology Survey Department, British Territories in Borneo, 319pp.
- Yamakura, T., Kanzaki, M., Itoh, A., Ohkubo, T., Ogino, K., Ernest, C., Lee, H. S., Ashton, P. S. 1995. Topography of a large-scale research plot established within a tropical rain forest at Lambir, Sarawak. *Tropics* 5:41-56.

Chapter 7

Conclusion

The overall goal of my study was to investigate the characteristics of spatial and seasonal variation in rainfall, the ENSO-rainfall relationship, the water and nutrient balances, the difference in water chemistry between tropical montane and lowland forests, and the cause of the streamwater chemistry in Malaysian Borneo.

I collected rainfall data established a series of experimental watersheds and conducted hydrological and hydrochemical observations in Malaysian Borneo.

Chapter 2 presents the site descriptions, tropical montane and tropical lowland rainforest sites were located inside the two national parks in Malaysian Borneo.

Chapter 3 deals with the spatial distribution of seasonal variation in rainfall and ENSO-rainfall relationship in 1000×1000 km scale included two study sites. The features of the data used in this chapter were data spanning from 20 to 41 years, multi-location derived data, and temporal resolution of the data. The rainfall–ENSO relationship and seasonal variation in rainfall over Sarawak and Sabah, Malaysian Borneo, was examined using rainfall data. Rainfall–ENSO relationships in Sarawak were first seen in Southwest Sarawak during JJA and move northeastward to Northeast Sarawak in the following DJF. The seasonal variation in rainfall over Sarawak was categorized into four clusters, JJA and DJF were dry and wet seasons, respectively, whereas for extremely limited region (C3), ONDJ and FM were relatively wet and dry seasons, respectively. The C3 region is the most vulnerable to El Niño-induced drought. In Sabah, the seasonal in rainfall was categorized into four clusters. For ENSO-rainfall relationship, after it returns from the dryness caused by El Niño, all areas experience higher rainfall than average in the period from July to September. The amount of rainfall and degree of seasonal variation widely vary by locations in this region; however, it was found that the effect of the dryness caused by El Niño occurs at almost the same timing throughout all areas, and it brings dryness in certain points that normally have low rainfall in such timing.

7. Conclusion

Chapter 4 describes the water and nutrient balance from 2006 to 2008 and the differences between the two sites. **(1) Water balance:** The annual discharge in KM was approximately twice that in LT because the annual rainfall in KM was 120–670 mm greater than that in LT. No clear correlation was found between mean annual rainfall and loss, but there was a significant (99%) negative correlation between elevation and mean annual loss. **(2) Hydrological characteristics:** The probability of daily rainfall greater than 1 mm in LT and KM was 54% and 60%, respectively. The probability of 0 mm daily rainfall in LT and KM was 41% and 33%, respectively. The fluctuation of daily discharge was smallest in SP and greatest in LT. The probability of daily discharge less than 1 mm in LT and KM was 27% and 20%, respectively. In LT and KM, there is water flow in the stream throughout the year. The differences between the daily discharge when the probability of occurrence exceeded 80% (D80) and 20% (D20) were compared. The differences between D20 and D80 in LT and KM were 2.6 and 6.5 mm, respectively, showing that the fluctuation of daily discharge in LT was smaller than in KM. The differences between D20 and D80 in LT, KM, SP, and UK were 2.6, 6.5, 5.6, and 2.2 mm, respectively, showing that the fluctuation of daily discharge was the smallest in UK and the greatest in KM. **(3) Nutrient balance:** The greatest difference in nutrient balance between LT and KM was in the $\text{SO}_4\text{-S}$ balance. There were no distinct differences between $\text{SO}_4\text{-S}$ AIF_R and AIF_T in KM and LT. However, in LT, the mean $\text{SO}_4\text{-S}$ AOF was 65 times that in KM. In LT, the $\text{SO}_4\text{-S}$ AOF was higher than the AIF_R and AIF_T , whereas in KM, the $\text{SO}_4\text{-S}$ AOF was smaller than the AIF_R and AIF_T . The inorganic N balance was smaller than the balance of K, Mg, and Ca in KM and LT. The AIF_R and AIF_T of $\text{NH}_4\text{-N}$ were greater than those of $\text{NO}_3\text{-N}$, and the $\text{NO}_3\text{-N}$ AOF was greater than the $\text{NH}_4\text{-N}$ AOF in both LT and KM. This suggests that most $\text{NH}_4\text{-N}$ and organic N supplied in rainfall was nitrified by microorganisms. The K AOF was one fifth of the AIF_T in KM; less of a difference was observed between the K AOF and AIF_T in LT. To explain the small differences between nutrient AOF and AIF_T in LT, I postulate that K, Mg, and Ca are supplied by chemical weathering of the bedrock and that the differences between KM and LT may be attributable to differences in chemical weathering. There were no differences in the AIF_R , AIF_T , and AOF values for Na and Cl in KM; there was a greater difference in the AIF_R , AIF_T , and AOF values for Na and Cl in LT. **(4) Output flux estimation methods:** I estimated the nutrient AOF from a watershed using six methods. First, AOF was calculated by multiplying annual discharge with the volume-weighted mean annual concentration of nutrients (Method I). Second, AOF was calculated from 10-min

7. Conclusion

interval discharge data and the relationship between discharge and concentration (C–Q equation). The exponential equation $\text{Log}(\text{Concentration}) = a + b \text{Log}(\text{Discharge})$ was adopted, and the coefficients of the C–Q equations were obtained from linear regression on log–log plots both without (Method II) and with (Method III) data from samples taken during rainfall-induced stormflow. The only data necessary for Method I were the annual discharge (which could be roughly estimated by subtracting rainfall from evapotranspiration), the concentration of periodically sampled water, and the simultaneous discharge at sampling times. For Methods II and V, continuously recorded discharge data were necessary. For Methods III and VI, the concentrations of samples during stormflow were added. Methods III or VI may have been more accurate, but they required the highest quality data. As a result of having examined the differences in the methods for AOF estimation, I identified Method VI as the most meaningful and the most accurate of the six methods.

Chapter 5 describes the characteristics of streamwater inorganic ion concentrations in a tropical montane forest and a tropical lowland forest in Malaysian Borneo and presents possible factors determining the differences between the two sites through comparisons with data reported at a number of other tropical forests. Watersheds in lowland forest had acidic streamwater, with pH values ranging from 4.2 to 4.8, and extremely high SO_4^{2-} concentrations that were approximately 100 times higher than those montane rainforest and those of other tropical watersheds. To understand the relationship between bedrock type and chemical weathering in tropical forest watersheds, I compared my watersheds with other watersheds and with data reported in the literature with regard to a number of other locations in the tropics. The absolute concentrations of total cations varied among sites with different bedrock. The component rate of cations is likely explained by bedrock geology. On the other hand, both the absolute concentrations and component rates of anions varied even among sites on the same type of geology. Because the main anion was SO_4^{2-} at lowland rainforest, the origin of SO_4^{2-} may be attributable to which sulfide is present in sedimentary rock and to the chemical weathering that takes place in sulfide-containing rocks. The first factor determining the pH of streamwater is likely whether the SO_4^{2-} concentration is lower or higher than that of rainwater. The second factor is whether the major anion is SO_4^{2-} and whether the cation runoff is sufficient to buffer SO_4^{2-} . For these factors, I discussed the results by comparing the four watersheds and comparing my findings with data reported for a number of other locations in the tropics.

Chapter 6 describes the possible generation mechanism for controlling ion concentrations of

7. Conclusion

streamwater in multi-scale. This chapter deals with the spatial and vertical variation of ion concentrations. I found that (1) the SO_4^{2-} concentration of soil water exhibited great spatial heterogeneity; (2) the SO_4^{2-} concentration of stream water at the watershed outlet was dissimilar to that of soil water in both the lower and upper parts of the catchment, but was similar to that of soil water, groundwater, and stream water at the spring (stream source); and (3) at the points where the SO_4^{2-} concentration of soil water was the highest (around $400 \mu\text{mol}_c\text{L}^{-1}$), high dissolved iron concentrations were detected, which may explain the ion and mass balance of FeS_2 , Fe^{3+} , and SO_4^{2-} . From these findings, I conclude that the high SO_4^{2-} concentrations in stream water may be generated by chemical and bacterial weathering of inorganic FeS_2 unevenly distributed in the watershed.

As mentioned above, in this study the characteristics of rainfall spatial and seasonal variation, ENSO-rainfall relationship, water and nutrient balances, water chemistry between tropical montane and lowland forests, the possible generation mechanism of streamwater chemistry in Malaysian Borneo had been become evident. These new findings help in determining the management and guideline for the natural tropical lowland and montane rainforest in the future.

Acknowledgements

First of all I appreciate Dr. Koichiro Kuraji (The University of Tokyo), Prof. Masakazu Suzuki (The University of Tokyo) and Prof. Kanehiro Kitayama (Kyoto University) as a graduate educator for giving the opportunity for studies on water and nutrient balances in tropical lowland and montane rainforests in Malaysian Borneo and for helpful suggestions and critical comments.

I thank Dr. Maklarin Lakim, Ms. Rimi Binti Repin of the Sabah Parks, Mr. Peter and Ms. Rosna at the Mount Kinabalu National Park in Sabah, Ms. Lucy Chong of Sarawak Forestry Corporation, and Mr. Matt at the Lambir Hills National Park for supporting my research activities from August 2005 to June 2009. I thank Dr. Mahmud Sudin, Dr. John Tay, and Dr. Phua Mui How for giving me the opportunity to perform my research activities at the University Malaysia Sabah from May 2008 to October 2008.

I have accepted help from many people throughout this study. I thank the editors and reviewers of journals, and the examiners of my thesis, namely Prof. Masakazu Suzuki, Dr. Koichiro Kuraji, Dr. Nobuhito Ohte, Prof. Takeshi Tange, and Hirofumi Shibano (The University of Tokyo), whose comments improved this study.

For help with Chapter 3, I am grateful to Dr. Koichiro Kuraji for teaching me to analyze rainfall data. I am also grateful to Prof. Masakazu Suzuki and Dr. Shinji Sawano. I thank Prof. Jun Matsumoto (Tokyo Metropolitan University) and Dr. Masayuki Maki (National Research Institute for Earth Science and Disaster Prevention) for helpful suggestions and critical comments. I thank Dr. Phua Mui How (University Malaysia Sabah) and Dr. Yap Siew Fah (DID, Sabah) for sharing their rainfall data. I thank Dr. Koichiro Kurajio and Dr. Nobuaki Tanaka (The University of Tokyo) for sharing long-term rainfall data from the Lambir Hills National Park and Prof. Kanehiro Kitayama for giving me long-term rainfall data from Mount Kinabalu National Park.

For help with Chapter 4 and Chapter 5, I am grateful to Dr. Katsushige Shiraki and Dr. Taeko Wakahara (United School of Agricultural and Science, Tokyo University of Agriculture and Technology) for giving me discharge data and a topographic map of the Lambir Hills National Park.

For help with Chapter 6, I am thankful to Dr. Koichiro Kuraji and Dr. Nobuhito Ohte (The University of Tokyo) who provided me with warm encouragement and helpful advice, Dr.

Acknowledgements

Tomoki Oda (The University of Tokyo) for useful comments in the initial stage of the field work and for on-site assistance, and Dr. Masamitsu Fujimoto (Kyoto University) for assisting with the laboratory work. I thank Prof. Takeshi Tange (The University of Tokyo), Dr. Toko Tanikawa (Forestry and Forest Products Research Institute), Dr. Shigehiro Kamoda (The University of Tokyo), and Dr. Kaoru Ueno (Chubu University) for giving me helpful advice and the opportunity to study in Japan.

I was supported by many people during this study, which has given me great happiness and pleasure. I thank the seniors of the laboratory (especially Dr. Norifumi Hotta, Dr. Shinji Sawano, Dr. Natsuko Yoshifuji, and Dr. Tomoki Oda) and other seniors (especially Dr. Rota Wagai and Dr. Masamitsu Fujimoto). I thank the juniors of the laboratory (especially Mr. Tetsuhiro Yamamoto). I thank the colleagues (especially Mr. Yusuke Kajiya) and other colleagues (especially Dr. Taeko Wakahara, Mr. Yuta Inoue, Ms. Chihiro Handa, Ms. Tamaki Kamoi, and Dr. Masayuki Ushio).

I am deeply grateful to all of the members of the laboratory (especially Ms. Takako Mori and Ms. Junko Fukushima) and all of the members of University Forest in Aichi, The University of Tokyo (especially Ms. Atsumi Kato and Ms. Yukiko Kamata) for their encouragement.

This research was supported by a Grant-in-Aid from the Japan Society for the Promotion of Science (JSPS) Fellows (no. 19 · 4231); the Japan Science and Technology Corporation (JST) Core Research for Evolutional Science and Technology (CREST) program “Effects of rainfall variability on water cycles and ecosystems in tropical forests under an Asian monsoon climate”; the JSPS Asia-Africa Science Platform Program “Building a Center for Ecosystem Ecology to Develop Societal Adaptability for the Land-use Change in Tropical Rain Forests”; and a Grant-in-Aid for Scientific Research from JSPS (no. 21405021).

Finally, I thank my parents (Mr. Kazuo Gomyo and Ms. Fusae Gomyo) and my sister (Ms. Yoshie Gomyo) for their affection and support.